Multipartite, Quantum, and Classical Correlation in the AdS/CFT correspondence

Koji Umemoto

Center for Gravitational Physics, Yukawa Institute for Theoretical Physics

Kyoto University

January 2021

Abstract

Many of the tools and ideas of quantum information theory have been employed to shed light on the holographic principle. The entanglement entropy in the AdS/CFT correspondence tells us that information of the bulk geometries is encoded in the boundary correlations. This thesis is aimed to deepen our understanding of this direction by studying various correlation measures in holography. We first derive a generalization of the holographic entanglement of purification conjecture for multipartite states. It turns out that this proposal is consistently supported in arbitrary n-partite states. We next study the entanglement of purification in quantum many body systems by numerical methods. That reveals a remarkable non-monotonicity of the entanglement of purification, attributed to the different sensitivities to quantum and classical correlations. We finally discuss the holographic duals of two classes of correlation measures: optimized correlation measures and axiomatic entanglement measures. The results suggest that classical correlation also plays an important role in encoding the geometrical information.

Contents

1 Introduction

That black holes have entropy is an important guidepost for capturing a theory of quantum gravity. A striking feature of this type of entropy is that they are proportional to the area of codimension-2 surface (e.g. event horizon), not the volume of the system [1, 2]. This fact makes a sharp distinction between the thermodynamics of black holes and that of usual matters, providing us with an insight that degrees of freedom in a spacetime region could be equivalently encodable in a matter theory on one lower dimensional spacetime without gravity. This concept is generically called "holographic principle" and has been intensively studied in the context of superstring theory [3, 4].

The most established realization of holographic principle would be the Anti-de-Sitter (AdS) / Conformal field theory (CFT) correspondence [5]. This duality argues that quantum gravity on an asymptotically AdS geometry is equivalent to a particular class of CFTs allocated on the asymptotic boundary. This equivalence provides a promising method to formulate quantum gravity from matter field theory in a non-perturbative way.

In the AdS/CFT correspondence, the origin of the black hole entropy can be attributed to a remnant of strong quantum entanglement. This picture is brought by the famous Ryu-Takayanagi formula or the holographic entanglement entropy formula [6, 7], that asserts the following equivalence; Suppose a holographic CFT is in a state $|\Psi\rangle$. Then the von Neumann entropy of the reduced density matrix $\rho_A := \mathrm{Tr}_{A^c}[|\Psi\rangle\langle\Psi|]$ associated with a spatial subregion A in CFTs,

$$S(\rho_A) := -\mathrm{Tr}\rho_A \log \rho_A, \tag{1.1}$$

is equivalent to the minimal area of certain codimension-2 surfaces γ_A in the dual AdS geometry,

$$S(\rho_A) = \min_{\gamma_A} \frac{\mathrm{Area}(\gamma_A)}{4G_N}, \tag{1.2}$$

at the leading order of $O(1/G_N)$ expansion, where G_N is the (d-dimensional) Newton constant. Here the von Neumann entropy $S(\rho_A) \equiv S_A$ is commonly called the entanglement entropy, because that represents an amount of quantum entanglement between A and its complement A^c based on the number of EPR pairs [8]. The codimension-2 surface $\gamma_A^{\min}$ that achieves the minimum on the right hand side, is called Ryu-Takayanagi surface. In the AdS black hole, the CFT (denoted by CFT_R) corresponding to the thermal state

$$\rho_{\mathrm{CFT}} = \rho_{\mathrm{thermal}} = \sum_n \frac{e^{-\beta E_n}}{Z} |E_n\rangle\langle E_n|_{\mathrm{CFT}_R}. \tag{1.3}$$

This state can be purified by a copy of the original CFT (denoted by CFT_L), results in a pure total state called thermofield double (TFD) state

$$|\Psi\rangle = \sum_n \frac{e^{-\beta E_n/2}}{\sqrt{Z}} |E_n\rangle_{\mathrm{CFT}_L} \otimes |E_n\rangle_{\mathrm{CFT}_R}. \tag{1.4}$$

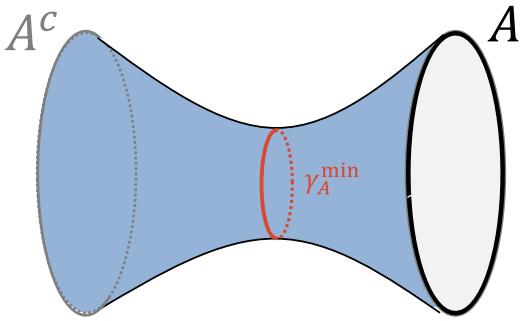

Figure 1.1: The two-sided eternal AdS wormhole geometry (on a constant time slice). The Ryu-Takayanagi surface $\gamma_A^{\min}$ denoted by the red line is located exactly on the event horizon of the black hole.

Then the corresponding AdS geometry is given by the eternal wormhole [9]. From the formula (1.2), the entropy of AdS black hole is now interpreted as the entanglement entropy between the two CFTs on the asymptotic boundaries ($A \equiv \mathrm{CFT}_R$ and $A^c \equiv \mathrm{CFT}_L$) (Fig. 1.1.). The expression of the TFD state (1.4) clearly illustrates existence of strong (sometimes we say "maximal") entanglement between these two CFTs. In this picture, the degree of of freedom of the black hole entropy is nothing but a remnant of the strong entanglement.

The Ryu-Takayanagi formula (1.2) itself is much more generic and applicable to various situations other than black holes. For example, the spatial region A is not necessarily a whole space of a boundary CFT, as well as the asymptotic AdS geometry does not necessarily contain a black hole. The formula is also generalized to non-static geometries (the Hubeny-Rangamani-Takayanagi formula) [10, 11], or to higher derivative gravity [12, 13], with an appropriate modification. In this sense, the Ryu-Takayanagi formula is an extensive generalization of the Bekenstein-Hawking formula in the AdS/CFT correspondence.

This powerful and universal connection between the entanglement entropy and spacetime geometry implies that the details of bulk spacetime geometry is secretly encoded in the structure of quantum entanglement on boundary CFTs. This mindset is sometimes mentioned as the slogan "It From Qbit", and has opened up a new era of holography cooperating with quantum information theory [14, 15, 16, 17]. The various tools and ideas of quantum information theory, such as information metrics, complexity, quantum teleportation, and quantum error corrections, have been employed to research of the AdS/CFT correspondence (e.g. [18, 19, 20, 21, 22, 23, 24, 25, 26, 27]). They have brought us pro-

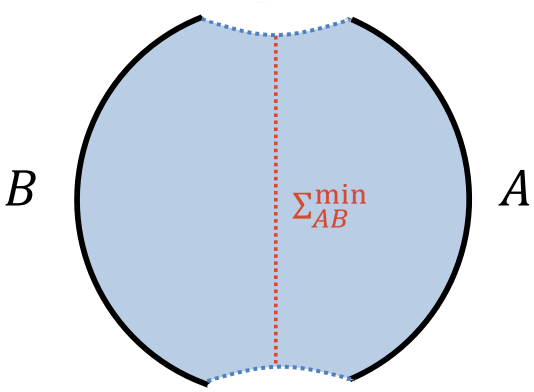

Figure 1.2: The entanglement wedge of $A \cup B$ (the blue colored region) and the entanglement wedge cross section (the red dotted line) in a pure AdS geometry on a constant time slice. The blue dotted curves of the entanglement wedge is the Ryu-Takayanagi surface $\gamma_{AB}^{\min}$.

found insights on the mechanism of the bulk/boundary duality. Moreover, inspired by the motivation from holography, new information theoretic quantities have been invented in recent years [28, 29, 30, 31].

There typically exists an equivalence between an information-theoretic quantity and a geometrical object. The entanglement entropy and the Ryu-Takayanagi surface is the first and the most well-studied example of such relations. One of such dual relations is the so-called holographic entanglement of purification conjecture, that is also deeply related to the structure of correlation and geometry [32, 33]. This relation argues that the entanglement of purification $E_P(\rho_{AB})$, an information measure of correlation on a bipartite system $\mathcal{H}_{AB} := \mathcal{H}_A \otimes \mathcal{H}_B$ [34], is equivalent to the minimal cross section of the entanglement wedge (a bulk region surrounded by the Ryu-Takayanagi surface of the subregion $A \cup B$),

$$E_P(\rho_{AB}) = \min_{\Sigma_{AB}} \frac{\text{Area}(\Sigma_{AB})}{4G_N}. \tag{1.5}$$

The right hand side is called the entanglement wedge cross section (EWCS), which is a plausible geometrical measure of correlation between the boundary subsystem A and B (Fig. 1.2). This relation is a generalization of the holographic entanglement entropy of the wormhole geometry for arbitrary geometries and for arbitrary partner subsystem $B \neq A^c$.

The quantum state on the bipartite system $A \cup B$ (such as depicted in Fig. 1.2)

is typically a mixed state because we trace out the remainder $\rho_{AB} := \mathrm{Tr}_{(AB)^c}[|\Psi\rangle\langle\Psi|]$. Remark that the von Neumann entropy S_A (or S_B) is no longer a measure of entanglement for mixed states; the entanglement entropy properly quantifies quantum entanglement only for pure states $\rho_{AB} = |\Psi\rangle\langle\Psi|_{AB}$. When ρ_{AB} is a mixed state, the entanglement entropy is not even a measure of classical correlation, as is obvious from that the totally decoupled mixed state $\rho_{AB} = \rho_A \otimes \rho_B$ can result in $S_A > 0$. Thus, the relation 1.5 implies that there still exists a profound connection between the correlations and the spacetime geometry for mixed states.

This conjecture and the entanglement wedge cross section itself have recently attracted much attention in the literature (e.g. [35, 36, 37, 38, 39, 40, 41, 42, 43, 44, 45, 46, 47, 48, 49, 50, 51, 52]). In particular, recent advances have revealed that the entanglement wedge cross section is a plausible dual candidate for several information measures, the odd entropy [28], the logarithmic negativity [53, 54], and the reflected entropy [55]. Interestingly, all of them satisfy the fundamental properties of correlation measure, which makes it more solid that the correlations in boundary is deeply connected with the bulk geometry. This view has inspired, for instance, the bit-thread formalism that is the construction of the AdS/CFT correspondence based on a bunch of correlated degree of freedom akin to EPR pairs [56, 57, 58, 59].

This thesis is aimed to promote this direction and to investigate concrete relations between boundary correlation and bulk geometry in the AdS/CFT correspondence. That will develop the further interaction between high energy physics and quantum information theory. In order to achieve this purpose, we will follow the three multifaceted approaches below:

First, one of the missing pieces of the above discussion is about multipartite correlations in three or more partite systems $A, B, C, \ldots$. In quantum information theory, it is well known that multipartite entanglement is more than just a combination of bipartite entanglement. Such multipartite correlation also plays an important role in extracting a distinct feature of holographic correlations. We will introduce a totally new information-theoretic measure of multipartite correlation, and propose a plausible geometrical counterpart of this quantity. That provides a fundamental tool to deal with multipartite correlations in the AdS/CFT correspondence [60].

Second, the entanglement of purification on the left hand side (1.5) is generically hard to compute, because that definition involves a highly non-trivial optimization procedure. Thus the behavior of this quantity in physical many body systems is less known, while the information-theoretic properties are well studied. As a first step, we perform a computation of the entanglement of purification in quantum body systems by a numerical method [61]. That reveals unusual behavior of the entanglement of purification as a measure of correlation, explained by a difference of quantum and classical correlations [1].

[1] Refer also to an analytic computation of the entanglement of purification based on the path-integral optimization, which shows an exact match of the conjecture (1.5) in particular configurations [62].

Finally, there are various classes of correlation measures in quantum information theory. We comprehensively deal with two classes of such correlation measures [63] to illustrate a unified view on the relation between correlations and geometry. The first one, called optimized correlation measure, is a generalization of the entanglement of purification and their holographic dual will be derived in an integrated manner. That will provide an interesting example for which these optimization procedures are executable owing to the power of holography. Then we present a no-go theorem for another class, called the axiomatic entanglement measures, that they can not be dual to the promising geometrical measures of correlation. That high-lightens the importance of classical correlation in the AdS/CFT correspondence.

The remainder of this thesis is organized as follows: In the section 2, we give a brief review on the holographic entanglement entropy, the entanglement wedge cross section, and the information-theoretic measure of correlation. That covers the fundamentals of the latter parts. In the section 3, the definition of the n-partite generalization of the entanglement of purification is introduced, and the properties of that are studied in detail. The holographic dual then will be derived and the consistency of their properties are shown. In the section 4, we discuss a numerical computation of the entanglement entropy in lattice regularized free scalar field theory and spin chain models. Varying the size and the location of the subsystem A and B will illustrate an outstanding behavior of the entanglement of purification common to both models. In the section 5, the holographic dual of the optimized correlation measures are discussed in a comprehensive way. That bring us a new bulk object inside the entanglement wedge, similar to but more complex than the entanglement wedge cross section. We also state a no-go theorem on the holographic dual of the axiomatic entanglement measures, that forbids them from being a dual to the geometrical measures of correlation. To close, we summarize the whole discussion and develop a future perspective in the section 6.

2 A review of quantum entanglement in the AdS/CFT Correspondence

2.1 Ryu-Takayanagi formula

We start by setting our conventions in the AdS/CFT correspondence. The entanglement entropy is defined on a reduced density matrix ρ_A, where the subsystem A in quantum field theories is typically taken as a spatial subregion on a time slice. The total Hilbert space of the field theory may be factorized into $\mathcal{H}_{tot} = \mathcal{H}_A \otimes \mathcal{H}_{A^c}$. The subsystem A can be a single connected subregion, or a total of multiple disconnected subregions. Then the entanglement entropy for the subsystem A in a total state ρ_{tot}, is defined as the von Neumann entropy of the reduced density matrix $\rho_A = \mathrm{Tr}_{A^c}\rho_{tot}$,

$$S(\rho_A) := -\mathrm{Tr}\rho_A \log \rho_A. \tag{2.1}$$

We usually denote $S(\rho_A)$ by S_A for simplicity unless the state ρ_A under consideration needs to be explicitly mentioned. This same caution will apply to the other entropic quantities such as the mutual information.

In the AdS/CFT correspondence, the holographic entanglement entropy formula [6, 64, 10] tells us how to calculate entanglement entropy in the dual gravity side. Consider a d-dimensional holographic CFT that has a classical $d+1$ dimensional gravity dual. In the present thesis, we will restrict ourselves to static geometries for simplicity. A covariant generalization is almost straightforward following the same method that extends the Ryu-Takayanagi formula to the Hubeny-Rangamani-Takayanagi formula [2]. On the dual gravity solution corresponds to ρ_{tot} , we consider a constant time slice. To compute the entanglement entropy for the chosen subsystem A, we have to search the codimension-2 (i.e. $d-1$-dimensional) surfaces γ_A on the time slice, under the two conditions that (i) they are anchored on the entangling surface $\partial\gamma_A = \partial A$ and (ii) γ_A is homologous to A. Then the entanglement entropy is given by the minimal area of such surfaces[3] [6],

$$S_A = \min_{\gamma_A} \frac{\mathrm{Area}(\gamma_A)}{4G_N} \ . \tag{2.2}$$

The right hand side is called the holographic entanglement entropy. The simplest example would be found in the (global) pure AdS, where the Ryu-Takayanagi surface $\gamma_A^{\min}$ is depicted in (Fig. 2.1).

The minimality of the Ryu-Takayanagi surface allows us to prove the properties of the holographic entanglement entropy, such as the strong subadditivity, purely by the

[2] A covariant discussion is not so straightforward for multipartite settings that will be discussed in the section 3. For instance, refer to [65] for the entropic inequalities for more than 4-partite systems.

[3] We deal with the leading order of large N limit (small $1/G_N$ limit) through the whole of present thesis.

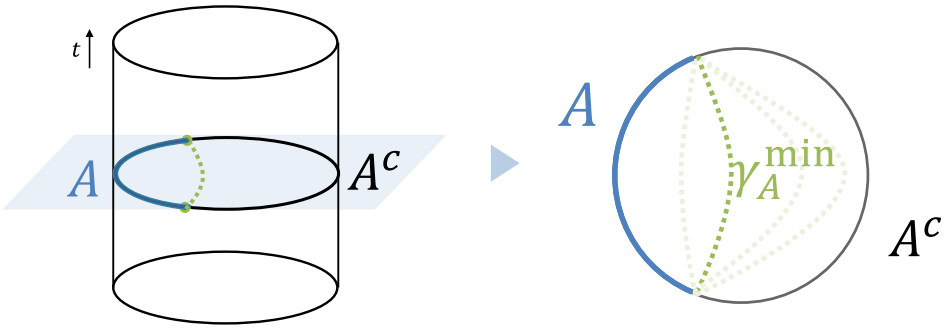

Figure 2.1: The holographic entanglement entropy of a given spatial subregion A on a constant time slice (the gray shaded region) in the global pure AdS. The dotted green lines are codimension-2 surfaces γ_A, and the Ryu-Takayanagi surface $\gamma_A^{\min}$ gives the minimal area.

geometrical methods [66, 67, 68, 69]. The derivation of (2.2) and of a covariant version are found in [7, 11].

2.2 The holographic Mutual Information

One of the generalizations of the entanglement entropy is the mutual information. The mutual information I is defined on quantum states ρ_{AB}, acting on a bipartite system $\mathcal{H}_{A\cup B}(\equiv \mathcal{H}_{AB}) = \mathcal{H}_A \otimes \mathcal{H}_B$ on two subsystems A and B, by

$$I(\rho_{AB}) := S_A + S_B - S_{AB}. \tag{2.3}$$

We denote $I(\rho_{AB})$ by $I(A:B)$ for simplicity. This quantity is a measure of correlation between A and B, satisfying the monotonicity on strict local operations. In particular, $I(A:B) \geq 0$ and $I(A:B) = 0$ if and only if $\rho_{AB} = \rho_A \otimes \rho_B$. The mutual information is usually UV-finite even in quantum field theories.

Because the mutual information is a linear combination of the entanglement entropies, the holographic dual of the mutual information is immediately induced from the Ryu-Takayanagi formula. To compute $I(A:B)$, we need to find the Ryu-Takayanagi surface of the subsystem $A \cup B$ that is typically a disconnected subregion. That makes the holographic dual of S_{AB} more complex than that of a single interval. There are two different phases for $\gamma_A^{\min}$, depending on the size and location of the subsystems (Fig. 2.2). When A and B are distant, the disconnected phase (Left) where we have $S_{AB} = S_A + S_B$ is chosen. That leads to

$$I(A:B) = 0. \tag{2.4}$$

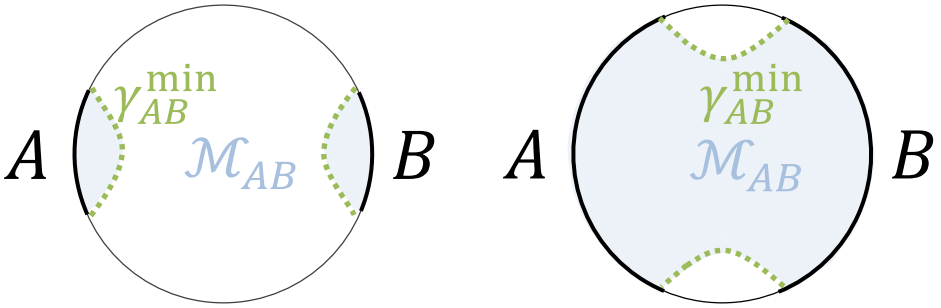

Figure 2.2: The Ryu-Takayanagi surface of S_{AB} in the two different configurations (Left and Right). The configuration that has smaller area of $\gamma_A^{\min}$ will be chosen. The blue shaded region is the (time slice of) entanglement wedge of $A \cup B$.

When A and B are close, the connected phase (Right) is preferred, and then we have

$$I(A:B) > 0. \tag{2.5}$$

This is called the phase transition of the holographic mutual information. The vanishing $I(A:B) = 0$ is a magic of the leading order approximation at $O(1/G_N)$; there still remains $O(1)$ positive value even in the disconnected phase.

2.3 Entanglement Wedge Cross Section

The entanglement wedge of a subsystem X is a bulk subregion $\mathcal{M}_X$ surrounded by the Ryu-Takayanagi surface $\gamma_X^{\min}$ [70, 71, 72]. [4] The entanglement wedge of $A \cup B$ is , for example, denoted by $\mathcal{M}_{AB}$ illustrated in the Fig. 2.2.

Given an entanglement wedge for a bipartite subsystem, the entanglement wedge cross section is defined as follows [32]. Suppose the boundary of $\mathcal{M}_{AB}$, consists of $A \cup B$ and $\gamma_{AB}^{\min}$, is divided into two imaginary subsystems $\mathcal{A}$ and $\mathcal{B}$ so that

$$\partial \mathcal{M}_{AB} = \mathcal{A} \cup \mathcal{B}, \ \mathcal{A} = A \cup A', \ \mathcal{B} = B \cup B', \tag{2.6}$$

where $A' \cup B' = \gamma_{AB}^{\min}$. The boundary $\partial \mathcal{M}_{AB}$ may include the horizon of black hole. Then the entanglement wedge cross section $E_W(A:B)$ of $\mathcal{M}_{AB}$ is defined by the minimum of the holographic entanglement entropy $S_{\mathcal{A}}$ optimized over all possible such partitions

[4] Precisely speaking, the entanglement wedge is a codimension-0 subregion in the bulk spacetime, but we call the time slice of that by the entanglement wedge with an abuse of terminology.

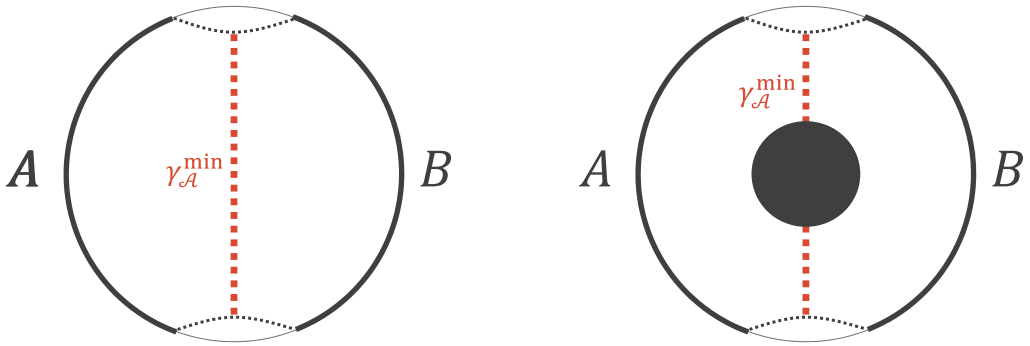

Figure 2.3: The entanglement wedge cross section (the red dashed lines) in the global pure AdS (Left) and in the global AdS black hole (Right). (The figure is cited from [63])

$$E_W(A:B) := \min_{\mathcal{A}:\partial\mathcal{M}_{AB}=\mathcal{A}\cup\mathcal{B}} S_{\mathcal{A}} \tag{2.7}$$

$$= \min_{\gamma_{\mathcal{A}}} \frac{\mathrm{Area}(\gamma_{\mathcal{A}})}{4G_N}, \tag{2.8}$$

where $\gamma_{\mathcal{A}}$ is the Ryu-Takayanagi surface of the subsystem $\mathcal{A}$. Examples in a typical subsystem $A\cup B$ in connected phases are shown in Fig.2.3. For the disconnected phase in Fig.2.2, the entanglement wedge cross section will automatically vanish $E_W(A:B)=0$ by definition.

The entanglement wedge cross section is a generalization of the holographic entanglement entropy for mixed states, in the sense that $\gamma_{\mathcal{A}}^{\min}$ reduces to the Ryu-Takayanagi surface $\gamma_A^{\min}$ if ρ_{AB} is pure. The entanglement wedge cross section is usually a UV-finite quantity. The several properties such as the sandwich inequality

$$\frac{1}{2}I(A:B) \leq E_W(A:B) \leq \min\{S_A, S_B\}, \tag{2.9}$$

are shown [32, 33]. These support that the entanglement wedge cross section is a plausible geometrical measure of correlation.

2.4 The Holographic Dual Conjectures

The entanglement wedge cross section is originally conjectured to be dual to the information-theoretic quantity called the entanglement of purification, based on agreements of their various information-theoretic properties as well as the compatibility with the tensor network description of the AdS/CFT correspondence [73, 74].

Surprisingly, several correlation measures other than the entanglement of purification have been shown to be essentially equal to the entanglement wedge cross section. These measures include the logarithmic negativity [53, 75, 76, 54], the odd entropy [28], and the reflected entropy [55]. They are computable in holographic CFTs and the results match with the form of the entanglement wedge cross section in many cases. Remarkably, the reflected entropy, a cousin of the entanglement of purification, shows that the entanglement wedge cross section is exactly analogous to the wormhole horizon in a geometry dual to the canonical purification.

2.4.1 The entanglement of purification

Here we will focus on the entanglement of purification for the latter use. The entanglement of purification is defined on a bipartite state ρ_{AB} as follows [34]. Consider a purification of ρ_{AB}, i.e. a pure state $|\psi\rangle_{ABE}$ that satisfies

$$\mathrm{Tr}_E[|\psi\rangle\langle\psi|_{ABE}] = \rho_{AB}, \tag{2.10}$$

with a decomposition of the ancillary system E into $\mathcal{H}_E \equiv \mathcal{H}_{A'} \otimes \mathcal{H}_{B'} = \mathcal{H}_{A'B'}$. There are infinite choices of $|\psi\rangle_{AA'BB'}$, and the dimension of the Hilbert space $\mathcal{H}_{A'B'}$ could be arbitrary large in general. Then the entanglement of purification E_P is defined by the entanglement entropy of the reduced density matrix $\rho_{AA'} = \mathrm{Tr}[|\psi\rangle\langle\psi|_{AA'BB'}]$,

$$E_P(\rho_{AB}) := \min_{|\psi\rangle_{AA'BB'}} S_{AA'}, \tag{2.11}$$

where the minimum is taken over all possible purifications. We concisely write $E_P(\rho_{AB}) \equiv E_P(A:B)$ unless a given state need to be specified.

This is an information-theoretic measure of both quantum and classical correlations between A and B. The $E_P(A:B)$ is positive semi-definite and vanishes only for product states $\rho_{AB} = \rho_A \otimes \rho_B$. This monotonically decreases under local operations, but not for classical communication. In this sense, the entanglement of purification is very similar to the mutual information. The regularized version of entanglement of purification

$$E_P^{\infty}(\rho_{AB}) := \lim_{n\to\infty} \frac{E_P(\rho_{AB}^{\otimes n})}{n}, \tag{2.12}$$

has an operational interpretation based on the number of EPR pairs under the local operation and asymptotically vanishing communication (LOq).

2.5 The Classes of the Correlation Measures

There are many types of correlation measures in quantum information theory. They have been invented historically in accordance with various purposes in the information theory. The entanglement measures are characterized by the monotonicity under strict local

operations (LO) and classical communication (CC), quantifying an amount of entanglement for given mixed states. A subclass of that called axiomatic entanglement measures satisfy a set of axioms such as the asymptotic continuity. This class includes the entanglement of formation [77], the relative entropy of entanglement [78], the entanglement cost [77, 79], the distillable entanglement [77, 80], the squashed entanglement [81], and so forth [82]. Most of them are defined using a certain type of minimization. For instance, the entanglement of formation E_F is defined by

$$E_F(\rho_{AB}) := \min_{\sum p_i |\psi^i\rangle\langle\psi^i|_{AB} = \rho_{AB}} \sum_i p_i S(\sigma_A^i),\ \sigma_A^i := \mathrm{Tr}_B[|\psi^i\rangle\langle\psi^i|_{AB}], \tag{2.13}$$

where the minimization is performed over all possible choices of $\{p_i, |\psi^i\rangle_{AB}\}$ subject to $\rho_{AB} = \sum_i p_i |\psi^i\rangle\langle\psi^i|_{AB}$ and $\sum p_i = 1,\ p_i \geq 0$. This procedure is called convex roof in general. The entanglement of formation is known to give a universal upper bound on various entanglement measures

$$E_X(\rho_{AB}) \leq E_F(\rho_{AB}), \tag{2.14}$$

where E_X is any of the other axiomatic entanglement measures listed above.

The entanglement of purification and the mutual information belong to the class called the total (quantum and classical) correlation measures. They are monotonically non-increasing under strict local operations, but may increase by classical communication. The other examples will be discussed in the section 5.

The entanglement of formation is closely related to the entanglement of purification by the inequality

$$E_F(\rho_{AB}) \leq E_P(\rho_{AB}). \tag{2.15}$$

An interpretation is that an amount of quantum correlation can never exceed the sum of quantum and classical correlation.

3 Multipartite entanglement in the AdS/CFT correspondence

The quantum entanglement is typically discussed as a bipartite correlation. In these case, as we saw in the previous sections, we usually divide the whole quantum system into two pieces, a subsystem A and its complement A^c, and then the entanglement entropy S_A uniquely represents the amount of quantum entanglement between them for pure states [8]. However, this bipartite model is not the only case we discuss the quantum entanglement on. It has been known that there are richer correlation structures in quantum systems consisting of three or more subsystems.

On multipartite quantum systems, there are various types and levels of the multipartite quantum entanglement. This diversity comes from the fact that the separable states on multipartite quantum system has different criteria depending on how one require the states to be un-entangled among the multi-subsystems. This fact results in the variety – and difficulty – of study of multipartite entanglement compared to the bipartite one [82]. For example, one needs (infinitely) many kinds of standard states like Bell pairs in bipartite case in order to characterize operational aspects of an amount of multipartite entanglement by means of (S)LOCC. Another way to illustrate an aspect of multipartite entanglement is given by the famous GHZ state in 3-qubits system:

$$|\mathrm{GHZ}\rangle_{ABC} = \frac{1}{\sqrt{2}}(|000\rangle_{ABC} + |111\rangle_{ABC}). \tag{3.1}$$

This type of entanglement is known to play an essential part of the building blocks of tripartite entanglement. Each of the three qubits is maximally entangled with the other systems in this state. After one of the subsystems is traced out, however, the remaining bipartite state becomes separable, and thus no quantum entanglement remains. This example shows that the structure of multipartite quantum entanglement is much richer than bipartite ones and is not just a sum of bipartite one.

To quantify an amount of correlations for multipartite states, there have been several proposals by generalizing the mutual information.

The multipartite entanglement has been studied in the holographic system also. A pioneer work on this context it the well-known property of holographic mutual information called "monogamy". This feature is characterized the following simple inequality on a tripartite system A, B, C:

$$I(A : BC) \geq I(A : B) + I(A : C). \tag{3.2}$$

This inequality is always true on the geometrical states for any tripartite subsystems at the leading order $O(\frac{1}{G_N})$. The proof relies only on the very basic properties of Ryu-Takayanagi surface and thus is flexible and robust. In general, this type of inequality (3.2) is conventionally called monogamy inequality also for the other measures of correlation.

If a measure of correlation satisfies the inequality (3.2) for a class of states, then this measure is called monogamous on the state class.

The key argument is that the inequality (3.2) is not always true in general quantum tripartite systems. For example, one can easily check that a fully mixed multipartite quantum state $\rho_{ABC} = \frac{1}{2}(|000\rangle\langle 000|_{ABC} + |111\rangle\langle 111|_{ABC})$ violates the inequality. Thus the monogamy of mutual information can be regarded as a characterization or a necessary condition of geometrical states. This is the tripartite subsystem case, but four- or more-partite case are also known to exhibit the distinctive behavior of correlation in a similar way [68, 69]. These examples indicate that multipartite entanglement tells us more fine-grained information about the holographic states and their structure.

This inequality (3.2) can be transformed into a more intuitive form using the tripartite information,

$$I_3(A, B, C) = I(A : B) + I(A : C) - I(A : BC) = I(A : B) - I(A : B|C), \tag{3.3}$$

where $I(A : B|C) = I(A : BC) - I(A : C)$ is the conditional mutual information. The tripartite information is one of the various generalizations of the mutual information. The monogamy of holographic mutual information can be rephrased as the negativity (or non-positivity, strictly speaking) of the tripartite information,

$$I_3(A, B, C) \leq 0. \tag{3.4}$$

This quantity attracts a lot of attention as a measure of correlation or a diagnostic of chaos (with a flipped sign, $-I_3$) in the context of holography [67, 83, 84, 85, 86, 87]. In generic quantum system, the tripartite information can be both positive and negative (as a consequence of the possible violation of the monogamy of mutual information), and can be zero even for correlated states e.g. GHZ state. This property complicates the situation and make it hard to extract the description of structure of multipartite correlation in geometric states.

Our goal in this section is to introduce a genuine informational measure of multipartite correlation both in generic quantum states and in holographic states. This procedure is conducted by generalizing the entanglement of purification to multipartite systems: we first define a multipartite version of the entanglement of purification, and then propose its holographic dual following a similar manner to the bipartite case. The properties of the multipartite entanglement of purification are studied in generic quantum systems, which assures that this quantity is a genuine measure of multipartite correlation. These feature include new upper bounds on the existing measures of multipartite correlation – called the total correlation and the dual total correlation [88, 89]– and on the novel information measures defined as generalizations of the tripartite information. The holographic counterpart typically has a form exemplified in Fig.3.1

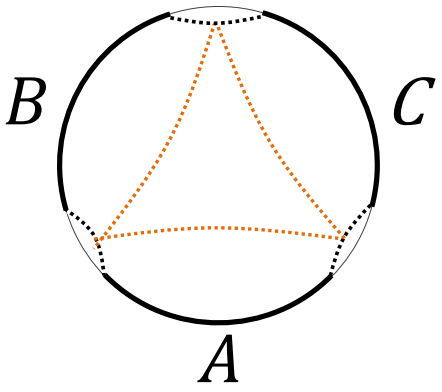

Figure 3.1: An typical example of the multipartite generalization of the entanglement wedge cross section, whose area gives $E_W(A:B:C)$ (The figure is cited from [60])

, and the its geometrical properties totally match with these of the multipartite entanglement of purification.

Finally, we remark that the word "monogamy" means that they can never correlated the other system. This is purely quantum phenomena and can not be seen in classical system (since one can always add a correlated system C by just classically mixing the states). A clear and simple argument related to this fact is the following: a pure quantum state $|\psi\rangle_{AB}$ can never be correlated with any other system C. In other words, any type of extension of $\rho_{AB} = |\psi\rangle\langle\psi|_{AB}$ must have a totally decoupled form $\rho_{ABC} = |\psi\rangle\langle\psi|_{AB} \otimes \rho_C$. This can easily seen by $I(AB:C) = S_{AB} + S_C - S_{ABC} = 0$ because of $S_{AB} = 0$ that also leads to $S_C \leq S_{ABC} \leq S_C$.

Note: This section is mainly based on the results in [60, 63].

3.1 The multipartite entanglement of purification

We first give a brief review of the properties of the bipartite entanglement of purification. Then we provide a generalization for generic multipartite quantum systems. The various information-theoretic properties necessary for a multipartite correlation measures will be shown in detail.

3.1.1 A review of the bipartite entanglement of purification

Recall the definition and basic properties of the entanglement of purification, discussed in the previous section 2.4. Given a quantum state ρ_{AB} on a bipartite quantum system $\mathcal{H}_{AB} = \mathcal{H}_A \otimes \mathcal{H}_B$, the entanglement of purification $E_P(A:B)$ is defined by

$$E_P(\rho_{AB}) := \min_{|\psi\rangle_{AA'BB'}} S_{AA'}, \tag{3.5}$$

where the minimization is taken over all possible purifications $|\psi\rangle_{AA'BB'}$ that satisfies $\rho_{AB} = \mathrm{Tr}_{A'B'}[|\psi\rangle\langle\psi|_{AA'BB'}]$. Using the fact $S_{AA'} = S_{BB'}$ for any pure states $|\psi\rangle_{AA'BB'}$, this expression can also be written as

$$E_P(\rho_{AB}) := \frac{1}{2}\min_{|\psi\rangle_{AA'BB'}}(S_{AA'} + S_{BB'}) = \frac{1}{2}\min_{|\psi\rangle_{AA'BB'}} I(AA' : BB'). \tag{3.6}$$

For the reader's convenience, we put a short list of the information-theoretic properties of E_P that will be related to the later discussion:

(I) For pure state $\rho_{AB} = |\psi\rangle\langle\psi|_{AB}$, this quantity reduces to the entanglement entropy:

$$E_P(A : B) = S_A = S_B \text{ on any pure states.} \tag{3.7}$$

This property is desirable for many bipartite correlation measure, especially for the entanglement measures, owing to the uniqueness theorem [8]. Namely, this feature allows us to regard E_P as a generalization of entanglement entropy for mixed state as an amount of correlations. Refer to the original paper [34] for the operational meaning of the EOP based on the number of EPR pairs. This property is also usually required for a class of axiomatic entanglement measures as a normalization condition, which enable us to compare their values meaningfully.

(II) This quantity is always non-negative $E_P(A : B) \geq 0$, and vanishes if and only if a given state ρ_{AB} is a product state,

$$E_P(A : B) = 0 \Leftrightarrow \rho_{AB} = \rho_A \otimes \rho_B. \tag{3.8}$$

This property is usually an essential requirement for a measure of correlation. Note that many important information-theoretic quantities, e.g. the conditional entropy or the tripartite information, can be both positive and negative in quantum systems.

(III) This quantity monotonically decreases by discarding an ancilla subsystem,

$$E_P(A : BC) \geq E_P(A : B). \tag{3.9}$$

This is also a natural property for a measure of correlation. The same inequality replaced with the mutual information $I(A : BC) \geq I(A : B)$ is also true, known as the strong subadditivity of the entanglement entropy.

(IV) This quantity is bounded from above by the entanglement entropy,

$$E_P(A : B) \leq \min\{S_A, S_B\}. \tag{3.10}$$

This inequality directly follows from the definition (3.5) by choosing an extremal purification $|\psi\rangle_{AA'BB'} = |\psi'\rangle_{AA'B} \otimes |\phi\rangle_{B'}$ for S_B, and also for S_A. It gives an upper bound on the entanglement of purification.

(Va) This quantity is bounded from below by a half of mutual information,

$$E_P(A:B) \geq \frac{I(A:B)}{2}. \tag{3.11}$$

(Vb) For any tripartite state ρ_{ABC}, this quantity is bounded from below as

$$E_P(A:BC) \geq \frac{I(A:B) + I(A:C)}{2}. \tag{3.12}$$

These follows from the second expression of the entanglement of purification (3.6), the monotonicity of mutual information, and the saturation of the monogamy of the mutual information on arbitrary tripartite pure states.

(VI) For any tripartite pure state $|\psi\rangle_{ABC}$, this quantity is polygamous,

$$E_P(A:BC) \leq E_P(A:B) + E_P(A:C). \tag{3.13}$$

This polygamous property is in contrast to the monogamy of the squashed entanglement, while the latter is a genuine entanglement measure.

(VIIa) For a class of states saturating the subadditivity, this quantity returns to the entanglement entropy,

$$E_P(A:B) = S_A \text{ when } S_{AB} = S_B - S_A. \tag{3.14}$$

(VIIb) For a class of states saturating the strong subadditivity, this quantity returns to the entanglement entropy,

$$E_P(A:B) = S_A \text{ when } S_{AB} + S_{AC} = S_B + S_C. \tag{3.15}$$

These properties are a consequence of the more powerful theorem which completely determine the structure of quantum states of such classes. We will revisit this point in the subsection 5.3.5.

The listed properties above are not independent from each other. For instance, (VI) follows from (I) and (Va). Refer to [34, 90] for the proofs of these properties in general quantum systems.

3.1.2 The definition of the multipartite entanglement of purification

The multipartite generalization of the entanglement of purification is defined as follows. The key observation is the second form of the definition of the bipartite EOP (3.6). This clearly shows that the entanglement of purification is the minimized mutual information over the all possible purified systems. Thus we can employ a generalization of mutual information for multipartite systems in order to extend the EOP for multipartite cases.

The mutual information $I(A:B)$ has various multipartite generalizations. For example, we have the tripartite information (3.3) for tripartite systems based on Ven diagram, as mentioned before. However, we cannot use this quantity in this purpose, because the tripartite information trivially vanishes for any tripartite pure states.

Another generalization is called the total correlation $T(A_1:\cdots:A_n)$, defined on a n-partite state $\rho_{A_1\cdots A_n}$ upon the n-composite system $\mathcal{H}_{A_1}\otimes\mathcal{H}_{A_2}\otimes\cdots\otimes\mathcal{H}_{A_n}$, defined by

$$T(A_1:\cdots:A_n) := S(\rho_A||\rho_{A_1}\otimes\cdots\otimes\rho_{A_n}) \tag{3.16}$$

$$= \sum_{i=1}^{n} S_{A_i} - S_{A_1\cdots A_n}. \tag{3.17}$$

where $S(\rho||\sigma)=\mathrm{Tr}\rho(\log\rho-\log\sigma)$ is the relative entropy. This generalization is motivated by a particular form of mutual information based on the relative entropy between a given original state and the local product state $I(A:B)=S(\rho_{AB}||\rho_A\otimes\rho_B)$ [88, 89]. This quantity satisfies basic requirement for a good multipartite correlation measure, e.g. this is clearly positive semi-definite and is monotonic under strict local operations. Note that we can rewrite $T(A_1:\cdots:A_n)$ as a suggestive form, which is a summation of the bipartite mutual information:

$$T(A_1:\cdots:A_n) = I(A_1:A_2)+I(A_1A_2:A_3)+\cdots+I(A_1\cdots A_{n-1}:A_n). \tag{3.18}$$

.

We then define a generalization of entanglement of purification for a n-partite state $\rho_{A_1\cdots A_n}$ using the total correlation measure.

Definition 1. The multipartite entanglement of purification E_P on a n-partite quantum states $\rho_{A_1\cdots A_n}$ is defined by [5]

$$E_P(\rho_{A_1:\cdots:A_n}) := \frac{1}{2}\min_{|\psi\rangle_{A_1A_1'\cdots A_nA_n'}} T(A_1A_1':\cdots:A_nA_n') \tag{3.19}$$

$$= \frac{1}{2}\min_{|\psi\rangle_{A_1A_1'\cdots A_nA_n'}} \sum_{i=1}^{n} S_{A_iA_i'}, \tag{3.20}$$

where the minimization is taken over all possible purifications of $\rho_{A_1\cdots A_n}$.

[5] The normalization factor is unessential in the following discussion. We omitted the half factor in the paper [60], in order to keep the inequalities simple. In this thesis we follow the convention in [63]. Remark that a multipartite factor $1/2$, but not $1/n$, sometimes has an operational background [91].

We usually denote $E_P(\rho_{A_1:\cdots:A_n})$ by $E_P(A_1:\cdots:A_n)$ briefly to keep the expression concise, unless the state under consideration must be specified. The fact that the entanglement entropy always vanishes for pure states was used to derive the second line. This expression indicate that the multipartite entanglement of purification is the (half of the) minimum value of the sum of bipartite entanglement between each of n-parties and the other $n-1$ parts in the purified systems. We note that the optimal purification that gives the minimal value in (3.5) can be non-unique in general. This is the same as in the case of the bipartite entanglement of purification.

In particular, the tripartite case is represented by

$$E_P(A:B:C) = \frac{1}{2} \min_{|\psi\rangle_{AA'BB'CC'}} [S_{AA'} + S_{BB'} + S_{CC'}]. \tag{3.21}$$

The entanglement entropies $S_{AA'}$, $S_{BB'}$, and $S_{CC'}$ characterize an amount of quantum entanglement between $AA' : BB'CC'$, $BB' : AA'CC'$, and $CC' : AA'BB'$, respectively. This is usually enough to prove a property of the multipartite entanglement of purification for this tripartite case, because its n-partite generalization follows easily from the 3-partite case.

3.1.3 The properties of the multipartite entanglement of purification

We explore the information-theoretic properties of E_P in generic quantum systems.

First, the following reduction property follows from the definition.

Lemma 2. *If one of the n-partite subsystems is totally decoupled* $\rho_{A_1\cdots A_n} = \rho_{A_1\cdots A_{n-1}} \otimes \rho_{A_n}$, *then the reduction holds*

$$E_P(A_1:\cdots:A_{n-1}:A_n) = E_P(A_1:\cdots:A_{n-1}). \tag{3.22}$$

Proof. The decoupled part can be separately purified apart from the remaining parts, like $\langle\psi\rangle_{A_1A_1'\cdots A_nA_n'} = |\psi'\rangle_{A_1A_1'\cdots A_{n-1}A_{n-1}'} \otimes |\phi\rangle_{A_nA_n'}$. This type of purifications guarantees $E_P(A_1:\cdots:A_{n-1}:A_n) \leq E_P(A_1:\cdots:A_{n-1})$ for this state. The opposite inequality $E_P(A_1:\cdots:A_{n-1}:A_n) \geq E_P(A_1:\cdots:A_{n-1})$ is inherited from the same property of the total correlation $T(A_1:\cdots:A_{n-1}:A_n) \geq T(A_1:\cdots:A_{n-1})$ on any states. □

This property means that the correlation measured by E_P is never disturbed by any uncorrelated systems.

Next, since we require E_P to be a natural generalization of the bipartite case, the similar properties suitably adjusted to the multipartite systems must hold. Indeed, one can prove the following properties which are the counterparts of those of the bipartite ones mentioned above.

Proposition 3. *If a given n-partite state is pure* $\rho_{A_1\cdots A_n} = |\phi\rangle\langle\phi|_{A_1\cdots A_n}$*, then the multipartite entanglement of purification is given by just the summation of entanglement entropy of each single subsystem,*

$$E_P(A_1 : \cdots : A_n) = \frac{1}{2}\sum_{i=1}^{n} S_{A_i}. \tag{3.23}$$

Proof. Notice that the original state $|\phi\rangle_{A_1\cdots A_n}$ itself is nothing but a purification which gives (3.23). The fact that any additional ancillary system always increases the sum of the entanglement entropy follows from that the any other purifications must have a form $|\psi\rangle_{A_1A_1'\cdots A_nA_n'} = |\phi\rangle_{A_1\cdots A_n} \otimes |\phi'\rangle_{A_1'\cdots A_{n'}'}$. □

This is a generalization of the property (I). Thus calculating E_P for pure states is trivial. Note that the total correlation also reduces to just the sum of entanglement entropy for pure states:

$$T(A_1 : \cdots : A_n) = \sum_{i=1}^{n} S_{A_i} - S_{A_1\cdots A_n} = \sum_{i=1}^{n} S_{A_i}. \tag{3.24}$$

Thus they essentially coincide with each other $E_P = \frac{1}{2}T$ on any pure multipartite states.

Proposition 4. E_P *vanishes if and only if a given n-partite state is a fully product state,*

$$E_P(A_1 : \cdots : A_n) = 0 \Leftrightarrow \rho_{A_1\cdots A_n} = \rho_{A_1} \otimes \cdots \otimes \rho_{A_n}. \tag{3.25}$$

Though this proposition can also be directly proven from the definition of E_P, we postpone the proof after the proposition (7). This property indicates that E_P can be positive not only for entangled states but also for non-separable states. This means that E_P is not a genuine measure of quantum entanglement, but a measure of both quantum and classical correlations. This property is expected as the bipartite case also a measure of quantum and classical correlation, not only of entanglement.

It is natural to expect E_P to always decrease when a part of the subsystems is traced out. This is actually true as we can see in the following proposition.

Proposition 5. E_P *monotonically decreases upon discarding ancilla systems,*

$$E_P(XA_1 : \cdots : A_n) \geq E_P(A_1 : \cdots : A_n). \tag{3.26}$$

Proof. This inequality follows from the simple fact that any purification of the larger system is also a purification of the smaller system. Namely, suppose that $|\psi\rangle_{XX'A_1A_1'\cdots A_nA_n'}$ is an optimal purification of $\rho_{XA_1\cdots A_n}$, then this state is also a (presumably non-optimal)

purification of $\rho_{A_1\cdots A_n}$. Thus the minimization of the smaller system does search strictly wider region than that of the larger system, and we have

$$\begin{aligned} E_P(XA_1:\cdots:A_n) &= \frac{1}{2}(S_{A_1X(A_1'X')} + S_{A_2A_2'} + \cdots + S_{A_nA_n'}) \\ &\geq \frac{1}{2}\min_{|\psi\rangle_{A_1A_1'\cdots A_nA_n'}} (S_{A_1(A_1'XX')} + S_{A_2A_2'} + \cdots + S_{A_nA_n'}) \\ &= E_P(A_1:\cdots:A_n). \end{aligned} \tag{3.27}$$

□

This property also guarantees that the E_P is monotonically non-increasing under strict local operations [29].

Now we provide an upper bound on E_P in terms of a sum of the entanglement entropy, as a generalization of the property (IV).

Proposition 6. *E_P is bounded from above by*

$$E_P(A_1:\cdots:A_n) \leq \frac{1}{2}\min_i[S_{A_1} + \cdots + S_{A_1\cdots A_{i-1}A_{i+1}\cdots A_i} + \cdots + S_{A_n}]. \tag{3.28}$$

Proof. We will prove this bound for tripartite state ρ_{ABC} for simplicity. The generalization to n-partite systems is straightforward. Let us consider a standard purification of a given state $\rho_{ABC} = \sum p_k |\phi^k\rangle\langle\phi^k|_{ABC}$ such that

$$|\psi\rangle_{AA'BB'CC'} = \sum_{k=1}^{\mathrm{rank}[\rho_{ABC}]} \sqrt{p_k}\,|\phi^k\rangle_{ABC} \otimes |0\rangle_{A'} \otimes |0\rangle_{B'} \otimes |k\rangle_{C'}\,. \tag{3.29}$$

On this purification any information of the original system is pushed into the ancilla C'. The definition leads to $2E_P(A:B:C) \leq S_{AA'} + S_{BB'} + S_{CC'}$ on this state. Note that $\rho_{AA'} = \rho_A \otimes |0\rangle\langle 0|_{A'}$, as well as the same for B, and $S_{CC'} = S_{AA'BB'}$ for this purification (3.29). Then it can be shown that

$$S_{AA'} = S_A,\ S_{BB'} = S_B,\ S_{CC'} = S_{AB}, \tag{3.30}$$

Thus we get

$$2E_P(A:B:C) \leq S_A + S_B + S_{AB}. \tag{3.31}$$

The three upper bounds on E_P follows by commuting A, B, C, and thus

$$E_P(A:B:C) \leq \frac{1}{2}\min\{S_A + S_B + S_{AB}, S_B + S_C + S_{BC}, S_C + S_A + S_{CA}\}. \tag{3.32}$$

□

The procedure of the proof and the results implies that the upper bound of $E_P(A:B:C)$ is totally determined by the information included in the reduced density matrix ρ_{AB}. In other words, the multipartite correlation can not be arbitrarily increased by adding ancillary systems which is compatible with the original system. This upper bounds can be obviously reached by a pure state $|\psi\rangle_{ABC}$, though this is not only the case as we will see in the corollary 10 and 11.

We now show a lower bound on E_P follows from the definition.

Proposition 7. *The n-partite entanglement of purification is bounded from below by*

$$E_P(A_1:\cdots:A_n) \geq \frac{1}{2}T(A_1:\cdots:A_n). \tag{3.33}$$

Proof. This is the direct consequence of the monotonicity of the total correlation:

$$E_P(\rho_{A_1:\cdots:A_n}) \coloneqq \frac{1}{2}\min_{|\psi\rangle_{A_1A_1'\cdots A_nA_n'}} T(A_1A_1':\cdots:A_nA_n') \tag{3.34}$$

$$\geq \frac{1}{2}\min_{|\psi\rangle_{A_1A_1'\cdots A_nA_n'}} T(A_1:\cdots:A_n) \tag{3.35}$$

$$= \frac{1}{2}T(A_1:\cdots:A_n). \tag{3.36}$$

where we used the property of the total correlation on generic states

$$T(A_1X:\cdots:A_n) \geq T(A_1:\cdots:A_n). \tag{3.37}$$

□

This is a generalization of the property (Va). It provides a generic order between two multipartite measure of correlation. It is worth to point out that E_P and T behave very similarly. The propositions 2, 3, 4, 5, and 6 are also true for the total correlation.

This proposition 7 also gives a easy proof of the proposition 4:

Proof. Suppose that a given n-partite state is totally product $\rho_{A_1\cdots A_n} = \rho_{A_1}\otimes\cdots\otimes\rho_{A_n}$. Then the absolute minimum $E_P = 0$ is easily reachable by a purification on which the each subsystem is purified independently.

On the other hand, $E_P(A_1:\cdots:A_n) = 0$ leads to $T(A_1:\cdots:A_n) = S(\rho_{A_1\cdots A_n}||\rho_{A_1}\otimes\cdots\otimes\rho_{A_n}) = 0$ from the proposition 7. Then the non-degeneracy of the relative entropy implies $\rho_{A_1\cdots A_n} = \rho_{A_1}\otimes\cdots\otimes\rho_{A_n}$. □

We also provide another lower bound on E_P in terms of the sum of the bipartite entanglement of purification.

Proposition 8. *E_P is bounded from below by*

$$2E_P(A_1 : \cdots : A_n) \geq \sum_{i=1}^{n} E_P(A_i : A_1 \cdots A_{i-1}A_{i+1} \cdots A_n). \tag{3.38}$$

Proof. We prove this inequality in tripartite cases for simplicity. For a given state ρ_{ABC}, we have

$$\begin{aligned} 2E_P(A : B : C) &= \min_{|\psi\rangle_{AA'BB'CC'}} [S_{AA'} + S_{BB'} + S_{CC'}] \\ &\geq \min_{|\psi\rangle_{AA'BB'CC'}} S_{AA'} + \min_{|\psi\rangle_{AA'BB'CC'}} S_{BB'} + \min_{|\psi\rangle_{AA'BB'CC'}} S_{CC'} \\ &= E_P(A : BC) + E_P(B : CA) + E_P(C : AB), \end{aligned} \tag{3.39}$$

then the bound follows. □

There are several properties of E_P follow from the above arguments as corollaries.

Corollary 9. *For any pure n-partite state, E_P is polygamous:*

$$E_P(A_1 : \cdots : A_{n-1} : BC) \leq E_P(A_1 : \cdots : A_{n-1} : B) + E_P(A_1 : \cdots : A_{n-1} : C). \tag{3.40}$$

Proof. For a pure state $|\phi\rangle_{A_1 \cdots A_n BC}$, the proposition 3 leads to

$$\begin{aligned} 2E_P(A_1 : \cdots : A_{n-1} : BC) &= \sum_{i=1}^{n-1} S_{A_i} + S_{BC} = \sum_{i=1}^{n-1} S_{A_i} + S_{A_1 \cdots A_{n-1}} \\ &\leq 2\sum_{i=1}^{n-1} S_{A_i} \\ &= \sum_{i=1}^{n-1} S_{A_i} + S_B - S_{A_1 \cdots A_{n-1}B} + \sum_{i=1}^{n-1} S_{A_i} + S_C - S_{A_1 \cdots A_{n-1}C} \\ &\leq 2E_P(A_1 : \cdots : A_{n-1} : B) + 2E_P(A_1 : \cdots : A_n : C), \end{aligned} \tag{3.41}$$

where the subadditivity of the von Neumann entropy is recursively used in the first inequality, as well as the proposition 7 is in the last inequality. □

The following shows that there is a class of quantum states for which one can rigorously compute E_P especially for tripartite systems:

Corollary 10. *For a class of tripartite states ρ_{ABC} that saturate the subadditivity $S_{ABC} = S_C - S_{AB}$, we have*

$$E_P(A : B : C) = \frac{1}{2}(S_A + S_B + S_{AB}). \tag{3.42}$$

.

Proof. The proposition 6 and 7 indicate a sandwich inequality

$$S_A + S_B + S_C - S_{ABC} \leq 2E_P(A:B:C) \leq S_A + S_B + S_{AB}. \tag{3.43}$$

Then the saturation $S_C - S_{ABC} = S_{AB}$ immediately leads to $2E_P(A:B:C) = S_A + S_B + S_{AB}$. □

Corollary 11. *For a class of tripartite states ρ_{ABC} that saturate both of the two forms of the strong subadditivity, $S_A + S_C = S_{AB} + S_{BC}$ and $S_B + S_C = S_{AB} + S_{AC}$, we have*

$$E_P(A:B:C) = \frac{1}{2}(S_A + S_B + S_{AB}). \tag{3.44}$$

Proof. The proposition 6 and 7 mean

$$2(S_A + S_B + S_C) - S_{AB} - S_{BC} - S_{CA} \leq 2E_P(A:B:C) \leq S_A + S_B + S_{AB}. \tag{3.45}$$

Note that the lower side can be deformed as

$$\begin{aligned} &2(S_A + S_B + S_C) - S_{AB} - S_{BC} - S_{CA} \\ =&S_A + S_B + S_{AB} + (S_A + S_C - S_{AB} - S_{BC}) + (S_B + S_C - S_{AB} - S_{AC}). \end{aligned} \tag{3.46}$$

Thus when the two types of the strong subadditivity are simultaneously saturated, we have $2E_P(A:B:C) = S_A + S_B + S_{AB}$. □

Remark that another way of generalization of (Va) was shown in [60] for tripartite states ρ_{ABC}. The result has a form

$$E_P(A:B:C) \geq \frac{1}{2}(T(A:B:C) + I_3(A:B:C)) \tag{3.47}$$

$$= \frac{1}{2}(I(A:B) + I(B:C) + I(C:A)). \tag{3.48}$$

This expression can also be generalized to n-partite system as discussed below.

3.1.4 Upper bounds on the other multipartite correlation measures

There are various measures of correlations that quantify multipartite correlations for mixed states, reflecting to the diversity of multipartite correlations (see [68] also in this context in holography). An approach is the total correlation T as we have discussed. Another generalization of the mutual information is the dual total correlation

$$D(A_1:\cdots:A_n) := S_{A_1\cdots A_n} - \sum_{i=1}^{n} S(A_i|A_1\cdot\overset{i}{\check{}}\cdot A_n) \tag{3.49}$$

$$\begin{aligned} &= I(A_1 : A_2\cdots A_n) + I(A_2 : A_3\cdots A_n|A_1) \\ &+ \cdots + I(A_{n-1} : A_n|A_1\cdots A_{n-2}), \end{aligned} \tag{3.50}$$

where $S(A|B) = S_{AB} - S_B$ is the conditional entropy, and $\cdots^{\overset{i}{\check{}}}\cdots$ denotes the exclusion of A_i. The D also possesses a good nature as a correlation measure. Namely, this quantity monotonically non-increases under strict local operations, vanishes if and only if the state is totally decoupled, and $D = \sum_{i=1}^n S_{A_i}$ holds for pure states.

We now introduce two non-negative information X, Y for three- or more-partite systems:

$$X(A_1 : \cdots : A_n) := \frac{(n-1)T(A_1 : \cdots : A_n) - D(A_1 : \cdots : A_n)}{n-2} \quad (n \geq 3), \tag{3.51}$$

$$Y(A_1 : \cdots : A_n) := \frac{(n-1)D(A_1 : \cdots : A_n) - T(A_1 : \cdots : A_n)}{n-2} \quad (n \geq 3). \tag{3.52}$$

They are positive semi-definite as it is clear from the following expressions,

$$X(A_1 : \cdots : A_n) = \frac{1}{n-2} \sum_{i=1}^n T(A_1 : \cdots^{\overset{i}{\check{}}}\cdots : A_n), \tag{3.53}$$

$$Y(A_1 : \cdots : A_n) = \frac{1}{n-2} \sum_{i=1}^n D(A_1 : \cdots^{\overset{i}{\check{}}}\cdots : A_n|A_i), \tag{3.54}$$

where

$$\begin{aligned} &D(A_1 : \cdots : A_n|E) \\ &\quad = I(A_1 : A_2 \cdots A_n|E) + I(A_2 : A_3 \cdots A_n|A_1E) + \cdots + I(A_{n-1} : A_n|A_1 \cdots A_{n-2}E), \end{aligned} \tag{3.55}$$

is the conditional dual total correlation. They are normalized so that

$$X(A_1 : \cdots : A_n) = Y(A_1 : \cdots : A_n) = \sum_{i=1}^n S_{A_i}, \tag{3.56}$$

holds on any pure states. The X is a generalization of the right hand side of (3.47).

The X is monotonically non-increasing under strict local operations as is clear from (3.53), while the Y is not necessarily. Moreover, both X and Y are not faithful: there exists a correlated state $\rho_A \neq \rho_{A_1} \otimes \cdots \otimes \rho_{A_n}$ whose X (or Y) vanishes. There is a balancing relation between these information,

$$T(A_1 : \cdots : A_n) + D(A_1 : \cdots : A_n) = X(A_1 : \cdots : A_n) + Y(A_1 : \cdots : A_n) \tag{3.57}$$

$$= \sum_{i=1}^n T(A_1 : \cdots^{\overset{i}{\check{}}}\cdots : A_n). \tag{3.58}$$

The multipartite entanglement of purification gives upper bounds on these information, generalizing the proposition 7 and (3.47). The statement can be generically expressed as follows:

Proposition 12. *Suppose an entropic measure $\Theta(A_1 : \cdots : A_n)$ defined on n-partite system satisfies (i) $\Theta(A_1 : \cdots : A_n) = \sum_{i=1}^{n} S_{A_i}$ for pure n-partite states, (ii) is non-increasing under strict local operations. Then*

$$E_P(A_1 : \cdots : A_n) \geq \frac{1}{2}\Theta(A_1 : \cdots : A_n). \tag{3.59}$$

The proof is totally the same as that of the proposition 7, because the monotonicity and the non-increasing property under strict local operations are equivalent on this class of measures [29].

The T, D, and X satisfy the both conditions of the proposition, while Y does not satisfy the condition (ii). Thus, the following three inequalities hold:

$$E_P(A_1 : \cdots : A_n) \geq \frac{1}{2}T(A_1 : \cdots : A_n). \tag{3.60}$$

$$E_P(A_1 : \cdots : A_n) \geq \frac{1}{2}D(A_1 : \cdots : A_n). \tag{3.61}$$

$$E_P(A_1 : \cdots : A_n) \geq \frac{1}{2}X(A_1 : \cdots : A_n). \tag{3.62}$$

The third inequality is nothing but a generalization of (3.47) for n-partite systems.

These three inequalities generically give independent lower bounds on the E_P. However, if the monogamy of mutual information holds for any partition on a state, e.g. in the case of geometric states, the ordering of them holds

$$X(A_1 : \cdots : A_n) \leq T(A_1 : \cdots : A_n) \leq D(A_1 : \cdots : A_n) \leq Y(A_1 : \cdots : A_n). \tag{3.63}$$

First, the middle inequality $T(A_1 : \cdots : A_n) \leq D(A_1 : \cdots : A_n)$ follows by the assumption of the monogamy $I(A : B|C) \geq I(A : B)$,

$$\begin{aligned}
&D(A_1 : \cdots : A_n) \\
&= I(A_1 : A_2 \cdots A_n) + I(A_2 : A_3 \cdots A_n|A_1) \\
&\quad + \cdots + I(A_{n-1} : A_n|A_1 \cdots A_{n-2}) \\
&\geq I(A_1 : A_2 \cdots A_n) + I(A_2 : A_3 \cdots A_n) \\
&\quad + \cdots + I(A_{n-1} : A_n) \\
&= T(A_1 : \cdots : A_n).
\end{aligned} \tag{3.64}$$

Given this fact, the remaining inequalities are obvious by

$$X(A_1 : \cdots : A_n) = T(A_1 : \cdots : A_n) - \frac{D(A_1 : \cdots : A_n) - T(A_1 : \cdots : A_n)}{n-2}, \tag{3.65}$$

$$Y(A_1 : \cdots : A_n) = D(A_1 : \cdots : A_n) + \frac{D(A_1 : \cdots : A_n) - T(A_1 : \cdots : A_n)}{n-2}. \tag{3.66}$$

3.2 The multipartite entanglement wedge cross section

We now return to the holographic world. Our aim is to find a geometrical object which appropriately captures multipartite correlations flowing in geometric states. Here we define a multipartite generalization of the entanglement wedge cross-section. The formulation is inspired by the tensor network description of the AdS/CFT correspondence [73, 74, 62].

3.2.1 The definition of the multipartite entanglement wedge cross section

Let us start to give a formal definition of the multipartite generalization of the entanglement wedge cross section. We mostly focus on the tripartite case i.e. there are three subsystems A, B, C, for simplicity. The generalization to the n-partite cases is straightforward.

First, take the subsystems A, B and C on the boundary. The reduced density matrix ρ_{ABC} is typically mixed. The holographic entanglement entropy S_A, S_B, S_C, and S_{ABC} can be computed following the Ryu-Takayanagi formula. The corresponding Ryu-Takayanagi surfaces are denoted by $\gamma_A^{\min}$, $\gamma_B^{\min}$, $\gamma_C^{\min}$, $\gamma_{ABC}^{\min}$, respectively. The entanglement wedge $\mathcal{M}_{ABC}$ is defined as a inner region of M [6] with the boundary A, B, C, and $\gamma_{ABC}^{\min}$:

$$\partial\mathcal{M}_{ABC} = A \cup B \cup C \cup \gamma_{ABC}^{\min}. \tag{3.67}$$

Notice that $\mathcal{M}_{ABC}$ is possibly disconnected if some of the subsystems A, B, C are totally decoupled. The boundary $\partial\mathcal{M}_{ABC}$ may include the bifurcation surfaces, not only the AdS boundary, in the AdS black hole geometry.

Next, divide the boundary $\partial\mathcal{M}_{ABC}$ – not the entanglement wedge $\mathcal{M}_{ABC}$ itself – into three pieces $\widetilde{A}, \widetilde{B}, \widetilde{C}$ so that

$$\widetilde{A} \cup \widetilde{B} \cup \widetilde{C} = \partial\mathcal{M}_{ABC}, \tag{3.68}$$

and

$$A \subset \widetilde{A}\ , B \subset \widetilde{B}\ , C \subset \widetilde{C}. \tag{3.69}$$

The boundary of $\widetilde{A}, \widetilde{B}, \widetilde{C}$ is denoted by $\mathcal{D}_{ABC}$. Now regarding the $\widetilde{A}, \widetilde{B}, \widetilde{C}$ as the subsystems on the new boundary inside the bulk, the sum of their entanglement entropies

$$S_{\widetilde{A}} + S_{\widetilde{B}} + S_{\widetilde{C}}, \tag{3.70}$$

are formally defined by using the Ryu-Takayanagi formula. This procedure is performed by finding a minimal surface Σ_{ABC}^{min} that consists of three parts Σ_A, Σ_B, Σ_C such that

$$\Sigma_{ABC}^{min} = \Sigma_A \cup \Sigma_B \cup \Sigma_C\ , \quad \partial\Sigma_{ABC}^{min} = \mathcal{D}_{ABC}, \tag{3.71}$$

[6] Precisely speaking, we are talking about a constant time slice of the entanglement wedge with an abuse of terminology. The former is codimension-1, and the latter is codimension-0 object.

and

$$\Sigma_{A,B,C} \text{ is homologous to } \widetilde{A}, \widetilde{B}, \widetilde{C} \text{ inside } M_{ABC}. \tag{3.72}$$

The $\partial\mathcal{M}_{ABC}$ is codimention-2, and thus the surfaces $\mathcal{D}_{ABC}$ is codimension-3.

Finally, minimize the area of Σ^{min}_{ABC} over all possible divisions $\widetilde{A}, \widetilde{B}, \widetilde{C}$ that satisfy the requirements (3.68) and (3.69). This minimum value (with a 1/2 prefactor) is the multipartite entanglement wedge cross section:

$$E_W(\rho_{ABC}) := \frac{1}{2} \min_{\widetilde{A},\widetilde{B},\widetilde{C}} \left[\frac{\text{Area}(\Sigma^{min}_{ABC})}{4G_N} \right]. \tag{3.73}$$

Examples in the case of $\text{AdS}_3/\text{CFT}_2$ are found in the Fig 3.2, 3.3.

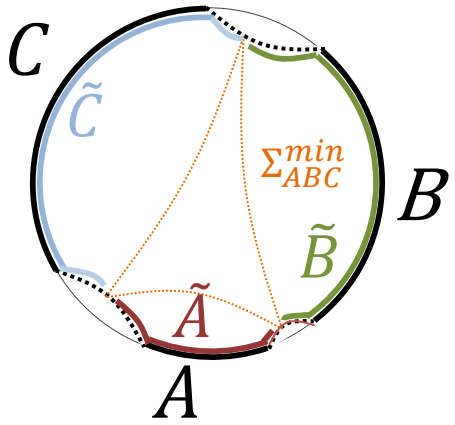

Figure 3.2: The tripartite entanglement wedge cross section. The black bold dashed lines represents the minimal surface $\gamma^{\text{min}}_{ABC}$, providing a part of the boundary of the entanglement wedge $\mathcal{M}_{ABC}$. The yellow thin dashed lines represents the codimension-2 surface Σ^{min}_{ABC}, whose area (divided by $8G_N$) is the E_W. (The figure is cited from [60])

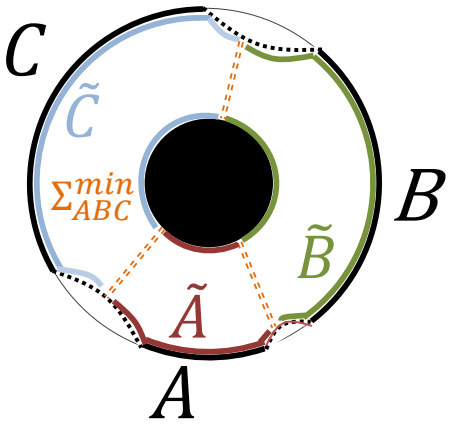

Figure 3.3: The tripartite entanglement wedge cross section in the AdS black hole geometry. Following the definition, each codimension-2 surface of Σ_{ABC}^{min} is doubly degenerated. (The figure is cited from [60])

The multipartite entanglement wedge cross section for n-partite systems is defined in the same manner. For the bipartite case $n = 2$, this definition is nothing but that of the bipartite entanglement wedge cross section. We usually write $E_W(\rho_{ABC}) = E_W(A : B : C)$ briefly whenever the target state is obvious from the context.

This quantity is expected to capture multipartite correlations in holography, as a generalization of the bipartite entanglement wedge cross section. We show several properties of E_W which assures this expectation below.

3.2.2 Properties of the multipartite entanglement wedge cross section

In the following, we study the holographic properties of E_W. Most of them are inspired by those of E_P. We mostly deal with the tripartite case for simplicity, but the properties are easily generalized to n-partite cases.

First, if ρ_{ABC} is a pure state, Σ_{ABC}^{min} coincides with $\gamma_A^{\min} \cup \gamma_B^{\min} \cup \gamma_C^{\min}$ by definition (3.71). Therefore E_W equals to the sum of the entanglement entropy of A, B and C in this case:

$$E_W(A : B : C) = \frac{1}{2}(S_A + S_B + S_C). \tag{3.74}$$

For a partly decoupled entanglement wedge e.g. $\mathcal{M}_{ABC} = \mathcal{M}_{AB} \bigsqcup \mathcal{M}_C$ (where $\bigsqcup$ denote a sum of the totally separated geometries), the $E_W(A : B : C)$ reduces to the bipartite entanglement wedge cross section $E_W(A : B)$. This leads the fact that $E_W = 0$ if and only if the entire entanglement wedge is totally decoupled $\mathcal{M}_{A_1 \cdots A_n} = \bigsqcup_{i=1}^{n} \mathcal{M}_{A_n}$

for multipartite setups.

The E_W decreases when we reduce the size of one of the sub-regions:

$$E_W(A \cup X : B : C) \geq E_W(A : B : C). \tag{3.75}$$

This property follows from the famous entanglement wedge nesting,

$$\mathcal{M}_X \subset \mathcal{M}_{XY}, \tag{3.76}$$

for any boundary sub-regions $X,\ Y$ [71, 70, 72].

An upper bound of E_W follows by a graph proof (Fig.3.4) (or obviously from the fact that the entanglement entropies are UV divergent while E_W is usually finite):

$$E_W(A : B : C) \leq \frac{1}{2}(S_A + S_B + S_{AB}), \tag{3.77}$$

Commuting A, B, C, we get

$$E_W(A : B : C) \leq \frac{1}{2}\min[S_A + S_B + S_{AB}, S_B + S_C + S_{BC}, S_A + S_C + S_{AC}]. \tag{3.78}$$

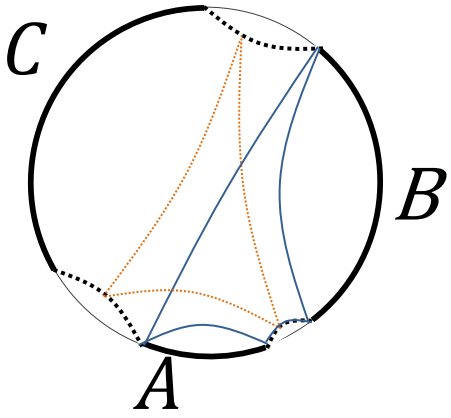

Figure 3.4: The proof of an upper bound of E_W by the entanglement entropies. The sum of blue lines is $S_A + S_B + S_{AB}$, and the sum of dashed yellow lines are $2E_W(A : B : C)$. Clearly $2E_W(\rho_{ABC}) \leq S_A + S_B + S_{AB}$ holds even if E_W has a UV divergence when two of the subsystems are adjacent, as shown the graph and the minimal property of the each surface. (The figure is cited from [60])

Furthermore, the lower bounds of E_P also can be shown for E_W by the graph proofs. For example, the bound by $T(A:B:C)$ and $X(A:B:C)$

$$2E_W(A:B:C) \geq T(A:B:C) = S_A + S_B + S_C - S_{ABC}, \tag{3.79}$$

$$2E_W(A:B:C) \geq X(A:B:C) = 2(S_A + S_B + S_C) - S_{AB} - S_{BC} - S_{AC}, \tag{3.80}$$

are shown in Fig.3.5 and Fig.3.6. In holography, we always have $T(A:B:C) \geq X(A:B:C)$ as mentioned before, thus the former is always tighter. Similarly, the bound by D and the n-partite generalization can also be shown by drawing a graph.

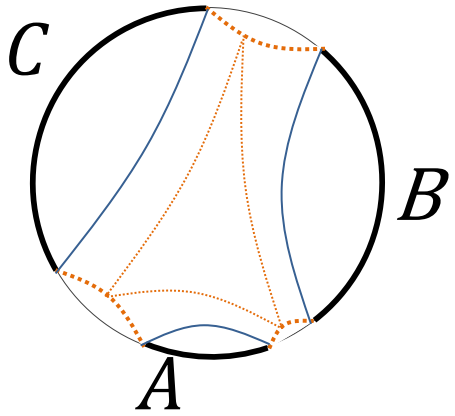

Figure 3.5: The proof of the lower bound of E_W by T. The sum of the dashed yellow lines is $2E_W(A:B:C) + S_{ABC}$, and the sum of the real blue lines are $S_A + S_B + S_C$. The inequality $2E_W(\rho_{ABC}) + S_{ABC} \geq S_A + S_B + S_C$ follows due to the minimality of the surfaces. (The figure is cited from [60])

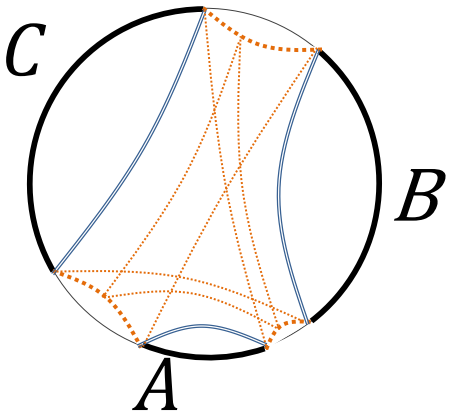

Figure 3.6: The proof of the lower bound of E_W by X. The sum of the dashed yellow lines is $2E_W(A:B:C)+S_{AB}+S_{BC}+S_{CA}$, and the sum of the real doubled blue lines is $2(S_A+S_B+S_C)$. The inequality $2E_W+S_{AB}+S_{BC}+S_{CA}\geq 2(S_A+S_B+S_C)$ follows due to the minimality of the surfaces. (The figure is cited from [60])

Note that the corollaries in the previous section follows also for E_W automatically, while they can also be shown by drawing a graph. The proposition 8 for E_W can also be easily shown graphically.

Conjecture

The above properties are the multipartite generalization of the properties of the bipartite entanglement wedge cross section. The coincidence of the properties of E_W and E_P tempt us to propose a conjecture: the multipartite entanglement wedge cross section E_W is holographically dual to the multipartite entanglement of purification E_P at the leading order $O(N^2)$:

$$E_W = E_P. \tag{3.81}$$

3.2.3 Computations of the multipartite entanglement wedge cross section

In the pure AdS_3

Unlike the entanglement of purification, the E_W is computable as a purely geometrical objects. We compute E_W in the AdS_3/CFT_2 setup. We work in the Poincaré patch with the ground state of a CFT_2 on an infinite line, which is described by the bulk metric

$$ds^2=\frac{dx^2+dz^2}{z^2},\quad x\in(-\infty,+\infty), z\in[0,+\infty). \tag{3.82}$$

We choose the three subsystems A, B, C as the intervals $A = [-b, -a-r]$, $B = [-a+r, a-r]$, $C = [a+r, b]$ where $b > a > 0$. Here r is relatively small compared to the a and b. We assume that the entanglement wedge of ABC is connected as shown in Fig.3.7. Following the definition of E_W, we need to find a triangle-like connected geodesics with the minimal length. The ending points of the geodesics (the corner of the triangle) must be located on the semi-circles in Fig.3.7. The reasonable minimal configuration should also keep the reflection symmetry of the original system $x \to -x$. This reduces the program to find a special angle θ^* whose the sum of length of the geodesics is minimal. Formally, the entanglement wedge cross section is given by

$$E_W(A:B:C) = \frac{1}{2} \min_{\theta} \left[\frac{L(\theta)}{4G_N} \right]. \tag{3.83}$$

Because a compact formula of the length L as a function of a, b, r and θ is rather complicated, we instead show numerical θ dependence of L as plotted in Fig.3.8, and evaluate the special values of both θ and L satisfying the minimal length condition for a given a, b, r. Note that the properties of E_W studied before can be easily checked in this particular setup.

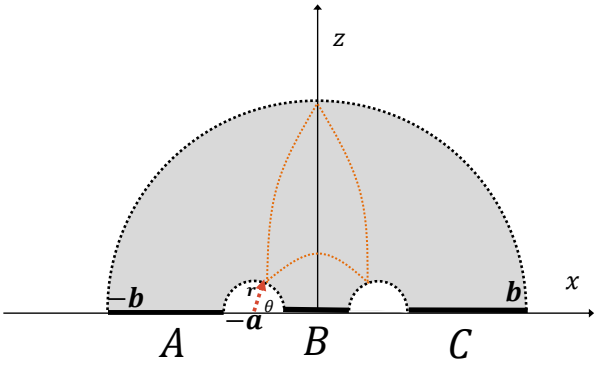

Figure 3.7: The computation of E_W in a setup in the pure AdS_3. (The figure is cited from [60])

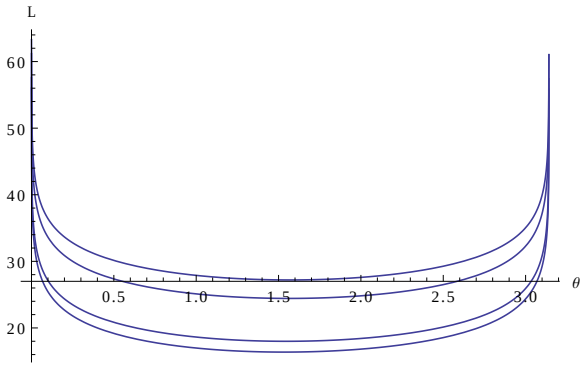

Figure 3.8: $L - \theta$ plot in the computation of E_W with different parameters. From top to bottom, the parameters of (a, b, r) are $(10, 100, 0.05), (10, 100, 0.1), (10, 100, 0.5), (10, 100, 0.75)$. $E_W * 8G_N$ and the the optimal value of θ are $(27.2046, \theta \to 1.56818)$ $(24.432, \theta \to 1.5657), (17.9942, \theta \to 1.54531), (16.3723, \theta \to 1.53255)$, respectively.

In the BTZ black hole

Now we discuss the BTZ black hole. A planar BTZ black hole describes a 2d CFT on an infinite line at finite temperature. The metric of a fixed time slice of the BTZ black hole is given by

$$ds^2 = \frac{1}{z^2}\left(\frac{dz^2}{f(z)} + dx^2\right), \quad f(z) = 1 - \frac{z^2}{z_H^2}, \tag{3.84}$$

where the inverse temperature is related to the horizon by $\beta = 2\pi z_H$.

We choose the three subsystems A, B, C as the intervals $[-\ell, 0]$, $[0, \ell]$, and the remaining of the infinite line, respectively.

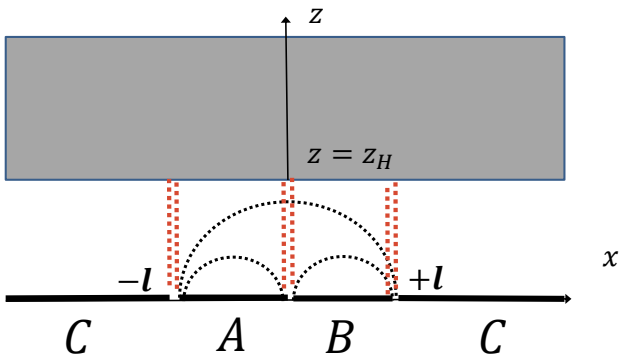

Figure 3.9: The computation of E_W in a setup in the BTZ black hole. (The figure is cited from [60])

As studied in [32], the geodesic length between the boundary and the horizon is given by

$$L_1 = \log \frac{\beta}{\pi\epsilon}, \tag{3.85}$$

where ϵ is the UV cutoff. The geodesic length between two points $(-\ell, 0)$ and $(0, 0)$ is

$$L_2 = 2 \log \frac{\beta \sinh(\pi\ell/\beta)}{\pi\epsilon}, \tag{3.86}$$

and the geodesic length between two points $(-\ell, 0)$ and $(\ell, 0)$ is

$$L_3 = 2 \log \frac{\beta \sinh(2\pi\ell/\beta)}{\pi\epsilon}. \tag{3.87}$$

At high temperature, Σ^{min}_{ABC} consists of six short lines of length L_1. In this configuration, the tripartite entanglement wedge cross section is given by

$$2E_W = 6L_1 = 6 \log \frac{\beta}{\pi\epsilon} \equiv A^{(1)}. \tag{3.88}$$

At low temperature, Σ^{min}_{ABC} consists of three geodesic lines connecting $(-\ell, 0)$, $(0, 0)$ and $(\ell, 0)$, and so the E_W is given by

$$2E_W = 2L_2 + L_3 = 4 \log \frac{\beta \sinh(\pi\ell/\beta)}{\pi\epsilon} + 2 \log \frac{\beta \sinh(2\pi\ell/\beta)}{\pi\epsilon} \equiv A^{(2)}. \tag{3.89}$$

The tripartite entanglement wedge cross section E_W is thus given by the minimum of them

$$E_W(A:B:C) = \frac{1}{8G_N}\min\{A^{(1)}, A^{(2)}\}. \tag{3.90}$$

Comparing $A^{(1)}$ and $A^{(2)}$, the critical temperature is given by

$$\beta_c = \frac{\log\sqrt{y_+}}{\pi\ell}, \tag{3.91}$$

where y_+ is the positive root of

$$(y + y^{-1} - 2)(y - y^{-1}) = 8. \tag{3.92}$$

$A^{(1)}$ is favored for the high temperature $\beta < \beta_c$, and $A^{(2)}$ is for the low temperature $\beta > \beta_c$.

3.3 The multipartite squashed entanglement in holography

There are a lot of measure of genuine quantum entanglement. Here we would like to mention one of them, the squashed entanglement [92, 81], whose definition is based on the same spirit as that of the (multipartite) entanglement of purification. They belong to the class called optimized correlation measure, which will be discussed in the section 5 in detail.

3.3.1 The multipartite squashed entanglement

The squashed entanglement is a promising measure of quantum entanglement for mixed states. This quantity satisfies all the known desirable properties e.g. the additivity or the monogamy for generic states. The squashed entanglement is defined by

$$E_{sq}(\rho_{AB}) := \frac{1}{2}\min_{\rho_{ABE}} I(A:B|E), \tag{3.93}$$

where $I(A:B|E) = I(A:BE) - I(A:E) = S_{AE} + S_{BE} - S_{ABE} - S_E$ is the conditional mutual information, and the minimization is taken over all possible extensions $\rho_{AB} = \mathrm{Tr}_E[\rho_{ABE}]$. Taking E as a trivial extension immediately leads to the inequality:

$$E_{sq}(A:B) \leq \frac{1}{2}I(A:B). \tag{3.94}$$

The two types of multipartite generalization of E_{sq} were also introduced in [88, 89]. One of them is defined based on the conditional multipartite mutual information,

$$T(A_1:\cdots:A_n|E) = I(A_1:A_2|E) + I(A_1A_2:A_3|E) + \cdots + I(A_1\cdots A_{n-1}:A_n|E). \tag{3.95}$$

Namely, the (q-)multipartite squashed entanglement for n-partite state $\rho_{A_1\cdots A_n}$ is given by

$$E_{sq}(A_1:\cdots:A_n) := \frac{1}{2}\min_{\rho_{A_1\cdots A_nE}} T(A_1:\cdots:A_n|E), \tag{3.96}$$

where the minimization is taken over all possible extensions of $\rho_{A_1\cdots A_n}$.

Again the trivial extension $\rho_{A_1\cdots A_nE} = \rho_{A_1\cdots A_n}\otimes|0\rangle\langle 0|_E$ gives an upper bound

$$E_{sq}(A_1:\cdots:A_n) \leq \frac{1}{2}T(A_1:\cdots:A_n), \tag{3.97}$$

where $T(A_1:\cdots:A_n|E) = T(A_1:\cdots:A_n)$ was used on the state.

The proposition 7 and this inequality indicates the generic order of the three types of multipartite correlation measure.

Corollary 13. *For any n-partite quantum states, we have*

$$E_{sq}(A_1:\cdots:A_n) \leq \frac{1}{2}T(A_1:\cdots:A_n) \leq E_P(A_1:\cdots:A_n). \tag{3.98}$$

Note that these bounds are saturated for any n-partite pure state. $E_P \geq E_{sq}$ is an expected property because E_P is a measure of both quantum and classical correlations while E_{sq} is only of quantum one.

3.3.2 Holographic dual of the multipartite squashed entanglement

The definition of the squashed entanglement (3.93) is very similar to that of the entanglement of purification (3.5). Both of them use a certain type of extension (purifications are, indeed, a special subset of extensions). This observation motivates us to seek for the holographic counterpart of E_{sq} in the same manner of E_P.

Let us regard a time slice of the AdS spacetime as a tensor network, which describes the quantum state of the boundary CFT. The tensor network description of the background enable us to define a quantum state for any codimension-2 convex surface. This argument is called the surface/state correspondence [74, 93, 94]. Then we consider a class of extensions from ρ_{AB} to ρ_{ABE} which have classical gravity duals, called geometrical extensions, described by tensor networks. These extensions are not necessarily defined on the original AdS boundary, but each extended geometry should at least contain the entanglement wedge $\mathcal{M}_{AB}$. We also require its boundary to be convex in order to the entanglement entropy of any part of the boundary is well-defined [74].

Then all the nontrivial extensions result in (at the leading order $O(1/G_N)$)

$$I(A:B|E) \geq I(A:B). \tag{3.99}$$

Indeed, this is equivalent to the well known non-positivity of the holographic tripartite information $I_3(A,B,E) \leq 0$. This property was originally proven for the subsystems on

the AdS boundary, but the proof does not rely on any peculiarity of asymptotic AdS boundary [7]. In particular, that does not concern whether the boundary is located on the asymptotic infinity or not. This situation can be graphically illustrated for example in Fig.3.10. This indicates that one can never reduce the correlation between A and B by knowing the extension E in geometrical states.

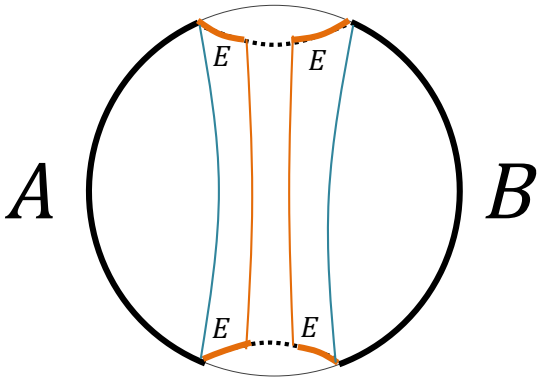

Figure 3.10: The proof of $I(A : B|E) \geq I(A : B)$ for an extension ρ_{ABE}, where the extended subsystem E is on the Ryu-Takayanagi surface of S_{AB}. The difference $I(A : B|E) - I(A : B)$ is given by the area of the orange codimension-2 surfaces subtracted by that of the blue ones. We illustrate the case that E is relatively small, but the same result is true for much large E.

Assuming that there exists an optimal extension for (3.93) in the geometrical class leads to the equivalence

$$E_{sq}(A : B) = \frac{1}{2} I(A : B). \tag{3.100}$$

This implies that the inequality $E_{sq}(A : B) \leq I(A : B)/2$ is saturated in holography, as observed in a tensor network model [95].

We can test this equivalence by checking their properties, especially one which is special for holography. The mutual information is not always monogamous on generic states, while the squashed entanglement must satisfy it for any tripartite states [96]. The holographic mutual information, however, becomes monogamous – that provides a non-trivial

[7] About the monogamy property, the area functional can be replaced with any geometrical functional as long as that is extensive. In particular, higher curvature corrections does not affect and this property would be common in all large-N field theories [67].

check of (3.100).

We can generalize the discussion of the bipartite case to the multipartite squashed entanglement as follows. The multipartite squashed entanglement can be rewritten as

$$E_{sq}(A_1 : \cdots : A_n) = \frac{1}{2}T(A_1 : \cdots : A_n) + \frac{1}{2}\min_{\rho_{A_1\cdots A_n E}} Q_n(A : E), \tag{3.101}$$

where

$$Q_n(A; E) \coloneqq I(A_1 \cdots A_n : E) - \sum_{i=1}^{n} I(A_i : E). \tag{3.102}$$

This quantity can be both positive and negative in generic quantum system. However, the monogamy of mutual information guarantees

$$Q_n(A : E) \geq 0. \tag{3.103}$$

In particular, this is nothing but the non-positivity of tripartite information $Q_2(AB; E) = I(AB : E) - I(A : E) - I(B : E) = -I_3(A, B, E) \geq 0$ for $n = 2$. Following the same logic and assumption leads to that holographic multipartite squashed entanglement is equivalent to half of the total correlation,

$$E_{sq}(A_1 : \cdots : A_n) = \frac{1}{2}T_n(A_1 : \cdots : A_n). \tag{3.104}$$

One of a non-trivial tests for n-partite case is given by the strong superadditivity of the multipartite squashed entanglement [88]:

$$E_{sq}(A_1B_1 : \cdots : A_nB_n) \geq E_{sq}(A_1 : \cdots : A_n) + E_{sq}(B_1 : \cdots : B_n). \tag{3.105}$$

This is true in any $2n$-partite state $\rho_{A_1B_1\cdots A_nB_n}$. Note that the total correlation does not satisfy this property in general. An example which violates this inequality for T is

$$\rho_{A_1B_1A_2B_2A_3B_3} = \frac{1}{\sqrt{2}}(|000000\rangle\langle 000000|_{A_1B_1A_2B_2A_3B_3} + |111111\rangle\langle 1111111|_{A_1B_1A_2B_2A_3B_3}), \tag{3.106}$$

Then we have $T(A_1B_1 : A_2B_2 : A_3B_3) = T(A_1 : A_2 : A_3) = T(B_1 : B_2 : B_3)$ and the inequality is violated.

However, in holographic CFTs, the total correlation indeed satisfies the strong superadditivity. This can be shown as follows:

$$\begin{aligned} T(A_1B_1 : \cdots : A_nB_n) &= T(A_1B_1 : A_2B_2) + T(A_1B_1A_2B_2 : A_3B_3) + \cdots \\ &\quad \cdots + T(A_1B_1A_2B_2\cdots A_{n-1}B_{n-1} : A_nB_n) \\ &\geq I(A_1 : A_2) + I(A_1A_2 : A_3) + \cdots + I(A_1A_2\cdots A_{n-1} : A_n) \\ &\quad + I(B_1 : B_2) + I(B_1B_2 : B_3) + \cdots + I(B_1B_2\cdots B_{n-1} : B_n) \\ &= I(A_1 : \cdots : A_n) + I(B_1 : \cdots : B_n), \end{aligned} \tag{3.107}$$

where the monogamy of holographic mutual information was used recursively. To our best knowledge, there is no counter example for such saturation conjecture.

4 The Numerical computation of the entanglement of purification in lattice models

There are various types of quantum entanglement for mixed states. This fact results in existence of the various quantum entanglement measures for mixed states, as described in the section 2.5. Many of them have a concrete operational meaning based on the number of the EPR pairs. They are, however, in general difficult to compute since their definition commonly includes a sort of minimization over some infinitely many operations or quantum states. Such minimizations are challenging in quantum field theories or even in spin chain systems.

The entanglement of purification is a cousin of these entanglement measures, as the definition (2.11) includes a minimization of correlation over all possible purifications. The entanglement of purification is not a genuine measure of quantum entanglement, but of both quantum and classical correlation. Nevertheless, the regularization of the entanglement of purification has an operational meaning based on the number of EPR pairs required to produce the given state under LOq [34]. The minimization involved in the entanglement of purification is comparatively simple, because that consists of a minimization of the single von Neumann entropy.

The conjectured formula of the entanglement of purification in the AdS/CFT correspondence could provide an alternative method to compute the entanglement of purification. In particular, [62] proves the holographic formula for specific examples. That also motivates us to study the field theoretical properties of the entanglement of purification.

In this section, we present numerical calculations of the entanglement of purification in a free scalar field theory and a spin chain system. In a free scalar field theory, we employ the Gaussian wave functional ansatz for a wider range of subsystem sizes than the earlier preliminary analysis [97]. In a spin chain, we perform the numerical optimization without assuming any ansatz for the minimal subsystems. The results in both models exhibit a common counter-intuitive behavior: The entanglement of purification $E_P(A:B)$ is not monotonically decreasing as a function of the physical distance d between A and B. This phenomena is also validated in an analytic method in a spin chain. We will discuss an interpretation of this property based on the difference between quantum and classical correlation. Moreover, there is a spontaneous breaking of the Z_2 reflection symmetry that exchanges A' and B', even for a system symmetric under the A, B reflection.

Note: This section is mainly based on the results in [61].

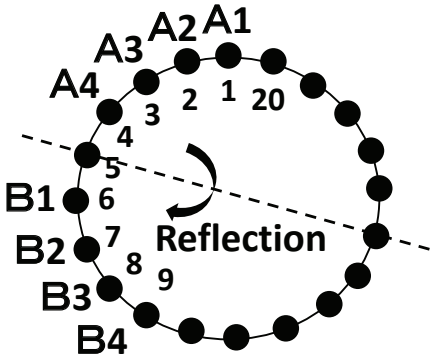

Figure 4.1: The setup for the lattice model for $N = 20$ and $|A| = |B| = 4$. The distance d between A and B is given by $d = 1$. The original subsystems obviously have the Z_2 reflection symmetry. (The figure is cited from [61])

4.1 The Gaussian entanglement of purification in free scalar field theories

First we consider a free massive scalar field theory in $1+1$ dimensions. The Hamiltonian is given by

$$H_0 = \frac{1}{2}\int_{-\infty}^{\infty} dx[\pi^2 + (\partial_x\phi)^2 + m^2\phi^2]. \tag{4.1}$$

Then the ground state wave functional of this lattice scalar theory is given by the Gaussian function [98, 99, 97]

$$\Psi_0[\phi] = \mathcal{N}_0 \exp\left(-\frac{1}{2}\sum_{n,n'=1}^{N}\phi'_n W_{nn'}\phi'_{n'}\right) =: \mathcal{N}_0 \exp\left(-\frac{1}{2}\phi^T W\phi\right). \tag{4.2}$$

Here W is symmetric and real-valued matrix defined by

$$W_{nn'} = \frac{1}{N}\sum_{k=1}^{N}\sqrt{m^2a^2 + 4\sin^2\left(\frac{\pi k}{N}\right)}\, e^{\frac{2\pi i k(n-n')}{N}}, \tag{4.3}$$

where N is the number of total lattice sites and the parameter a is the lattice spacing. We set a as unit by rescaling the mass m. The masses are taken to be small from $m = 10^{-4}$ to $m = 10^{-1}$ near the conformal (massless) limit.

By choosing the sites A and B, we divide the total system into three parts $\mathcal{H}_{\rm tot} = \mathcal{H}_A \otimes \mathcal{H}_B \otimes \mathcal{H}_E$. The number of lattice sites in $A, B, \cdots$ is denoted by $|A|, |B|, \cdots$, and the distance between A and B is by d. A sketch of the setup is illustrated in Fig. 4.1.

We rewrite (4.2) as

$$\Psi_0[\phi] = \mathcal{N}_0 \exp\left[-\frac{1}{2}\begin{pmatrix}\phi_{AB}\\ \phi_E\end{pmatrix}^{\rm T}\begin{pmatrix}P & Q\\ Q^{\rm T} & R\end{pmatrix}\begin{pmatrix}\phi_{AB}\\ \phi_E\end{pmatrix}\right], \tag{4.4}$$

with the matrices P, Q, R induced from the relative position of the subsystems A and B.

From the wave functional (4.4), we can derive the reduced wave functional Ψ_{AB} by the partial trace out of the environmental system E (see also [97]). Namely, the functional of $\rho_{AB} = \mathrm{Tr}_E \left[|\Psi\rangle \langle\Psi| \, |_{ABE} \right]$ is given by

$$\begin{aligned}\rho_{AB}[\phi_{AB}, \phi'_{AB}] &= \int D\phi_E \Psi_0^*[\phi_{AB}, \phi_E] \Psi_0[\phi'_{AB}, \phi_E] \\ &\propto \exp\left(-\frac{1}{2}\phi_{AB} M \phi_{AB}^T - \frac{1}{2}\phi'_{AB} M (\phi'_{AB})^T - \frac{1}{4}(\phi_{AB} - \phi'_{AB}) N (\phi_{AB} - \phi'_{AB})^T \right),\end{aligned} \tag{4.5}$$

where M and N are symmetric real matrices defined by

$$M = P - QR^{-1}Q^T, \ N = QR^{-1}Q^T. \tag{4.6}$$

The normalization is determined by the trace condition $\mathrm{Tr}\rho_{AB} = 1$.

4.1.1 The mutual information and the logarithmic negativity

From the expression of the density matrix (4.5), we can compute the mutual information $I(A:B) = S_A + S_B - S_{AB}$ and the logarithmic negativity $\mathcal{E}_N(\rho_{AB})$. The latter is a useful probe of quantum entanglement between A and B defined as [100]

$$\mathcal{E}_N(\rho_{AB}) = \log ||\rho_{AB}^{\Gamma_B}||_1, \tag{4.7}$$

where $\rho_{AB}^{\Gamma_B}$ is the partial transposition with respect to B and $||\cdot||_1$ is the trace norm. Their results are shown in Fig. 4.2. Refer to the appendix 7.1 for the details of computing $\mathcal{E}_N(\rho_{AB})$. The $\mathcal{E}(\rho_{AB})$ exhibits an exponential decay with increasing the distance d. On the other hand, the mutual information slowly decreases as function of d, following a power-law.

4.1.2 The Gaussian entanglement of purification

Now we compute the entanglement of purification $E_P(A:B)$ in this system by employing the gaussian purifications [8]. The generic form of the Gaussian purifications have the form

$$\begin{aligned}\Psi_{AA'BB'}[\phi] &= \mathcal{N}_{AA'BB'} \exp\left(-\frac{1}{2}\phi^{\mathrm{T}} V \phi \right) \\ &= \mathcal{N}_{AA'BB'} \exp\left[-\frac{1}{2} \begin{pmatrix} \phi_{AB} \\ \phi_{A'B'} \end{pmatrix}^{\mathrm{T}} \begin{pmatrix} J & K \\ K^{\mathrm{T}} & L \end{pmatrix} \begin{pmatrix} \phi_{AB} \\ \phi_{A'B'} \end{pmatrix} \right],\end{aligned} \tag{4.8}$$

[8] Refer to [101] for the study of the gaussian entanglement of formation.

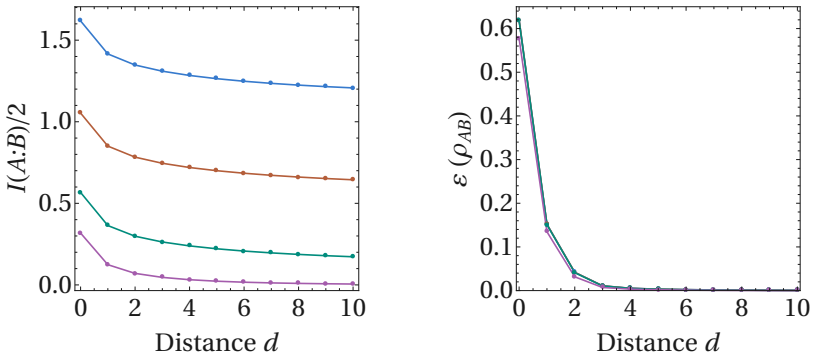

Figure 4.2: The half of mutual information $\frac{1}{2}I(A:B)$ (left) and the logarithmic negativity $\mathcal{E}(\rho_{AB})$ (right) as a function of the distance d. The subsystems are taken as $|A| = |B| = 4$ and $N = 60$, the four colors corresponds to the mass $m = 10^{-1}, 10^{-2}, 10^{-3}, 10^{-4}$ (bottom to top). (The figure is cited from [61])

where V is the Gaussian coupling matrix, and J, K, L are the decomposed matrices. Assuming the widths of subsystems are the same $w = |A| = |B|$, L becomes a $w \times w$ square matrix. The trace condition

$$\mathrm{Tr}_{A'B'}[|\Psi\rangle \langle\Psi|_{AA'BB'}] = \rho_{AB}, \tag{4.9}$$

requires

$$J = P, \tag{4.10}$$

and L must be related to K by

$$L^{-1} = (K^{-1}Q)R^{-1}(K^{-1}Q)^{\mathrm{T}}. \tag{4.11}$$

The symmetry transformation [97] which does not affect the value of $S_{AA'}$ allows us to simplify the K to the form,

$$K = \begin{pmatrix} 1_w & K_{A,B'} \\ K_{B,A'} & 1_w \end{pmatrix}. \tag{4.12}$$

Thus, all the free parameters we need to tune for the optimization are contained in the $w \times w$ matrices $K_{A,B'}$ and $K_{B,A'}$. This procedure determines the matrix $V \equiv V_{AA',BB'}$, from which we can compute the entanglement entropy $S_{A\tilde{A}}$ by

$$S_{A\tilde{A}} = \sum_k \left[\log \frac{\sqrt{\lambda_k}}{2} + \sqrt{1+\lambda_k} \log \left(\frac{1}{\sqrt{\lambda_k}} + \sqrt{1+\frac{1}{\lambda_k}} \right) \right], \tag{4.13}$$

where $\{\lambda_k\}$ is the eigenvalue spectrum of the matrix $\Lambda := -V^{-1}_{AA',BB'}V_{BB',AA'}$ [98].

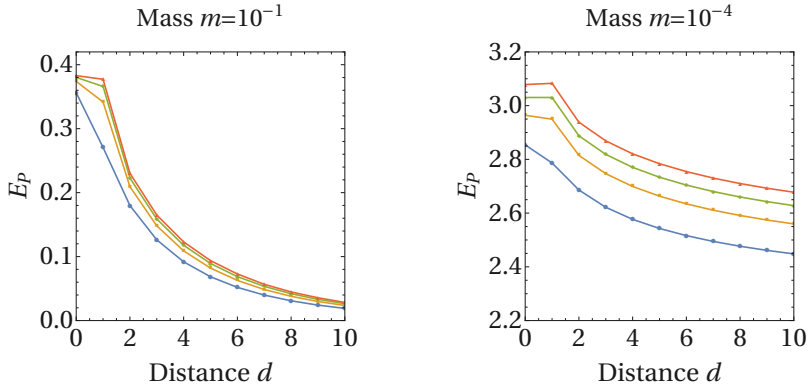

Figure 4.3: The Gaussian entanglement of purification $E_P(A:B)$ at $N = 60$ for $w = |A| = |B| = 1, 2, 3, 4$ (bottom to top). The left plot is for the massive limit $m = 10^{-1}$, and the right one is for the massless limit $m = 10^{-4}$. (The figure is cited from [61])

The Gaussian entanglement of purification is the minimum of $S_{A\tilde{A}}$ over all possible purifications $\Psi_{AA'BB'}[\phi]$ of the form (4.8), i.e. over varying the components of $K_{A,B'}$ and $K_{B,A'}$,

$$E_P(A:B) := \min_{K_{A,B'}, K_{B,A'}} S_{AA'}(V(K_{A,B'}, K_{B,A'})). \tag{4.14}$$

For the class of purifications which have the Z_2 symmetry reflecting AA' and BB', the K should satisfy

$$K_{A,B'} = K^{\mathrm{R}}_{B,A'}, \tag{4.15}$$

where M^{R} is the matrix M of the inverse ordering of all rows and columns,

$$(M^{\mathrm{R}})_{j,k} := M_{w+1-j,w+1-k}. \tag{4.16}$$

Note that the optimal purification is not necessarily in this symmetric class, as we will see in the following. Then the we may evaluate the degree of the breaking of the Z_2 symmetry by

$$\mathcal{A}(K) := ||K_{A,B'} - K^{\mathrm{R}}_{B,A'}||_2, \tag{4.17}$$

where $||M||_2$ is the 2-norm over all entries of M.

We calculated the Gaussian entanglement of purification (4.14) for the subsystem sizes $w = 1, 2, 3, 4$, changing the distance d. The results were computed using a numerical L-BFGS optimization implemented with the C++ package *dlib*.

4.1.3 The properties in the free scalar field theory

The results are shown in Fig. 4.3 for $N = 60$. There is a plateau-like behavior of E_P in the close configuration (from $d = 0$ to $d = 1$) at large w. The width of plateau seems independent of w, which suggests a finite-size effect.

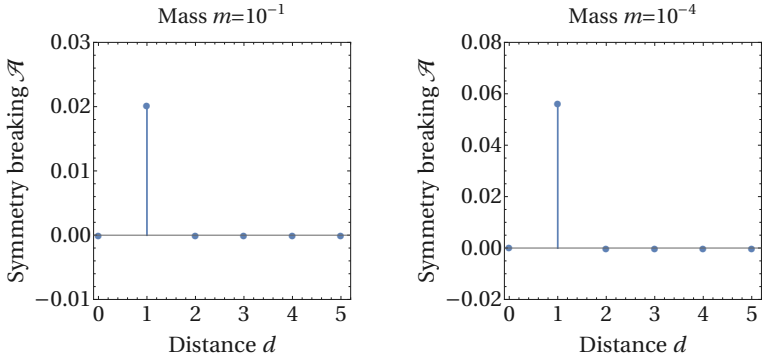

Figure 4.4: The asymmetry parameter $\mathcal{A}$ at masses $m = 10^{-1}$ and $m = 10^{-4}$ with the width $w = 4$ and total size $N = 60$. The positive value $\mathcal{A} > 0$ Z_2 indicates the breaking of the Z_2 symmetry. (The figure is cited from [61])

The Z_2 reflection symmetry is a property of the original system A and B, and leaves the entanglement of purification invariant i.e.

$$E_P(A:B) = E_P(B:A). \tag{4.18}$$

Then it would be natural to expect that the optimal purification is also Z_2-symmetric i.e. $\mathcal{A}(K) = 0$. Surprisingly, the optimal purification indeed violates the Z_2 symmetry for some states and $\mathcal{A}(K) > 0$ is observed. The Z_2 symmetry breaking clearly appears at $d = 1$, as shown in Fig. 4.4. Within numerical accuracy, the Z_2 symmetry is kept for any $d \neq 1$. Note that the symmetry breaking at $d = 1$ gets enhanced by increasing w.

The results for the smaller total system N is more intriguing: The entanglement of purification, at small N, does not need to monotonically decrease and can even increase with d, as shown in Fig. 4.5. As we increase N, this non-monotonicity is gradually relaxed. One may consider that this strange behavior as a correlation measure could be just a magic of the Gaussian purifications, we will conclusively show that the E_P is indeed not a monotonic function in the next section.

4.2 The entanglement of purification in spin chain models

We then compute the entanglement of purification in spin chain systems. Let us denote the dimension of a Hilbert space of a subsystem X by

$$D_X = \dim \mathcal{H}_X. \tag{4.19}$$

In order to purify a given mixed state ρ_{AB}, the dimension of the auxiliary Hilbert space $\mathcal{H}_{A'B'}$ should be at least as large as the rank of ρ_{AB},

$$D_{A'B'} = D_{A'} D_{B'} \geq \mathrm{rank}\rho_{AB}. \tag{4.20}$$

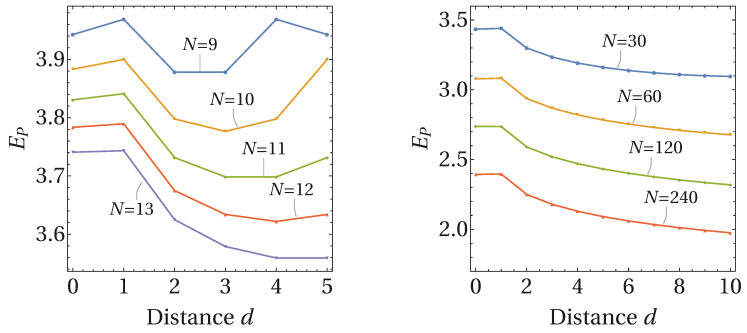

Figure 4.5: The entanglement of purification for the various system sizes N at mass $m = 10^{-4}$. The width is $w = 2$ for the left, and $w = 4$ for the right. (The figure is cited from [61])

The dimension $D_{A'B'}$ can be arbitrarily large in principle. However, it was shown that the minimum of $S_{AA'}$ is reachable within

$$D_{A'} \leq \mathrm{rank}\rho_{AB}, \ D_{B'} \leq \mathrm{rank}\rho_{AB} \tag{4.21}$$

in a finite-dimensional Hilbert space [102]. This fact enables us to compute the entanglement of purification in practice. For the latter convenience, we call the purification *minimal* when

$$D_{A'}D_{B'} = \mathrm{rank}\rho_{AB}, \tag{4.22}$$

and *maximal* when

$$D_{A'} = D_{B'} = \mathrm{rank}\rho_{AB}. \tag{4.23}$$

A typical example of purification of a mixed state

$$\rho_{AB} = \sum_i p_i \left|i\right\rangle \left\langle i\right|_{AB}, \ \sum_i p_i = 1, p_i \geq 0, \tag{4.24}$$

is so called the canonical purification

$$\left|\psi^c\right\rangle_{AA'BB'} = \sum_i \sqrt{p_i} \left|i\right\rangle_{AB} \left|i\right\rangle_{A'B'}, \tag{4.25}$$

where the ancilla state $\rho_{A'B'}$ is identical to the original state ρ_{AB}.

All purifications (of the fixed dimension $D_{A'B'}$) can be obtained by acting with the unitary operators on the auxiliary systems

$$\left|\psi(U)\right\rangle_{AA'BB'} = I_{AB} \otimes U_{A'B'} \left|\psi_0\right\rangle_{AA'BB'}, \tag{4.26}$$

where $\left|\psi_0\right\rangle_{AA'BB'}$ is an arbitrary initial state. For example, all possible purifications of $D_{A'B'} = \mathrm{rank}\rho_{AB}$ are obtained by setting $\psi_0 = \psi^c$ and using the unitary operators $U_{A'B'}$

on $\mathcal{H}_{A'B'}$. We also need to enlarge the dimension of the auxiliary systems $D_{A'}$ and $D_{B'}$ up to the limit (4.21). In many cases, we will find that the minimal purification is enough to reach the minimum of $S_{AA'}$.

Our numerical minimization relies on a variation of the steepest descent method. We start from several random initial purifications and then ensure that the same minimum is reached after the convergence. The possible existence of narrow local optimal valleys cannot be excluded due to the nature of the technique, in which case the results provide an upper bound to the true entanglement of purification.

4.2.1 In the transverse-field Ising model

We consider the 1d transverse-field Ising model

$$H_{\text{Ising}} = -\sum_{\langle i,j\rangle} \sigma_i^z \otimes \sigma_j^z - h\sum_{i=1}^{N} \sigma_i^x, \tag{4.27}$$

where $\langle i,j\rangle$ denotes the summation over the nearest neighbors with periodic boundary condition. We first focus on the ground state of the critical Ising model ($h = 1$). The entanglement of purification for the subsystems $|A| = |B| = 1$ as a function of the distance d is plotted Fig. 4.6 ($N = 10$ and $N = 4$). It turns out that the optimal purification corresponds to the minimal purification for these cases.

We see the non-monotonic behavior as function of d for $N = 4$, like in the free scalar cases. Remarkably, the non-monotonicity for $N = 4$ can be rigorously proven. The point is that $E_P(A:B)$ should equal to S_A at $d = 1$ for $N = 4$, because the density matrix ρ_{AB} has support only on a symmetric subspace [103]. On the other hand, $E_P(A:B) < S_A$ at $d = 0$ is obvious from the numerical results. Then we have

$$E_P(d=0) < E_P(d=1). \tag{4.28}$$

This provides an analytic example in which the entanglement of purification behaves non-monotonically with the physical distance d.

In fact, the non-monotonicity of the entanglement of purification for $N = 4$ (Fig. 4.6) is common in *any* homogeneous spin chain. Note that that the symmetric and anti-symmetric projectors $P_{\text{sym}}, P_{\text{asym}}$ on A and B at $d = 1$ commute with any of the term $\sum_{<ij>} \sigma_i^l \otimes \sigma_j^l, \sum_i \sigma_i^l$ ($l = x, y, z$). Then they are symmetries of the system, i.e. they commute with the Hamiltonian $[H, P_{\text{sym}}] = [H, P_{\text{asym}}] = 0$, regardless of the coupling parameters. Because of the orthogonality $P_{\text{sym}}P_{\text{asym}} = P_{\text{asym}}P_{\text{sym}} = 0$, the unique vacuum (and any other non-degenerate excited state) should belong to either symmetric or anti-symmetric subspace of $\mathcal{H}_{AB}$. For instance, we have $\rho_{AB} = \frac{1}{3}P_{\text{sym}}$ in the vacuum of the anti-ferromagnetic isotropic Heisenberg model. Therefore, following the statement in

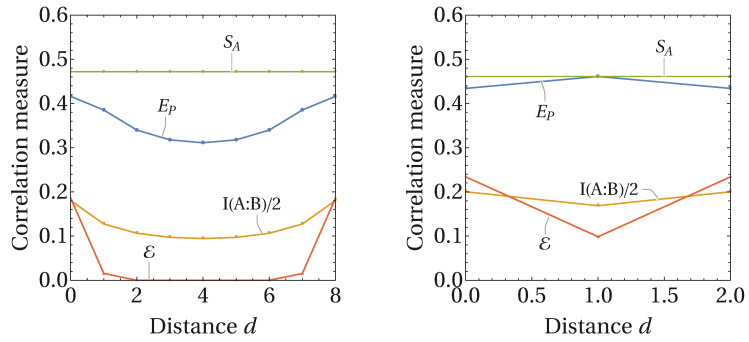

Figure 4.6: The entanglement of purification in the critical Ising model of width $|A| = |B| = 1$. The system size is $N = 10$ (left) and $N = 4$ (right). (The figure is cited from [61])

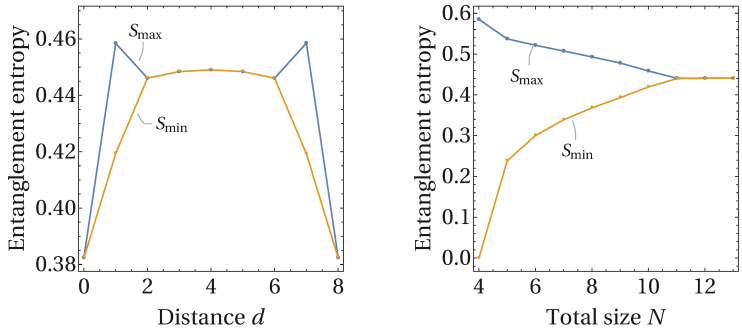

Figure 4.7: $S_{\max} = \max\{S_{A'}, S_{B'}\}$ and $S_{\min} = \min\{S_{A'}, S_{B'}\}$ under the optimal purifications ($|A| = |B| = 1$). The plot with distance d shows the Z_2 symmetry breaking at $d = 1$ (left). The reflection symmetry at $d = 1$ is getting recovered in the large N limit (right). (The figure is cited from [61])

[103], we must have $E_P(d = 1) = S_A(= S_B)$ for such states. Thus any ansatz that shows $E_P(d = 0) < S_A$ implies the non-monotonicity of the entanglement of purification.

The Z_2 reflection symmetry of exchanging AA' and BB' is explicitly broken at $d = 1$, as shown in the Fig. 4.7. The property $S_A \neq S_{A'}$ indicates that the optimal purification is non-trivially different from the canonical purification. Note that the Z_2 symmetry is gradually recovered as N gets larger for $|A| = |B| = 1$.

We also compute the entanglement of purification with larger subsystem size $|A| = |B| = 2$. In this case, the optimization was done within minimal purifications to expedite the computation. Interestingly, we again observe a non-monotonic behavior with d, which weakens as N increases (Fig. 4.8). Note that the Z_2 symmetry breaking is also found at

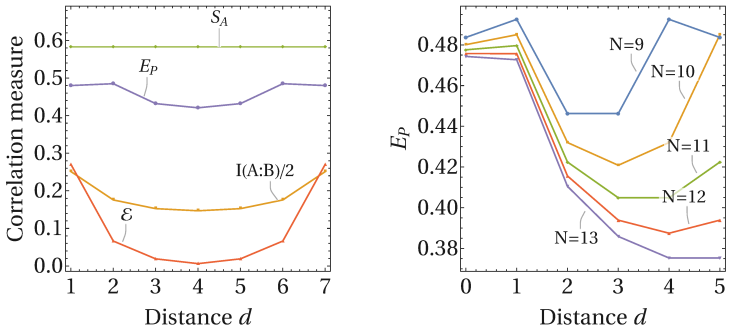

Figure 4.8: The entanglement of purification for the larger subsystem $|A| = |B| = 2$ and $N = 10$ (left). The non-monotonic behavior at $d = 0$ to $d = 1$ gets weaker as N increases (right). All results for $|A| = |B| = 2$ are optimized within minimal purifications. (The figure is cited from [61])

$d = 1$, which remains even in the large N limit.

Both a plateau-like behavior and the Z_2 symmetry breaking occur also for a class of two-qubit states called *Werner states*, the ground state of the Heisenberg spin chain (For details, refer to the appendix C).

Next, we compute the entanglement of purification as a function of the magnetic field h in the thermodynamic limit $N \to \infty$. The subsystems are taken as the nearest-neighbor minimum subsystems ($|A| = |B| = 1$ and $d = 0$). We consider the thermal ground state, in which the analytic expression of the reduced density matrices ρ_{AB} is obtained [104, 105]. The result is shown in Fig. 4.9. There is an inflection point at $h = 1$, which indicates that the entanglement of purification correctly captures the phase transition. The Z_2 reflection symmetry gets broken only, remarkably, in the ferromagnetic phase $h < 1$.

4.2.2 In the Heisenberg model and a Chaotic Spin Chain

We also consider the anti-ferromagnetic isotropic Heisenberg model,

$$H_{\text{Heisenberg}} = \sum_{\langle i,j \rangle} (\sigma_i^x \otimes \sigma_j^x + \sigma_i^y \otimes \sigma_j^y + \sigma_i^z \otimes \sigma_j^z). \tag{4.29}$$

For even N, the reduced density matrix ρ_{AB} of size $|A| = |B| = 1$ in the ground state is equivalent to the Werner state [106], which is discussed in the appendix 7.3. The result is shown in Fig. 4.10. Interestingly, the entanglement of purification exhibits a small peak at the farthest distance $d = 5$ for $N = 12$, while the other measures monotonically decrease. This is also an example of the non-monotonicity of the entanglement of purification.

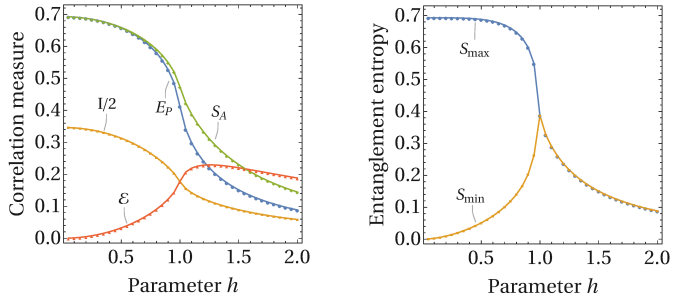

Figure 4.9: The entanglement of purification as a function of the magnetic field h in $N \to \infty$ limit. We took the nearest neighbor $d = 0$ with $|A| = |B| = 1$ (left). The Z_2 symmetry is broken in the ferromagnetic phase $h < 1$, and recovered in the paramagnetic phase $h > 1$ (right). (The figure is cited from [61])

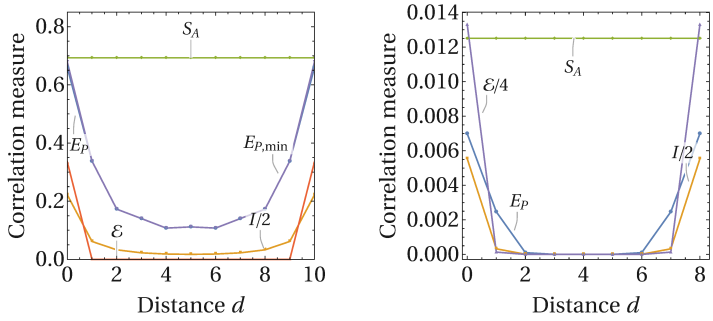

Figure 4.10: The entanglement of purification for the anti-ferromagnetic isotropic Heisenberg model (left) and for a chaotic spin chain (right). (The figure is cited from [61])

Finally, we consider a non-integrable model by adding a parallel magnetic field to the Ising model,

$$H_{\text{Chaos}} = -\sum_{\langle i,j \rangle} \sigma_i^z \otimes \sigma_j^z - h \sum_{i=1}^{N} \sigma_i^x - g \sum_{i=1}^{N} \sigma_i^z. \tag{4.30}$$

The parameters are set $h = 1.05$ and $g = -0.5$, following the work [107]. The long range correlations are almost vanishing in the vacuum, while the entanglement of purification is still relatively enhanced at $d = 1$ (Fig. 4.10).

4.3 Interpretation: Quantum and Classical correlations in a toy model

The plateau-like behavior, or the non-monotonicity, of the entanglement of purification are common both in the free scalar theory and in the critical Ising model. This behavior

is very special to the entanglement of purification E_P as that cannot be found in the mutual information $I(A:B)$ or the logarithmic negativity $\mathcal{E}(A:B)$. In particular, both E_P and I have almost equivalent information-theoretic properties as measure of quantum and classical correlation. Thus this outstanding difference between E_P and I is intriguing.

In order to interpret the difference, we focus on the following facts: for purely quantum correlations, i.e. any pure states, they should coincide with each other (with the appropriate factor $\frac{1}{2}$),

$$E_P(A:B) = \frac{1}{2} I(A:B), \tag{4.31}$$

while for purely classical correlations, i.e. any separable states, the entanglement of purification is actually enhanced at least twofold [34]

$$E_P \geq 2 \cdot \frac{1}{2} I(A:B). \tag{4.32}$$

This observation tempt us to assume that the half of the mutual information evaluates the quantum and classical correlation equivalently, while that the entanglement of purification enhances classical correlations.

Based on this picture, we can explain the non-monotonic behavior of the EOP as follows: Because the quantum entanglement falls off quickly as the physical distance d, the correlations at $d = 0$ mainly come from quantum entanglement and those at $d \geq 1$ arise from classical correlations. This structure enhance the entanglement of purification at $d \geq 1$, while does not at $d = 0$. That results in a plateau-like or the non-monotonic behavior of the entanglement of purification at $d = 0$ to $d = 1$. Indeed, for $d \gg 1$, the entanglement of purification is at least twice as large as the half of the mutual information. Moreover, both the mutual information and the entanglement of purification monotonically decrease following a similar power law. These facts imply that the correlation $d \geq 1$ consists of mostly classical correlation.

We illustrate a toy model of a purified system with only bipartite nearest-neighbor entanglement, depicted in Fig. 4.11. This picture also explains the Z_2 symmetry breaking at $d = 1$ as follows: First, remark that there is only quantum entanglement between AA' and BB' after purification. Thus the minimization procedure can be viewed as a transformation of the classical correlation into the smallest possible quantum entanglement. Then, at $d = 0$, the two boundary sites of A and B are strongly entangled, and this entanglement remains dominant after the purification. At $d = 1$, where A and B are separated by one extra site C, tracing it out will lead to a highly mixed and classically correlated state C is strongly entangled with both A and B. On the other hand, the direct quantum entanglement between A and B is very small. Therefore, the optimal purification requires strong entanglement injected into $A \leftrightarrow A'$, $B \leftrightarrow B'$, $A' \leftrightarrow B'$, $A' \leftrightarrow B$, and $A \leftrightarrow B'$ for the transformation of classical correlation, while the entanglement $A \leftrightarrow B$ is negligible. This complicated competition results in a Z_2 reflection symmetry breaking, where only either $A' \leftrightarrow B$ or $A \leftrightarrow B'$ exhibits strong entanglement (Fig. 4.11, center). For $d \geq 2$,

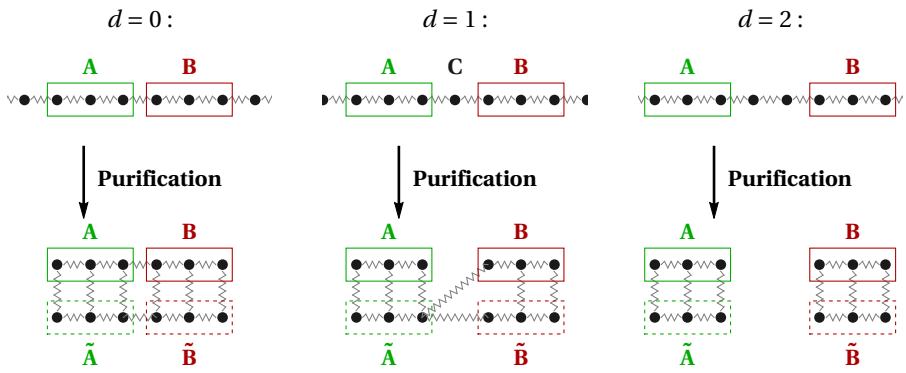

Figure 4.11: A simplified toy model of the entanglement of purification with only short-range quantum entanglement (zigzag lines). The original system $|\Psi\rangle_{ABC}$ is shown above, and the purification $|\Psi\rangle_{A\tilde{A}B\tilde{B}}$ below. (The figure is cited from [61])

however, A and B are separated by multiple sites and there is no longer a strong classical correlation nor quantum entanglement between A and B. Then the entanglement of purification decreases along with the small remaining classical correlations as d increases. This picture is indeed confirmed both for the free scalar field theory and the Ising model.

5 Holographic Dual of the Optimized Correlation Measures

The entanglement of purification and the squashed entanglement belong to a class of correlation measures, so called the optimized correlation measures. The measures in this class are defined by a type of optimization (minimization) of a linear combination of von Neumann entropy over all possible purifications or extensions. This optimization procedure is highly compatible with the AdS/CFT correspondence through geometric states that can be regarded as extended geometry of the entanglement wedge.

In this section, we comprehensively introduce the holographic duals of the optimized correlation measures. Besides the entanglement of purification and the squashed entanglement, there are three other measures of correlation: the conditional entanglement of mutual information (CEMI), the Q-correlation, and the R-correlation [91, 29]. The first one is a genuine entanglement measure, and the latter two are measures of both quantum and classical correlation. It turns out that, when the optimization is taken over all possible geometrical extensions, the CEMI and the R-correlation return to the known geometrical objects in the bulk. On the other hand, the holographic dual of the Q-correlation provides a totally new geometrical object inside the entanglement wedge: we call this geometrical object by the *entanglement wedge mutual information* (EWMI). The detailed property of the entanglement wedge mutual information will be studied in the following discussion. These dual relations again exhibit the consistency of all the properties of correlation measures. These results support a common framework of these quantity: the geometrical optimization works in holography.

As an application of these dual relations, we point out an implication to the structure of correlation in geometric states. Note that the monogamy of holographic mutual information tempts us to consider that correlations in the geometric states are dominated by quantum entanglement. However, we will show that both the entanglement wedge cross section and the entanglement wedge mutual information can be strictly larger than various types of the axiomatic entanglement measures and the quantum discord at the leading order $O(N^2)$. This means that they can not be a dual of the quantum correlation measures. It implies that these quantities captures more than quantum entanglement in the entanglement wedge, and it must be sensitive to classical correlations as well.

Note: This section is mainly based on the results in [63].

5.1 Holographic Dual of the Optimized Entanglement Measures

5.1.1 The squashed entanglement

We have already discussed the holographic dual of the squashed entanglement E_{sq} [81] in the section 3. Recall that the squashed entanglement is given by

$$E_{sq}(A:B) := \frac{1}{2}\min_{\rho_{ABE}} I(A:B|E) \tag{5.1}$$

$$= \frac{1}{2}I(A:B) - \frac{1}{2}\max_{\rho_{ABE}} I_3(A,B,E), \tag{5.2}$$

where ρ_{ABE} is extension of ρ_{AB} i.e. $\mathrm{Tr}_E\rho_{ABE} = \rho_{AB}$, and $I_3(A,B,C) = S_A + S_B + S_C - S_{AB} - S_{BC} - S_{CA} + S_{ABC}$ is the tripartite information. Then the assumption that the minimization over all possible geometrical extensions is enough to reach the minimum leads to

$$E_{sq}(A:B) = \frac{1}{2}I(A:B). \tag{5.3}$$

This relation, if it is true, requires that the mutual information in holography must satisfy the all properties of the squashed entanglement at $O(N^2)$. In particular, the squashed entanglement is known to satisfy the monogamy relation $E_{sq}(A:BC) \geq E_{sq}(A:B) + E_{sq}(A:C)$, which is usually considered as a characteristic of quantum entanglement and the mutual information does not satisfy in general. The holographic mutual information indeed satisfies this property.

This equality is the saturation of the generic inequality (3.97). The saturation occurs when ρ_{AB} is, for instance, a pure state. Moreover, the class of states saturating the Araki-Lieb inequality also saturates that, in which the correlation between A and B is essentially pure. Then a question is whether such pure correlation is the only possibility of the saturation or not. The answer is no: the so-called flower state $\rho_{A_1A_2B_1B_2}$ defined by tracing out C from

$$|\psi\rangle_{A_1A_2B_1B_2C} = \frac{1}{\sqrt{2d}}\sum_{i=0}^{d}\sum_{j=0,1}|i\rangle_{A_1}|j\rangle_{A_2}|i\rangle_{B_1}|j\rangle_{B_2}U_j|i\rangle_C, \tag{5.4}$$

where $U_0 = I$ and U_1 is a quantum Fourier transform,

$$U_k : |n\rangle \to |\psi_n\rangle := \frac{1}{\sqrt{N}}\sum_{k=0}^{N-1} e^{\frac{2\pi ik}{N}\cdot n}|k\rangle, \tag{5.5}$$

is known to satisfy $E_{sq}(A:B) = I(A:B)/2$ ($\neq S_A$) [103]. One might then naively expect that the structure of holographic states has a similar form to the flower state. For the flower state, however, the equality

$$E_P(A:B) = S_A = S_B, \tag{5.6}$$

must hold, which is not what we expect on the holographic states. Giving a characterization on the states saturating (3.97) will be an interesting problem in the context of holography.

5.1.2 The conditional entanglement of mutual information

Another entanglement measure in the class of the optimized correlation measures is the conditional entanglement of mutual information E_I [91][9]. That is given by

$$\begin{aligned} & E_I(A:B) \\ & := \frac{1}{2} \min_{\rho_{ABA'B'}} (I(AA':BB') - I(A':B')) \qquad (5.7) \\ & = \frac{1}{2} I(A:B) \\ & \quad + \frac{1}{2} \min_{\rho_{ABA'B'}} (I(AA':BB') - I(A:B) - I(A':B')), \qquad (5.8) \end{aligned}$$

where $\rho_{ABA'B'}$ is extension of ρ_{AB}. The monogamy of mutual information for geometric extensions $\rho_{AA'BB'}$ leads to

$$I(AA':BB') - I(A:B) - I(A':B') \geq I(A:B') + I(B:A') \geq 0, \qquad (5.9)$$

which again leads to

$$E_I(A:B) = \frac{1}{2} I(A:B). \qquad (5.10)$$

Interestingly, both results imply that the half of the mutual information in holography seems to capture only quantum entanglement. This fact might tempt us to assume that the holographic correlation is made of mostly quantum correlation. The entanglement wedge cross section, however, still indicates the existence of classical correlations in holography, as we will discuss later. This difference of the two geometrical quantities remind us the result in the previous section: the entanglement of purification is more sensitive to classical correlations than the mutual information. To our best knowledge, there is no obstruction to speculate that the other axiomatic entanglement measures (such as E_C and E_F) also coincide with the half of mutual information in holography. We leave investigating this possibility as a future work.

[9]The optimal correlation measures are originally defined by extensions of single ancillary system, that do not include the conditional entanglement of mutual information [29]. We include E_I here generalizing their definition to discuss E_I holographically.

5.2 Holographic Duals of the Optimized Total Correlation Measures

5.2.1 The Q-correlation and R-correlation

There are two other optimized correlation measures, the Q-correlation and the R-correlation, introduced in [29]

$$E_Q(A:B) \coloneqq \frac{1}{2}\min_{\rho_{ABE}}(S_A + S_B + S_{AE} - S_{BE}) \tag{5.11}$$

$$\equiv \min_{\rho_{ABE}} f^Q(A,B,E). \tag{5.12}$$

$$E_R(A:B) \coloneqq \frac{1}{2}\min_{\rho_{ABE}}(S_{AB} + 2S_{AE} - S_{ABE} - S_E) \tag{5.13}$$

$$\equiv \min_{\rho_{ABE}} f^R(A,B,E). \tag{5.14}$$

They are symmetric between A and B, which is obvious in the equivalent expression ($E \equiv A'$),

$$E_Q(A:B)$$

$$= \frac{1}{2}\min_{|\psi\rangle_{AA'BB'}}(S_A + S_B + \frac{S_{AA'} + S_{BB'} - S_{BA'} - S_{AB'}}{2}) \tag{5.15}$$

$$\equiv \min_{|\psi\rangle_{AA'BB'}} f^Q(A,A',B,B'). \tag{5.16}$$

$$E_R(A:B)$$

$$= \frac{1}{2}\min_{|\psi\rangle_{AA'BB'}}(S_{AB} + S_{AA'} + S_{BB'} - S_{A'} - S_{B'}) \tag{5.17}$$

$$\equiv \min_{|\psi\rangle_{AA'BB'}} f^R(A,A',B,B'). \tag{5.18}$$

The Q-correlation and the R-correlation are non-increasing under strict local operations, but not necessarily under LOCC. Thus they are not genuine entanglement measures.

There is inequalities

$$\frac{1}{2}I(A:B) \leq E_Q(A:B), E_R(A:B) \leq E_P(A:B). \tag{5.19}$$

The R-correlation is a kind of reminiscent to the CEMI. That is clear from the following

$$E_R(A:B) = \frac{1}{2}\min_{|\psi\rangle_{AA'BB'}}(I(AA':BB') - I(A':B')). \tag{5.20}$$

This is almost equivalent to the definition of the CEMI (5.7), though the minimization is taken over all possible extensions but not purifications.

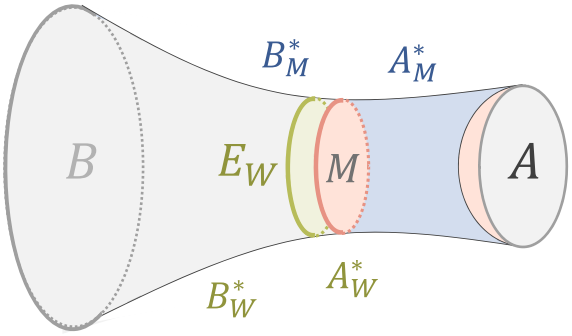

Figure 5.1: The definition of the entanglement wedge mutual information. In the above picture, E_M is given by the area of red codimension-2 surfaces subtracted by the area of blue codimension-2 surface (divided by $2{\cdot}4G_N$). Notably, this quantity may be understood as the mutual information between A and M: $E_M = \frac{1}{2}I(A:M)$. The symmetry $E_M(A:B) = E_M(B:A)$ comes from the fact that the RT-surface of $S_{BA'}$ and $S_{AB'}$ share the same configurations. The optimal partition of the entanglement wedge mutual information is not necessarily equivalent to that of the entanglement wedge cross section. (The figure is cited from [63])

5.2.2 The entanglement wedge mutual information

We first investigate the holographic dual of the Q-correlation. The definition of the holographic dual of E_Q is given as follows (let us focus on the static case):

Given an entanglement wedge $\mathcal{M}_{AB}$, divide the boundary into two pieces $\partial\mathcal{M}_{AB} = \mathcal{A}\cup\mathcal{B}$ such that $\mathcal{A} = A\cup A'$ and $\mathcal{B} = B\cup B'$. Then find the configuration of A' and B' that minimizes the holographic entanglement entropy $f^Q(A,A',B,B')$ over all possible partitions. The minimum value (divided by $8G_N$), called the *entanglement wedge mutual information* (entanglement wedge mutual information), is denoted by E_M,

$$E_M(A:B) := \min_{A'\cup B'} f^Q(A,A',B,B'). \tag{5.21}$$

The entanglement wedge mutual information is the possible counterpart of E_Q. An example is depicted in the Fig.5.1.

There are many configurations of A' and B' appear in the minimization of f^Q, which makes the geometrical computation of E_M highly complicated in general. We found,

however, that this quantity can be represented by a simple formula based on the mutual information in all the cases we deal with here.

Expressions based on the mutual information

In fact, for two disjoint intervals in $\mathrm{AdS}_3/\mathrm{CFT}_2$, the symmetry of the setup leads to an expression

$$E_M(A:B) = \frac{1}{2}\min_M(\max\{I(A:M),\ I(B:M)\}), \tag{5.22}$$

where M corresponds to the cross section of the partition $A' \cup B'$. This is also valid e.g. in the Araki-Lieb transition configuration discussed below. This formula indicates a useful property

$$I(A:M^*) = I(B:M^*), \tag{5.23}$$

on (at least) one of the optimal cross section. We emphasize that the optimal purification M^* is not necessarily unique, nor does necessarily agree with that of E_W (Fig.5.1). Both examples will be described in the next subsection.

The formula (5.22) is not always true and must be generalized in more complicated configurations. For example, if we set $|B_1| > |B_2|$ in the Araki-Lieb saturating configuration, an optimal configuration is neither of $I(A:M^*)$ nor $I(B:M^*)$, but of a combination $I(A:M_A^*) + I(B:M_B^*)$ where $M_A^* \cup M_B^* = M$. This example indicates a formula

$$E_M(A:B) = \frac{1}{2}\min_{M_A \cup M_B = M}(\max\{I(A:M_A) + I(B:M_B)\}). \tag{5.24}$$

To our best knowledge, there is no counter example of this expression. These suggestive expressions clearly shows that the Q-correlation is a measure of correlation, which is difficult to read from the original definition. Proving or disproving this formula in generic configurations is an interesting future work.

Another suggestive form of E_M is

$$\begin{aligned} &E_M(A:B) \\ &= \frac{1}{2}\left[\frac{1}{2}I(A:B) + \min_{A' \cup B'}\left(S_{AA'} + \frac{I(A:B') + I(B:A')}{2}\right)\right], \end{aligned} \tag{5.25}$$

where we have used $S_{AB} = S_{A'B'} = S_{A'} + S_{B'}$ for A' and B' on the RT-surface. The optimization term is obviously larger than the entanglement wedge cross section.

In particular, the balancing condition (5.23) for the simple setups leads to $I(A:B^*) = I(B:A^*)$. Note that at least one of $I(A:B')$ or $I(B:A')$ must vanish for these setups, because $S_{AB'} < S_A + S_{B'}$ read to $S_{BA'} = S_B + S_{A'}$ and vice versa. Therefore both of

$I(A:B')$ and $I(B:A')$ should vanish for the balanced optimal partition, and then we have

$$E_M(A:B) = \frac{1}{2}\left[\frac{1}{2}I(A:B) + S_{AA_b^*}\right], \tag{5.26}$$

where A_b^* denotes the balanced optimal partition that is minimal and reaches $I(A:B^*) = I(B:A^*)$. This is nothing but an average of $\frac{1}{2}I$ and the cross-section $S_{AA_b^*}$. When the balanced optimal partition of E_M is equivalent to that of E_W, we will have

$$E_M(A:B) = \frac{1}{2}\left[\frac{1}{2}I(A:B) + E_W\right]. \tag{5.27}$$

Roughly speaking, the E_M is an average of $\frac{1}{2}I$ and E_W with a deviation due to the term $S_{BA'}$ in general. Then let us define the deviation by

$$D_b(A:B) := S_{AA_b^*} - E_W(A:B) \geq 0, \tag{5.28}$$

and

$$E_M(A:B) = \frac{1}{2}\left[\frac{1}{2}I(A:B) + E_W + D_b(A:B)\right]. \tag{5.29}$$

The validity of these formula will be checked by direct computation in the following discussion.

5.2.3 The property of the entanglement wedge mutual information

Now we investigate the detailed properties of the entanglement wedge mutual information. First, this quantity can not be greater than the E_W,

$$E_M \leq E_W. \tag{5.30}$$

This inequality is expected from $E_W = E_P$ and (5.19). Though this can be proven by drawing a picture, a simpler way is by the property of the von Neumann entropy (representing the area of the corresponding codimension-2 surfaces). Given the optimal partition of E_W by A_W^* and B_W^*, we have

$$E_W(A:B) = S_{AA_W^*} \geq \frac{1}{2}(S_A + S_B + S_{AA_W^*} - S_{BA_W^*}) \geq E_M(A:B), \tag{5.31}$$

where the strong subadditivity and the definition (5.21) were used.

Next, E_M is bounded from below by the half of the mutual information,

$$\frac{1}{2}I(A:B) \leq E_M(A:B). \tag{5.32}$$

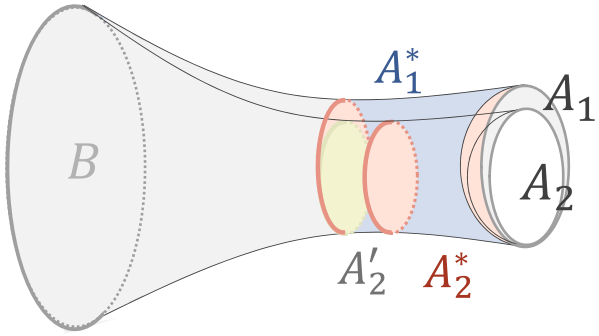

Figure 5.2: The extensivity $E_M(A_1 : B) \geq E_M(A_2 : B)$ for $A_1 \supset A_2$ is depicted in the figure. The B' labels are omitted for simplicity. The optimal partition A_1^* for A_1 naturally induces a partition A_2' on $\partial\mathcal{M}_{A_2B}$ so that $A_1^* \cap \gamma_{A_2B} = A_2' \cap \gamma_{A_2B}$. Then $E_M(A_1 : B) \geq f^Q(A_2, B, A_2')$ follows because of the minimality of RT-surface. Finally, $f^Q(A_2, B, A_2') \geq E_M(A_2 : B)$ is trivial by definition. (The figure is cited from [63])

This is clear from the definition for any optimal partition M^*,

$$
\begin{aligned}
& E_M(A : B) \\
&= \frac{1}{2}(S_A + S_B + S_{AA_M^*} - S_{BA_M^*}) && (5.33) \\
&= \frac{1}{2}I(A : B) + \frac{1}{2}(S_{AB} + S_{AA_M^*} - S_{BA_M^*}) && (5.34) \\
&\geq \frac{1}{2}I(A : B) + \frac{1}{2}(S_B + S_{A_M^*} - S_{BA_M^*}) \\
&\geq \frac{1}{2}I(A : B),
\end{aligned}
$$

where the strong additivity and the subadditivity were used.

These sandwich inequalities show that $E_M(A : B) = S_A = S_B$ for pure states, and that E_M vanishes if and only if the state is totally decoupled.

The extensivity $E_M(A_1 : B) \geq E_M(A_2 : B)$ for $A_1 \supset A_2$ can also be followed from the entanglement wedge nesting, see Fig.5.2 . The additivity $E_M(\rho_{A_1B_1} \otimes \sigma_{A_2B_2}) = E_M(\rho_{A_1B_1}) + E_M(\sigma_{A_2B_2})$ is obvious.

Conjecture All of these properties are consistent with these of E_Q. tempt us to propose the relation (at the leading order $O(N^2)$)

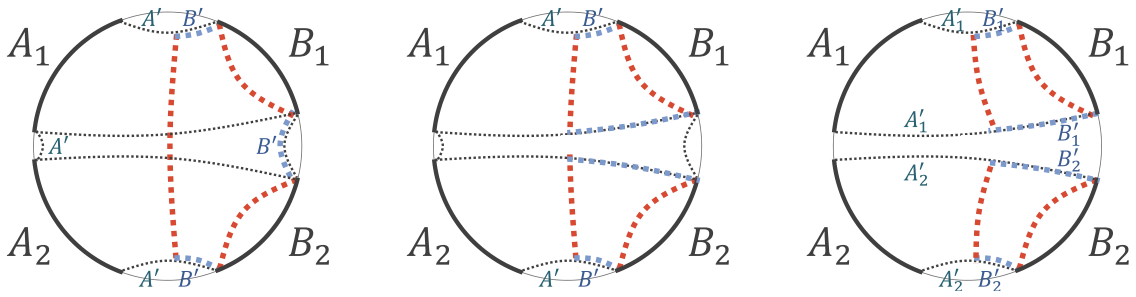

Figure 5.3: The proof of the strong superadditivity of the entanglement wedge mutual information. The areas with plus sign for red and minus sign for blue leads to (Left) $\geq$ (Middle) $\geq$ (Right). (The figure is cited from [63])

$$E_Q = E_M. \tag{5.35}$$

Remark that the entanglement wedge mutual information satisfies the strong superadditivity

$$E_M(\rho_{A_1A_2B_1B_2}) \geq E_M(\rho_{A_1B_1}) + E_M(\rho_{A_2B_2}). \tag{5.36}$$

This is the same property of E_W [32]. The geometrical proof is given in Fig.5.3 . This inequality (5.36) is not a property of E_Q, hence that will be a characteristic of holographic correlations as with the holographic entropy cone [68].

5.2.4 Examples in the AdS_3/CFT_2

In the pure AdS_3, the entanglement wedge mutual information for two disjoint intervals is given by Fig.5.4.

The optimal partition is obvious from the conformal symmetry, which coincides with that of E_W . The expression is (5.26),

$$E_M(A:B) = \frac{1}{2}\left[\frac{1}{2}I(A:B) + E_W(A:B)\right]. \tag{5.37}$$

All the properties of E_M mentioned above can be directly confirmed also by this form.

In generic setups, such as three or more multipartite intervals, or in the black hole geometry, the expression gets more complicated as we will see later.

5.2.5 The dual of R-correlation

The holographic dual of the R-correlation is introduced in the same manner replacing f^Q with f^R. It turns out, however, that this procedure gives nothing but the entanglement

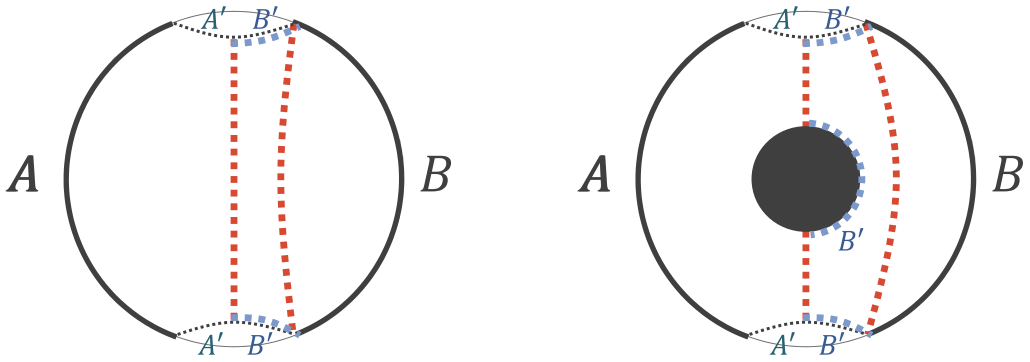

Figure 5.4: The E_M in the pure global AdS_3 (Left) and in the global BTZ (Right). The subsystems are taken as two disjoint intervals. (The figure is cited from [63])

wedge cross section again. A simple way to see this conclusion is to notice that one only need for the minimization to consider the ancillary systems A' and B' located on the RT-surface of S_{AB}. This has been used implicitly in the above discussion and can be proven geometrically.

In these configuration, we always have

$$I(A' : B') = S_{A'} + S_{B'} - S_{A'B'} \tag{5.38}$$
$$= S_{A'} + S_{B'} - S_{AB} \tag{5.39}$$
$$= 0, \tag{5.40}$$

since A' and B' should cover the all part of the Ryu-Takayanagi surface. Then it is obvious that

$$E_R = E_P, \tag{5.41}$$

from a form (5.20).

We also state it as a holographic proposal:

$$E_R = E_W. \tag{5.42}$$

Note that the additivity of the entanglement wedge cross section is consistent with that of the R-correlation, while the entanglement of purification is believed to be non-additive from numerical results [108].

5.3 A no-go theorem for the holographic entanglement measures

We have discussed the promising holographic duals of the information-theoretic quantities so far. The other view point would be that whether the geometrical objects, in particular

the entanglement wedge cross section and the entanglement wedge mutual information, can be dual of some information measures. Indeed, the mutual information seems to be degenerated to both the squashed entanglement and the CEMI under the geometrical extensions. That also strongly implies that quantum entanglement dominates holographic correlations. This observation tempts us to speculate that some of axiomatic entanglement measures could be equivalent to the entanglement wedge cross section or the entanglement wedge mutual information in holographic CFTs.

There is, however, a no-go theorem in this direction: the entanglement wedge cross section and the entanglement wedge mutual information can not be dual to the various quantum correlation measures. This is shown by noting that these geometrical quantities must be strictly larger than the information measures (at $O(N^2)$) in a configuration near to the holographic saturation of the Araki-Lieb inequality [109, 110]. These information measures include most of the axiomatic entanglement measures [82] as well as the quantum discord [111, 112]. This implies that the entanglement wedge itself captures more than quantum entanglement, encoding classical correlations as well geometrically.

5.3.1 The phase transition of the mutual information

First of all, we note the upper bounds on the entanglement measures,

$$E_D(A:B) \leq I(A:B), \tag{5.43}$$
$$E_{RE}(A:B) \leq I(A:B), \tag{5.44}$$
$$E_{sq}(A:B) \leq I(A:B), \tag{5.45}$$
$$E_I(A:B) \leq I(A:B), \tag{5.46}$$

where E_D is the distillable entanglement, E_{RE} is the relative entropy of entanglement. There is also an upper bound on the quantum discord

$$D_q(A:B) \leq I(A:B). \tag{5.47}$$

This type of upper bound is already enough to exclude the possibility that the quantum correlation measures are dual to the entanglement wedge cross section or the entanglement wedge mutual information. That can be seen in a configuration of

$$E_W(A:B) > I(A:B), \tag{5.48}$$
$$E_M(A:B) > I(A:B), \tag{5.49}$$

at the leading order $O(N^2)$ near to the phase transition of the mutual information [32]. This contradicts the generic upper bounds by the mutual information for the correlation measures. In fact, the same discussion holds any type of bipartite information measure E_X that satisfies

$$E_X(A:B) \leq \alpha I(A:B), \tag{5.50}$$

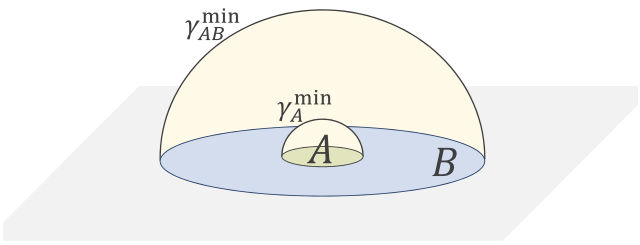

Figure 5.5: The boundary subsystems and the Ryu-Takayanagi surfaces in AdS_4/CFT_3, in which the Araki-Lieb inequality is saturated $S_A + S_{AB} = S_B$. (The figure is cited from [63])

where α is arbitrary constant.

Note that the E_C and E_F can possibly exceed $I(A:B)$, so they are not excluded by this method. In fact, they can be greater than $\frac{1}{2}I(A:B)$ [113].

5.3.2 The phase transition of the Araki-Lieb inequality

The Araki-Lieb inequality

$$S_A + S_{AB} \geq S_B, \tag{5.51}$$

can be saturated in certain configurations in holographic CFTs at the leading order $O(N^2)$ [109, 110]. A typical case is taking the subsystem A totally surrounded by the sufficiently large B (Fig.5.5)

. Suppose one shrinks the size of the subsystem B gradually, then the phase transition of the Ryu-Takayanagi surface of S_B occurs at some point. Then the saturation will turn into the strict inequality $S_A + S_{AB} > S_B$. We call this type of phase transition by the Araki-Lieb phase transition.

Let us focus on a configuration in the Poincaré AdS_3 for simplicity. The metric is given by

$$ds^2 = \frac{dz^2 - dt^2 + dx^2}{z^2}. \tag{5.52}$$

The subsystems A and B are taken to be symmetric, given by $A = [-a, a],\ B = [-b, -a] \cup [a, b] \equiv B_1 \cup B_2$ for $0 < a < b$ (see Fig.5.6). The relative size of subsystems is denoted by

$$p := \frac{a}{b},\ (0 < p < 1) \tag{5.53}$$

The two types of the mutual information

$$I(A : B_1B_2) = S_A + S_{B_1B_2} - S_{AB_1B_2}, \tag{5.54}$$
$$I(B_1 : B_2) = S_{B_1} + S_{B_2} - S_{B_1B_2}, \tag{5.55}$$

exhibit the phase transition due to the term $S_{B_1B_2}$. If p is sufficiently small, the connected phase $I(B_1 : B_2) > 0$ is preferred. If p is large, the disconnected phase $I(B_1 : B_2) = 0$ is. The terms S_A and $S_{AB_1B_2}$ have the single configurations, and thus there is no phase transition for them. Then $I(A : B_1B_2)$ can be computed as

$$I(A : B_1B_2) = \min\{\frac{2c}{3}\log\frac{2a}{\epsilon}, \frac{2c}{3}\log\frac{\sqrt{a/b}(b-a)}{\epsilon}\},$$

where c is the central charge of holographic 2d CFTs, and ϵ is the UV cutoff. The mutual information is divergent, while that is usually a finite quantity in field theories, because we are dealing with the adjacent limit of A and B.

The phase transition point of $I(A : B_1B_2)$ (i.e. of $S_{B_1B_2}$) is given by

$$p^*_{\rm MI} \equiv \frac{a^*_{\rm MI}(b)}{b} = 3 - 2\sqrt{2}. \tag{5.56}$$

Then we have the Araki-Lieb transition with respect to p by

$$S_{B_1B_2} = S_A + S_{AB_1B_2},\ (0 < p < p^*_{\rm MI}), \tag{5.57}$$
$$S_{B_1B_2} < S_A + S_{AB_1B_2},\ (p^*_{\rm MI} < p < 1). \tag{5.58}$$

In other words, there is a phase transition of the half of the mutual information $I(A : B_1B_2)$ as

$$\frac{1}{2}I(A : B_1B_2) = S_A,\ (0 < p < p^*_{\rm MI}), \tag{5.59}$$
$$\frac{1}{2}I(A : B_1B_2) < S_A,\ (p^*_{\rm MI} < p < 1). \tag{5.60}$$

5.3.3 The phase transition of the entanglement wedge cross section

Next, in the same setup, the $E_W(A : B)$ also enjoys a phase transition as depicted in Fig.5.6. In the left phase, the $E_W(A : B)$ just returns to S_A. In the right phase, the $E_W(A : B)$ consists of two disconnected surfaces that is equivalent to $E_W(AB_1 : B_2)$. Then the value is given by

$$\begin{aligned} E_W(A : B_1B_2) &= \min\{S_A,\ 2E_W(AB_1 : B_2)\} \\ &= \min\{\frac{c}{3}\log\frac{2a}{\epsilon},\ \frac{c}{3}\log[\frac{b^2-a^2}{b\epsilon}]\}. \end{aligned} \tag{5.61}$$

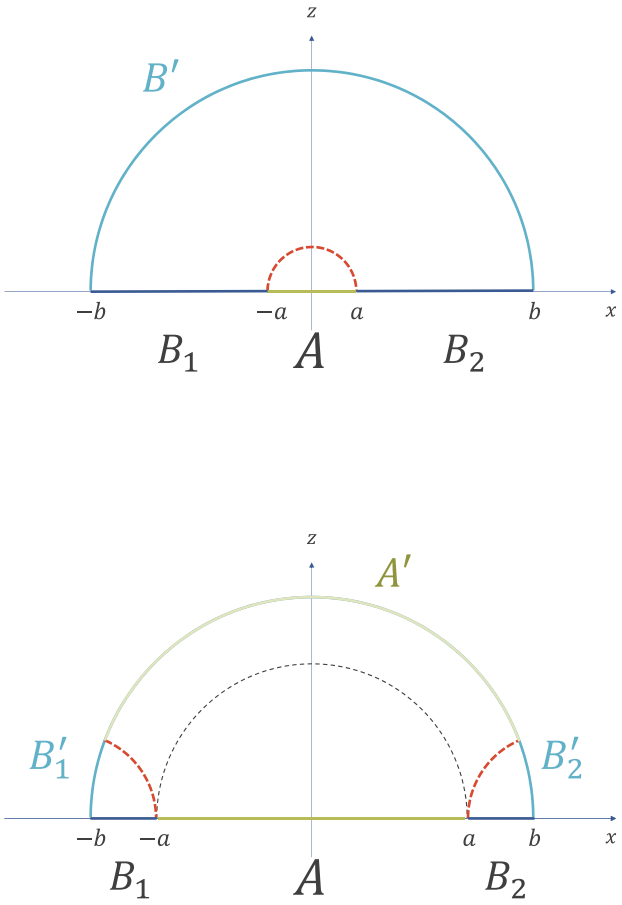

Figure 5.6: The two phases of the $E_W(A : B_1B_2)$ depicted by the orange dashed line. The left (right) configuration is preferred if $p < p^*_{\text{EW}}$ ($p > p^*_{\text{EW}}$). The symbols with a prime $'$ denote the partition of the Ryu-Takayanagi surface so that $\mathcal{A} = A \cup A'$ and $\mathcal{B} = B_1 \cup B_2 \cup B'_1 \cup B'_2$. (The figure is cited from [63])

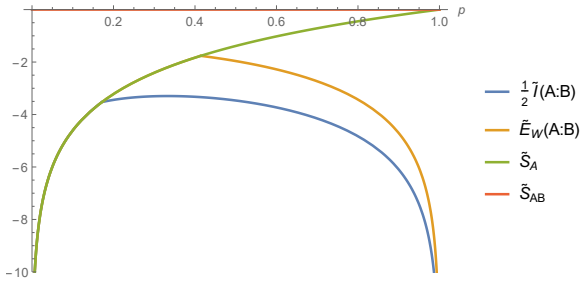

Figure 5.7: The half of the mutual information $\frac{1}{2}I(A:B_1B_2)$ and the entanglement wedge cross section $E_W(A:B_1B_2)$ in the Araki-Lieb transition. The UV divergent parts are normalized by subtracting S_{AB}. (The figure is cited from [63])

The phase transition of the entanglement wedge cross section therefore occurs at the critical point

$$p^*_{\rm EW} \equiv \frac{a^*_{\rm EW}(b)}{b} = \sqrt{2}-1. \tag{5.62}$$

We again have the two phases of the entanglement wedge cross section

$$E_W(A:B_1B_2) = S_A, \ \ (0 < p < p^*_{\rm EW}), \tag{5.63}$$
$$E_W(A:B_1B_2) < S_A, \ \ (p^*_{\rm EW} < p < 1). \tag{5.64}$$

The key observation is that the phase transition point of the Araki-Lieb transition does not match with that of the entanglement wedge cross section. The results above indicate $p^*_{\rm MI} < p^*_{\rm EW}$. The dependence on p of these quantity is plotted in Fig.5.7.

In particular, for or $p \in (p^*_{\rm MI}, p^*_{\rm EW})$, the entanglement wedge cross section saturates the upper bound $E_W(A:B) = S_A$ while the Araki-Lieb inequality is *not* saturated:

$$E_W(A:B) = S_A \text{ and } S_A + S_{AB} > S_B \text{ for } p^*_{\rm MI} \le p \le p^*_{\rm EW}. \tag{5.65}$$

This provides the crucial argument for any correlation measure $E(A:B)$: if $E(A:B) = S_A$ inevitably leads to the saturation of the Araki-Lieb inequality $S_A + S_{AB} = S_B$ on generic states, then E can never be dual to the entanglement wedge cross section. This property is indeed a common feature for various type of quantum correlation measures.

Note that the Araki-Lieb transition also happens in the global BTZ black hole

$$ds^2 = \frac{f^{-1}(z)dz^2 - f(z)dt^2 + dx^2}{z^2}, \tag{5.66}$$
$$f(z) = 1 - \frac{z^2}{z_H^2}, \tag{5.67}$$

with the inverse temperature $\beta = 2\pi z_H$. We impose the periodic boundary condition $x \simeq x + 2\pi$. The subsystems are chosen by $A = [-l/2, l/2]$ for $l \in (0, \pi)$ and B is the reminder. This system exhibits the Araki-Lieb saturation with respect to the size of A [109].

The phase transition points of the Araki-Lieb inequality and the entanglement wedge cross section can be computed in a similar way. We found

$$l^*_{\rm MI}(z_H) = \pi - z_H \log\cosh(\frac{\pi}{z_H}), \tag{5.68}$$

$$l^*_{\rm EW}(z_H) = 2z_H \log(1+\sqrt{2}). \tag{5.69}$$

This again indicates $l^*_{\rm MI}(z_H) \leq l^*_{\rm EW}(z_H)$ for any $z_H > 0$, and

$$E_W(A:B) = S_A \text{ and } S_A + S_{AB} > S_B \text{ for } l^*_{\rm MI} \leq l \leq l^*_{\rm EW}. \tag{5.70}$$

This is another example that confirms the above argument about the necessary condition for a correlation measure E.

5.3.4 The phase transition of the entanglement wedge mutual information

Finally, we study the phase transition of $E_M(A : B_1B_2)$ in the setups above. That will be a demonstration of the geometrical computation of the entanglement wedge mutual information.

Remark that $E_M(A : B_1B_2) = S_A$ should hold for $p < p^*_{\rm MI}$. That follows from the generic inequality

$$\frac{1}{2}I(A:B_1B_2) \leq E_M(A:B_1B_2) \leq E_W(A:B_1B_2), \tag{5.71}$$

and the previous result $\frac{1}{2}I(A : B_1B_2) = E_W(A : B_1B_2) = S_A$.

For $p > p^*_{\rm MI}$, the computation of the entanglement wedge mutual information is more complicated than the entanglement wedge cross section. There are now the four configurations of $S_{AA'} - S_{BA'}$ due to the symmetry of the system. Here we fix the size b to unit, dealing with the relative size p as the parameter for simplicity.

The two phases of $S_{AA'}$ and the two phases of $S_{BA'}$, are depicted in Fig.5.8. The ancillary subsystem A' is parameterized by $q \in (0, 1)$. Given the size p, our task is to seek the optimal configuration among them and the critical value $q^*(p)$ that gives the minimal value.

After some computations, the phase transition point q^* of $S_{AA'}$, or $S_{BA'}$, is given by

$$q^*_{AA'}(p) = \frac{(1-p)^2}{4p}, \tag{5.72}$$

$$q^*_{BA'}(p) = -\frac{1-6p+p^2}{(1+p)^2}, \tag{5.73}$$

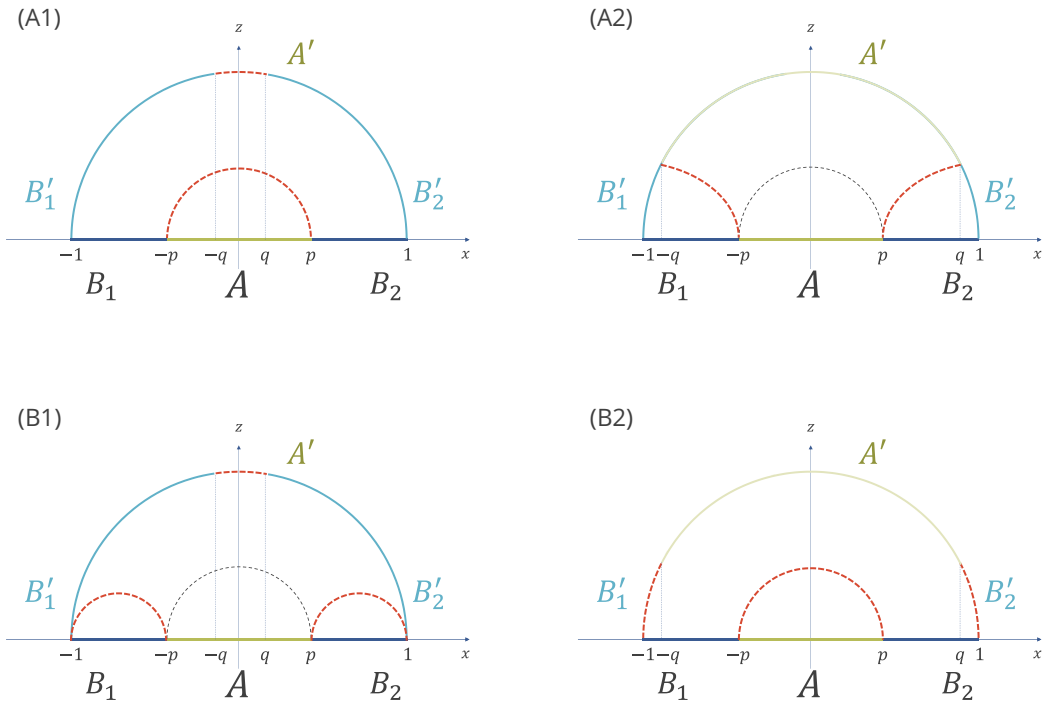

Figure 5.8: The two phases of $S_{AA'}$ (above panels) and the two phases of $S_{BA'}$ (below panels). The Ryu-Takayanagi surfaces are denoted by the red dashed lines. (The figure is cited from [63])

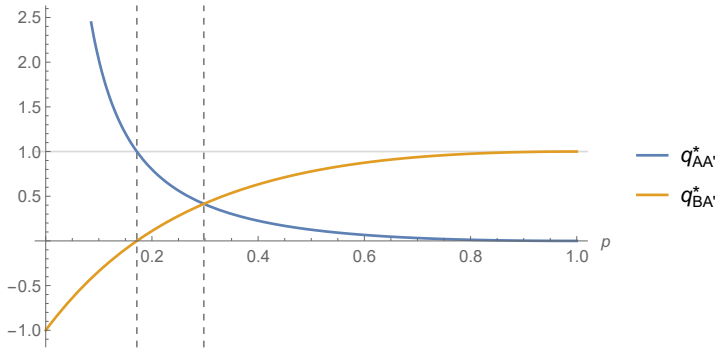

Figure 5.9: The phase transition point of $S_{AA'}$ (blue), and that of $S_{BA'}$ (yellow). The vertical dashed lines denote the critical points $p^*_{\mathrm{MI}} = 3 - 2\sqrt{2} \simeq 0.17$ and $p^*_{\mathrm{EM}} = -1 + 2\sqrt{2} - 2\sqrt{2-\sqrt{2}} \simeq 0.30$. (The figure is cited from [63])

respectively. They are plotted in Fig. 5.9. The region $q < q^*_{AA'}$ corresponds to the phase (A1), and $q^*_{AA'} < p$ does to the (A2) for $S_{AA'}$. Similarly, the region $q < q^*_{BA'}$ corresponds to the phase (B1), and $q^*_{BA'} < q$ does to the (B2) for $S_{BA'}$. The crossing point of $q^*_{AA'}(p)$ and $q^*_{BA'}(p)$ is denoted by $p^*_{\rm EM}$,

$$p^*_{\rm EM} = -1 + 2\sqrt{2} - 2\sqrt{2-\sqrt{2}} \simeq 0.30. \tag{5.74}$$

In order to find the minimal configuration, recall that the assumption $p > p^*_{\rm MI}$ leads to $I(B_1 : B_2) = S_{B_1} + S_{B_2} - S_{B_1B_2} = 0$. Then, in the small A' limit ($q \to 0$), one can show that the phase (A1) is preferred for $S_{AA'}$, and that the phase (B1) is for $S_{BA'}$. Similarly, in the large A' limit ($q \to 1$), the phase (A2) is preferred for $S_{AA'}$, and the phase (B2) is for $S_{BA'}$. This indicates that the phase transition happens as q is increased from 0 to 1 following either path

$$\text{(I)} \quad (\text{A1}, \text{B1}) \to (\text{A1}, \text{B2}) \to (\text{A2}, \text{B2}), \tag{5.75}$$

or

$$\text{(II)} \quad (\text{A1}, \text{B1}) \to (\text{A2}, \text{B1}) \to (\text{A2}, \text{B2}). \tag{5.76}$$

The path is determined by the value of p. The dependence of the critical points on p in Fig. 5.9 shows that the path (I) is chosen for the $p < p^*_{\rm EM}$ and the path (II) is for $p > p^*_{\rm EM}$.

Note that the target $S_{AA'} - S_{BA'}$ can decrease as increasing q only in the phase (A2, B1). In the phase (A1, B1), the size of A' does not affect at all. In the phase (A1, B2) and (A2, B2), the $S_{AA'} - S_{BA'}$ increases as the size of A' get increased. Then the path (II) is the only possibility that a nontrivial ($q \neq 0$) optimal partition for E_M can exist.

Therefore, for the $p < p^*_{\rm EM}$, the minimal configuration of the entanglement wedge mutual information is given by the trivial one $q = 0$ (or *any* size $q \leq q^*_{BA'}$), which leads to $E_M(A : B_1B_2) = S_A$. On the other hand, for the $p > p^*_{\rm EM}$, the non-trivial configuration (A2, B1) provides smaller value. The minimum is obtained at the q where the phase transition (A2, B1) to (A2, B2) occurs i.e. at $q^*_{BA'}(p)$. In this case, we can compute E_M for the optimal partition A^* as

$$\begin{aligned} E_M(A : B) &= \frac{1}{2}(S_A + S_B + S_{AA^*} - S_{BA^*}) \\ &= \frac{1}{2}(S_A - S_{A^*} + S_{AA^*}) \\ &= \frac{1}{2}(\frac{1}{2}(S_A + S_B - S_{AB}) + S_{AA^*}), \end{aligned} \tag{5.77}$$

where the properties

$$S_{BA^*} = S_B + S_{A^*}, \tag{5.78}$$

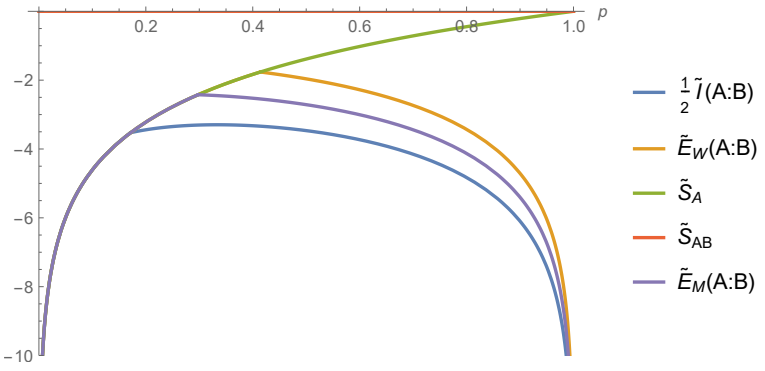

Figure 5.10: The phase transition of the $E_M(A : B_1B_2)$. The all quantities in the plot are normalized by subtracting S_{AB}. (The figure is cited from [63])

as in the (A2) phase, and

$$S_{A^*} = \frac{1}{2}(S_A + S_{AB} - S_B), \tag{5.79}$$

followed by the equality condition (B1)=(B2) were used.

Then the E_M is given by

$$E_M(A : B_1B_2) = \begin{cases} S_A & (p < p^*_{\mathrm{EM}}) \\ \frac{1}{2}\left[\frac{1}{2}I(A : B_1B_2) + S_{AA^*}(p, q^*_{BA'}(p))\right] & (p > p^*_{\mathrm{EM}}) \end{cases}, \tag{5.80}$$

where $S_{AA^*}(p, q^*_{BA'}(p))$ represents the contribution from the geodesics connecting ∂A and ∂A^*, given by

$$S_{AA^*}(p, q^*_{BA'}(p)) = \frac{c}{3}\log\left(\frac{(1-p)(1+6p+p^2)}{4\sqrt{p}\epsilon}\right). \tag{5.81}$$

The plot of E_M is given in Fig.5.10. This result (5.80) confirms the short-cut formula (5.26). In the above discussion, the condition (B1)=(B2) corresponds to the balancing condition $I(A : M^*) = I(B : M^*)$. Note that the balanced optimal partition for $p \in (p^*_{\mathrm{MI}}, p^*_{\mathrm{EM}})$ is the A' of the size $q = q^*_{BA'}(p)$, not $q = 0$. Both of them give the optimal value $E_M(A : B_1B_2) = S_A$. This is an example of non-uniqueness of the optimal partition of the entanglement wedge mutual information.

The deviation (5.28) in this case is given by

$$D_b(p) = S_{AA^*}(p, q^*_{BA'}) - E_W(p) = \frac{c}{3}\log\frac{1+6p+p^2}{4\sqrt{p}(1+p)} \ (p > p^*_{\mathrm{EW}}). \tag{5.82}$$

The plot of D_b is given in Fig.5.11. The positive deviation $D_b(p) > 0$ implies that the optimal partition of the entanglement wedge cross section and that of the entanglement wedge mutual information is different. The difference will disappear as $p \to 1$.

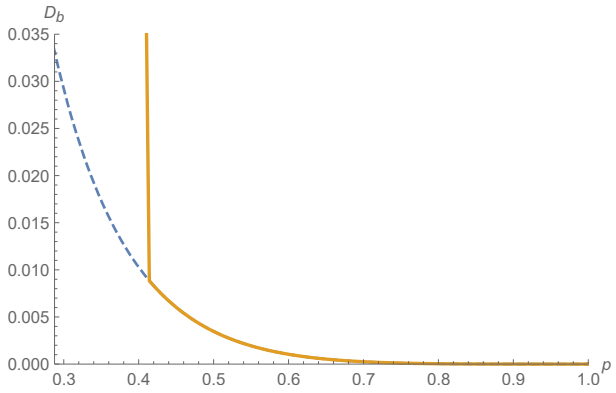

Figure 5.11: The deviation D_b of the phase transition of the entanglement wedge mutual information. The yellow solid line denotes the configuration $p^*_{\mathrm{EW}} \leq p$, and the blue dashed line does $p^*_{\mathrm{EM}} \leq p \leq p^*_{\mathrm{EW}}$. (The figure is cited from [63])

We rephrase the important results

$$E_M(A : B_1B_2) = S_A, \ (0 < p < p^*_{\mathrm{EM}}), \tag{5.83}$$
$$E_M(A : B_1B_2) < S_A, \ (p^*_{\mathrm{EM}} < p < 1). \tag{5.84}$$

This leads to the same conclusion again for a correlation measure $E(A : B)$: if $E(A : B) = S_A$ inevitably leads to the saturation of the Araki-Lieb inequality $S_A + S_{AB} = S_B$ on generic states, then E can never be dual to the entanglement wedge mutual information.

Remark that the E_M exhibits the same type of phase transition in the global BTZ black hole, which results in the same argument.

5.3.5 The Axiomatic Entanglement Measures and the Araki-Lieb Saturation

We now state a no-go theorem applicable to wide class of correlation measures. The following is a purely information theoretical statement.

Proposition 14. *Suppose that a quantum correlation measure $E(A : B)$ on $\mathcal{H}_{AB} = \mathcal{H}_A \otimes \mathcal{H}_B$ satisfies the following properties:*
(i) The monotonicity $E(A : B_1B_2) \geq E(A : B_1)$,
(ii) $E(A : B) = S_A = S_B$ for pure states,
(iii) $E(A : B) \leq E_F(A : B)$ $(\leq \min\{S_A, S_B\})$ for generic states.
Then the saturation $E(A : B) = S_A$ is equivalent to the Araki-Lieb saturation $S_A + S_{AB} = S_B$ on generic states.

Proof. First, the saturation $E(A : B) = S_A$ leads to $E_F(A : B) = S_A$ by the upper bound on E_F (iii). That is equivalent to the Araki-Lieb saturation [114]. Next, the opposite is

shown by the uniquely determined structure (up to isometries) of states saturating the Araki-Lieb inequality [115]

$$\rho_{AB} = |\psi\rangle\langle\psi|_{AB_L} \otimes \rho_{B_R}, \tag{5.85}$$

where the Hilbert space $\mathcal{H}_B$ is decomposed into $\mathcal{H}_B = \mathcal{H}_{B_L} \otimes \mathcal{H}_{B_R}$. Then we have

$$S_A \geq E(A : B_L B_R) \geq E(A : B_L) = S_A, \tag{5.86}$$

from the properties of (i) and (ii). □

Then the observation of the Araki-Lieb transitions in holography leads to the theorem.

Theorem 15. *Suppose that a quantum correlation measure $E(A : B)$ on $\mathcal{H}_{AB} = \mathcal{H}_A \otimes \mathcal{H}_B$ satisfies the properties in the above proposition. Then E can never be dual to the entanglement wedge cross section nor the entanglement wedge mutual information.*

This class of correlation measures includes the E_{RE}, E_D, E_{sq}, E_I, as well as the entanglement cost E_C, and the entanglement of formation E_F itself. Thus these information measures can not be a dual candidate of the entanglement wedge cross section or the entanglement wedge mutual information.

Note that this class of entanglement measures must be *strictly less* than E_W (or E_M) for the states of $p \in (p^*_{\mathrm{MI}}, p^*_{\mathrm{EW}})$ (or $p \in (p^*_{\mathrm{MI}}, p^*_{\mathrm{EM}})$). That is because in these region we have

$$E(A : B) < S_A = E_W(A : B) \quad (p^*_{\mathrm{MI}} < p < p^*_{\mathrm{EW}}), \tag{5.87}$$

$$E(A : B) < S_A = E_M(A : B) \quad (p^*_{\mathrm{MI}} < p < p^*_{\mathrm{EM}}). \tag{5.88}$$

Then the entanglement wedge cross section and the entanglement wedge mutual information are generically larger than these entanglement measures in holographic CFTs, unless these 1-parametrized states are singular among the holographic states.

5.3.6 Interpretation from the Holographic Entanglement of Purification

In contrast to the entanglement measures, the entanglement of purification, the Q-correlation, and the R-correlation evade the above no-go theorem. That is because the criteria (iii) is not true for them, and they can be still a possible dual of the entanglement wedge cross section or the entanglement wedge mutual information. Notably, the flower state satisfies $E_P(A : B) = S_A$ without the Araki-Lieb saturation. Similarly, the logarithmic negativity, the odd entropy, and the reflected entropy do not satisfy (iii).

Furthermore, there is interpretation of the behavior of the entanglement wedge cross section in the phase transition. There is a remarkable geometrical equality after the phase transition $p > p^*_{\mathrm{EW}}$,

$$E_W(A : B_1 B_2) = E_W(AB_1 : B_2) + E_W(AB_2 : B_1). \tag{5.89}$$

In fact, for $p > p^*_{\rm EW}$, we have $I(\mathcal{B}_1 : \mathcal{B}_2) = 0$ where $\mathcal{B}_1 = B_1 \cup B'_1$ and $\mathcal{B}_2 = B_2 \cup B'_2$. That implies the decoupled form

$$\rho_{\mathcal{B}_1\mathcal{B}_2} = \rho_{\mathcal{B}_1} \otimes \rho_{\mathcal{B}_2}. \tag{5.90}$$

From the information-threoretical point of view, any purification of this state must have the unique form [116]

$$|\psi\rangle_{\mathcal{A}\mathcal{B}_1\mathcal{B}_2} = |\phi^1\rangle_{\mathcal{A}\mathcal{B}_1} \otimes |\phi^2\rangle_{\mathcal{A}\mathcal{B}_2}\,, \tag{5.91}$$

up to the isometries on $\mathcal{H}_{\mathcal{A}}$ that are irrelevant to the correlation between A and B. In other words, all possible purification of $\rho_{\mathcal{B}_1\mathcal{B}_2}$ can be transformed to the decoupled purification by an appropriate decomposition of $\mathcal{A}$. This type of the purifications is clearly compatible with the equality (5.89).

On the other hand, for $p < p^*_{\rm EW}$, the remaining correlation $I(\mathcal{B}_1 : \mathcal{B}_2) > 0$ may drastically change the structure of purifications, results in the optimal purification by just setting A' empty. In this sense, the phase transition point $p^*_{\rm EW}$ is the point at which the optimal purification switches from the standard purification to the decoupled purification (5.91). This type of switching was indeed observed in the numerical study in the section 4.

6 Conclusion

We finally summarize the previous discussions and make some comments on the future directions.

First, in the section 3, we introduced a multipartite correlation measure both in quantum information theory and in the AdS geometries. That is a generalization of the entanglement of purification, or the entanglement wedge cross section, for multipartite states. We proved the various properties of them, that are consistent with the proposal for arbitrary n-partite cases. These multipartite setups are also shown to be compatible with the picture of bit-threads formalism [59]. It would be interesting to prove these properties on time-dependent backgrounds. The multipartite entropic inequalities in covariant cases were discussed in [65], where it was pointed out that some new techniques (apart from the maximin surfaces [70]) is needed for $n \geq 5$. Looking for new properties satisfied by the multipartite entanglement wedge cross section but not always by the multipartite entanglement of purification, will provide new constraints on holographic states. We also expect that there is an operational interpretation for the multipartite entanglement of purification based on (S)LOCC.

Next, in the section 4, we presented numerical computations of the entanglement of purification in free scalar field theories and in the spin chain models. There is a common feature that the entanglement of purification can be enhanced with the physical distance d, which is highly comparative with all the other correlation measures. We gave an explanation of this behavior based on the different sensitivities to quantum and classical correlation. There the entanglement of purification is expected to be more sensitive to classical correlations than the mutual information is. We also found the Z_2 reflection symmetry breaking in the optimal purifications. In the transverse-field Ising model, especially, the Z_2-broken region coincides with the ferromagnetic phase. Further studies on this direction are given in [117], there much larger subsystem size are taken into account. These numerical methods are also applicable to the other optimized correlation measures such as the squashed entanglement.

Finally, in the section 5, we comprehensively discussed the holographic duals to the optimized correlation measures. That derives a new geometrical quantity, the entanglement wedge mutual information, as a dual of Q-correlation. The crucial assumption of the equivalence is that the geometrical extensions are enough to achieve their minimum in holographic CFTs. Their properties are completely consistent with the original information-theoretic measures. We also showed that the two plausible geometrical measures of correlation, the entanglement wedge cross section and the entanglement wedge mutual information, are strictly larger than all of the axiomatic entanglement measures in the Araki-Lieb transition. In addition, they do not satisfy the monogamy but do the strong superadditivity, where the latter is the weaker property of quantum entanglement than the former. These observations tempt us to assume that these measures are sensitive to classical correlations even in holographic CFTs; the same conclusion obtained in the

field-theoretic studies for the entanglement of purification. Then it will be an interesting future work to investigate a role of classical correlation (e.g. separable states) in holographic CFTs. The multipartite generalization of these measures would also provide a new tool to probe a specific aspect of the holographic correlations, which was done for $n = 3$ case [30].

We remark that all of our discussions are restricted to the leading order $O(N^2)$. In particular, the discussion about the Araki-Lieb phase transition relies on the saturation of the holographic entanglement entropy at this order. Including quantum corrections from the bulk entanglement entropy will violate the exact saturation at $O(N^0)$ [118, 119], and the structure of state (5.85) is not robust against small corrections [120].

Acknowledgment

I would like to greatly thank my supervisor Tadashi Takayanagi for his encouragement and support throughout my PhD program. The great time I had collaborating with him on a variety of topics is an invaluable asset to me.

I am also grateful to my excellent collaborators, Arpan Bhattacharyya, Pawel Caputa, Alexander Jahn, Yuya Kusuki, Masamichi Miyaji, Yuki Suzuki, Tomonori Ugajin, and Yang Zhou for a lot of stimulating discussions. I also thank to Jan Boruch, Jesse C. Cresswell, Souvik Dutta, Kanato Goto, Jonathan Harper, Naotaka Kubo, Nilay Kundu, Yoshifumi Nakata, Masahiro Nozaki, Tokiro Numasawa, Kotaro Tamaoka, Massimiliano Rota, Kento Watanabe, and Zixia Wei for fruitful discussions and comments. I also thank to my colleagues and staff in Yukawa Institute for Theoretical Physics and in Department of Physics in Kyoto University for their long-standing support and the enjoyable time.

These works were supported by Grant-in-Aid for JSPS Fellows No.18J22888.

7 Appendix

7.1 Appendix A: The logarithmic negativity in Free Scalar Field Theory

One simple characterization of quantum entanglement between subsystems A and B for a mixed state ρ_{AB} is the logarithmic negativity [100]. A criteria of existence of quantum entanglement is given by the partial transposition Γ_B, which is the transposition acting only for the subsystem B. For separable states, the partially transposed density matrix $\rho_{AB}^{\Gamma_B}$ must be non-negative, while for non separable states this property is not preserved in general. Thus if $\rho_{AB}^{\Gamma_B}$ is negative, the subsystem A and B must be entangled. We can not, however, say there is no entanglement even if $\rho_{AB}^{\Gamma_B}$ is non-negative. This kind of criteria are called entanglement witness.

The logarithmic negativity is a famous example of entanglement witness, defined by

$$\mathcal{E}_N(\rho_{AB}) = \log ||\rho_{AB}^{\Gamma_B}||_1, \tag{7.1}$$

where we introduced the trace norm

$$||\rho_{AB}^{\Gamma_B}||_1 = \mathrm{Tr}\sqrt{(\rho_{AB}^{\Gamma_B})^\dagger \rho_{AB}^{\Gamma_B}}, \tag{7.2}$$

Given the eigenvalues of $\rho_{AB}^{\Gamma_B}$ as λ_i, we can write

$$\mathcal{E}_N(\rho_{AB}) = \log\left(\sum_i |\lambda|\right). \tag{7.3}$$

It is clear from this expression that the logarithmic negativity is vanishing if and only if all the eigenvalues λ_i are non-negative. Note that the normalization $\sum_i \lambda = 1$ means $\sum_i |\lambda| \geq 1$, which leads to $\mathcal{E}_N \geq 0$. This quantity is known to be monotonic under LOCC. When the total state ρ_{AB} is pure, $\mathcal{E}_N(\rho_{AB})$ is not equal to the entanglement entropy S_A, but is equal to the $n = 1/2$ Rényi entropy defined by

$$S_A^{(1/2)} = 2\log \mathrm{Tr}(\rho_A)^{1/2}. \tag{7.4}$$

.

Now we compute the logarithmic negativity for the ground state Ψ_0 for the free scalar lattice model. We divide the total lattice system into subregions A, B and E such that $\mathcal{H}_{tot} = \mathcal{H}_A \otimes \mathcal{H}_B \otimes \mathcal{H}_E$. In this setup, we wish to compute the logarithmic negativity $\mathcal{E}_N(A:B)$ which measures the quantum entanglement between A and B. First remember that the reduced density matrix ρ_{AB} is given by (4.5). For later purpose, it is useful to decompose M and N, which are $(|A|+|B|)\times(|A|+|B|)$ matrices, into $|A|\times|A|$,$|A|\times|B|$ and $|B|\times|B|$ matrices as follows:

$$M = \begin{pmatrix} M_1 & M_2 \\ M_2^T & M_3 \end{pmatrix},\ N = \begin{pmatrix} N_1 & N_2 \\ N_2^T & N_3 \end{pmatrix}. \tag{7.5}$$

Given this density matrix we now proceed to compute $\mathcal{E}_N(A:B)$. We have to first perform the partial transpose Γ_B, which is equivalent to interchanging ϕ_B and ϕ'_B. After we rearrange this as a matrix whose arguments are of the form $\phi_{AB} = (\phi_A, \phi_B)$, $\phi'_{AB} = (\phi'_A, \phi'_B)$, we obtain:

$$\rho_{AB}^{\Gamma_B}[\phi_{AB}, \phi'_{AB}] \propto \exp\left(-\frac{1}{2}\phi_{AB}M\phi_{AB}^T - \frac{1}{2}\phi'_{AB}M(\phi'_{AB})^T - \frac{1}{4}(\phi_{AB} - \phi'_{AB})\tilde{N}(\phi_{AB} - \phi'_{AB})^T\right), \tag{7.6}$$

where

$$\tilde{N} = \begin{pmatrix} N_1 & -N_2 - 2M_2 \\ -N_2^T - 2M_2^T & N_3 \end{pmatrix}. \tag{7.7}$$

Now we can perform a field redefinition,

$$\hat{\phi}_{AB} := M_D^{\frac{1}{2}} V \phi_{AB}, \tag{7.8}$$

where V is a orthogonal matrix and M_D is a diagonal matrix so that we have

$$M = V^T M_D V. \tag{7.9}$$

We apply the same transformation on ϕ'_{AB}. Then we find

$$\rho_{AB}^{\Gamma_B}[\hat{\phi}_{AB}, \hat{\phi}'_{AB}] \propto \exp\left(-\frac{1}{2}\hat{\phi}_{AB}\hat{\phi}_{AB}^T - \frac{1}{2}\hat{\phi}'_{AB}(\hat{\phi}'_{AB})^T - \frac{1}{4}(\hat{\phi}_{AB} - \hat{\phi}'_{AB})\tilde{N}'(\hat{\phi}_{AB} - \hat{\phi}'_{AB})^T\right), \tag{7.10}$$

where

$$N' = M_D^{-\frac{1}{2}} V \tilde{N} V^T M_D^{-\frac{1}{2}} \tag{7.11}$$

In order to diagonalize N' we perform another transformation,

$$\tilde{\phi}_{AB} = S\hat{\phi}_{AB}, \tag{7.12}$$

where S is another orthogonal matrix. Finally, up to a normalization factor, we have

$$\rho_{AB}^{\Gamma_B}[\tilde{\phi}_{AB}, \tilde{\phi}'_{AB}] \propto \exp\left(-\frac{1}{2}\tilde{\phi}_{AB}(\tilde{\phi}_{AB})^T - \frac{1}{2}\tilde{\phi}'_{AB}(\tilde{\phi}'_{AB})^T - \frac{1}{4}(\tilde{\phi}_{AB} - \tilde{\phi}'_{AB})\hat{N}(\tilde{\phi}_{AB} - \tilde{\phi}'_{AB}w)^T\right), \tag{7.13}$$

where

$$\hat{N} = \begin{pmatrix} \mu_1 & & \\ & \ddots & \\ & & \mu_{|A|+|B|} \end{pmatrix}. \tag{7.14}$$

Here μ_i are the eigenvalues of the matrix $\tilde{N}'$, equivalently the eigenvalues of the matrix $M^{-1}\tilde{N}$. This is because we can write $\tilde{N}'$ as $\tilde{N}' = (\sqrt{M_D}V)M^{-1}\tilde{N}(\sqrt{M_D}V)^{-1}$.

Once we obtain these eigenvalues μ_i, we can calculate the logarithmic negativity in a similar way to the entanglement entropy in [98, 99]. As a simple toy model, consider a scalar ϕ (i.e. $N = 1$ as quantum mechanics) with the density matrix

$$\rho[\phi, \phi'] \propto \exp\left(-\frac{1}{2}(\phi^2 + \phi'^2) - \frac{\mu}{4}(\phi - \phi')^2\right). \tag{7.15}$$

We can diagonalize this matrix and find the eigenvalues

$$(1-\lambda)\lambda^m, \ (m = 0, 1, \dots), \tag{7.16}$$

where λ is defined by

$$\lambda = 1 + \frac{2(1 - \sqrt{1+\mu})}{\mu}. \tag{7.17}$$

Thus we obtain

$$\log ||\rho||_1 = \log\left[(1-\lambda)\sum_{k=0}^{\infty}|\lambda|^k\right] = \log\frac{1-\lambda}{1-|\lambda|}. \tag{7.18}$$

Now notice that $\rho_{AB}^{\Gamma_B}$ given by (7.13) can be regarded as $|A| + |B|$ copies of this kind of quantum mechanics. Thus, finally, we can evaluate the logarithmic negativity by

$$\mathcal{E}_N(A:B) = \sum_{i=1}^{|A|+|B|}\log\frac{1-\lambda_i}{1-|\lambda_i|}, \tag{7.19}$$

where

$$\lambda_i = 1 + \frac{2(1-\sqrt{1+\mu_i})}{\mu_i}. \tag{7.20}$$

7.2 Appendix B: The Scaling Properties in Free Scalar Field Theory

The scale invariance

$$E_P(w, d, m) = E_P(nw, nd, m), \ (n \in \mathbb{N}) \tag{7.21}$$

holds for small masses m and block widths $1 \ll w \ll N$, as that should correspond to the conformal limit. We find a power low $E_P(d, w, m \ll 1) = a(m)\,(d/w)^{-p(m)}$ in the continuous limit, with positive scaling coefficients $a(m)$ and $p(m)$ in Fig. 7.1. The $a(m)$ diverges logarithmically as $m \to 0$, while $p(m)$ converges sublinearly to zero.

In the conformal limit $m \ll 1$ and at distances $d \gg 0$ larger than the lattice spacing, we observe a power law scaling of the entanglement of purification E_P:

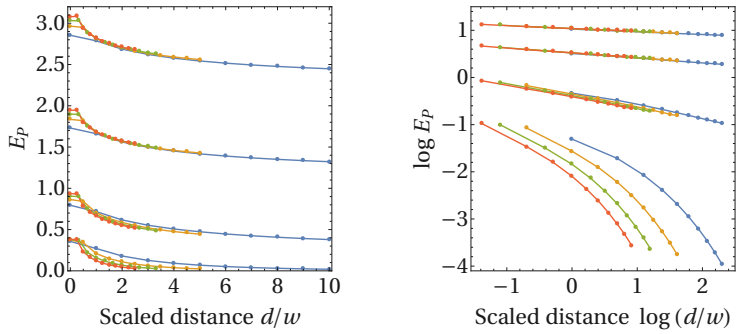

Figure 7.1: The $E_P(A:B)$ for $w = 1, 2, 3, 4$ (blue, yellow, green, red) for a mass $m = 10^{-1}, 10^{-2}, 10^{-3}, 10^{-4}$ (bottom to top) at $N = 60$. That is a function of d/w (left), and the same plot is also shown in log-log scaling (right). (The figure is cited from [61])

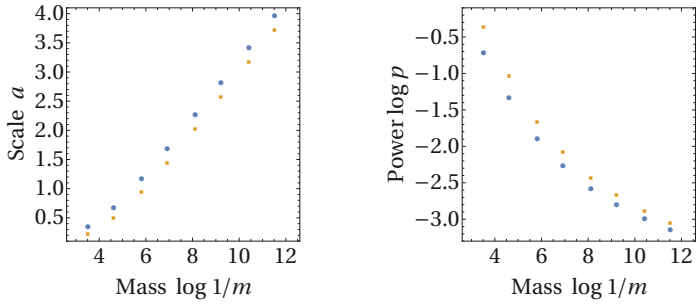

Figure 7.2: The coefficients $a(m)$ (left) and $p(m)$ (right) of a power law regression (7.22) for the entanglement of purification $E_P(A:B)$ (blue) and mutual information $I(A:B)$ (yellow) at $w = 3$, $1 \leq d \leq 10$. (The figure is cited from [61])

$$E_P(d, w, m) = a(m) \left(\frac{d}{w}\right)^{-p(m)} , \tag{7.22}$$

For $a(m)$ and $p(m)$ refer to Fig. 7.2. The mutual information also exhibits similar power law behavior in the same limits. The corresponding $a(m)$ and $p(m)$ are shown along with their EOP counterparts in Fig. 7.2. We observe that the entanglement of purification decays slower than the mutual information in this range.

7.3 Appendix C: Computing the EOP in Spin Chain

Given a bipartite state ρ_{AB} in a finite dimensional system, all possible purification of ρ_{AB} can be obtained by acting with local unitary operators on an arbitrary initial purification

$|\psi_0\rangle$,

$$|\psi(U_{A'B'})\rangle_{AA'BB'} = I_{AB} \otimes U_{A'B'} |\psi_0\rangle_{AA'BB'} . \tag{7.23}$$

One may use the standard purification

$$|\psi_{\rm std}\rangle_{AA'BB'} = \sum_i \sqrt{p_i} |i\rangle_{AB} |i\rangle_{A'} |0\rangle_{B'} , \tag{7.24}$$

or the canonical purification (4.24) as an initial purification. Note that we can embed a purification into a higher-dimensional Hilbert space. Therefore, the minimization of the entanglement of purification can be equivalently expressed in terms of unitary operators on the maximal purification $D_{A'} = D_{B'} = {\rm rank}\rho_{AB}$,

$$E_P(A:B) = \min_{\{U_{A'B'}, A'\cup B'\}} S(\rho_{AA'}), \tag{7.25}$$

$$\rho_{AA'} = {\rm Tr}_{BB'} \left[U_{A'B'} |\psi_0\rangle \langle\psi_0| U_{A'B'}^\dagger \right], \tag{7.26}$$

where where the minimization is also taken over all possible divisions of the ancilla Hilbert space into $\mathcal{H}_{A'}$ and $\mathcal{H}_{B'}$. The purifications have a trivial redundancy induced from a local unitary $U_{A'B'} = U_{A'} \otimes U_{B'}$, which does not affect $S_{AA'}$ at all. On the other hand, the optimal purification is (at least doubly) degenerated if one finds $S_{A'} \neq S_{B'}$.

7.3.1 Werner state

As an example, we deal with the Werner state on 2 qubits system following [34, 108]

$$\rho_{AB}(p) = \frac{p}{3} P_{\rm sym} + (1-p) P_{\rm asym} \tag{7.27}$$

$$= \frac{p}{3} I_4 + (1 - \frac{4p}{3}) |{\rm Bell}\rangle \langle{\rm Bell}| , \tag{7.28}$$

where $p \in [0,1]$ is a parameter of states, $P_{\rm sym}$ and $P_{\rm asym}$ are the projection operators onto the symmetric/anti-symmetric subspace in $\mathcal{H}_{AB}$

$$P_{\rm sym} = \begin{pmatrix} 1 & & & \\ & \frac{1}{2} & \frac{1}{2} & \\ & \frac{1}{2} & \frac{1}{2} & \\ & & & 1 \end{pmatrix}, \; P_{\rm asym} = \begin{pmatrix} 0 & & & \\ & \frac{1}{2} & -\frac{1}{2} & \\ & -\frac{1}{2} & \frac{1}{2} & \\ & & & 0 \end{pmatrix}, \tag{7.29}$$

in the $\{|00\rangle, |01\rangle, |10\rangle, |11\rangle\}$ basis. I_4 is the 4×4 identity matrix and

$$|{\rm Bell}\rangle := \frac{1}{\sqrt{2}} (|01\rangle - |10\rangle). \tag{7.30}$$

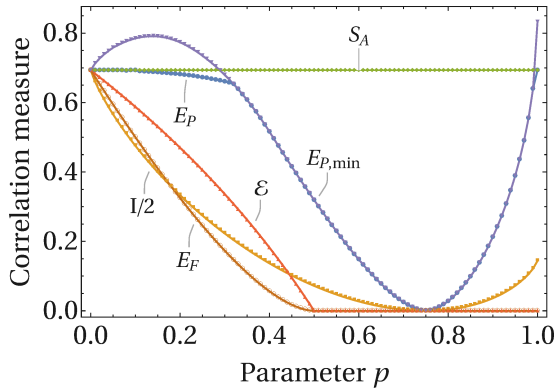

Figure 7.3: The E_P for the Werner state. There are shown the entanglement of formation E_F (from [121]), the logarithmic negativity $\mathcal{E}_N$, the mutual information $\frac{1}{2}I$, and the entanglement of purification under the minimal purifications $E_{P,\min}$. (The figure is cited from [61])

The Werner state can also be expressed in an isotropic form,

$$\rho_{AB}(p) = \frac{I}{4} + \frac{1}{4}(\frac{4p}{3} - 1) \sum_{i=x,y,z} \sigma_A^i \otimes \sigma_B^i, \tag{7.31}$$

and appears as the ground state of the anti-ferromagnetic Heisenberg model.

In order to find the entanglement of purification, we need to search at least $D_{A'}D_{B'} = \mathrm{rank}\rho_{AB} = 4$ and at most $D_{A'} = D_{B'} = 4$ for $p \neq 0, 1$. The result is shown in Fig. 7.3. It turns out that there are four different phases classified by the configuration of the optimal purifications:

(a) Non-minimal purification phase $0 \leq p \lesssim 0.319$, which requires $D_{A'} = 2$, $D_{B'} = 3$ (or $D_{A'} = D_{B'} = 3$),

(b) Minimal purification phase $0.319 \lesssim p \lesssim 0.401$, which requires $D_{A'} = D_{B'} = 2$,

(c) Canonical purification phase $0.401 \lesssim p \lesssim 0.995$, where the optimal purification is given by the canonical purification,

(d) Non-minimal purification phase $0.995 \lesssim p \lesssim 1$, which requires $D_{A'} = 2$, $D_{B'} = 4$.

These phase transitions are depicted in Fig. 7.4. In the phase (a), there are two non-equivalent optimal purifications, $D_{A'} = 2, D_{B'} = 3$ and $D_{A'} = D_{B'} = 3$, up to certain the numerical accuracy. In fact, they give the same value of $S_{AA'}$ up to 10 digits! In the phase (d), the EOP is strictly smaller than S_A (except $p = 1$), which is a more fine-grained structure than that found in the previous works [34, 108].

About the Z_2 symmetry breaking, the $S_{A'}$, $S_{B'}$ and $\frac{1}{2}I(A' : B')$ around the transition points $p_1 \simeq 0.319$ and $p_2 \simeq 0.401$ are shown in Fig. 7.5. It is clear from $S_{A'} \neq S_{B'}$ that the optimal purification breaks the Z_2 reflection symmetry in the phase (a). This phenomena

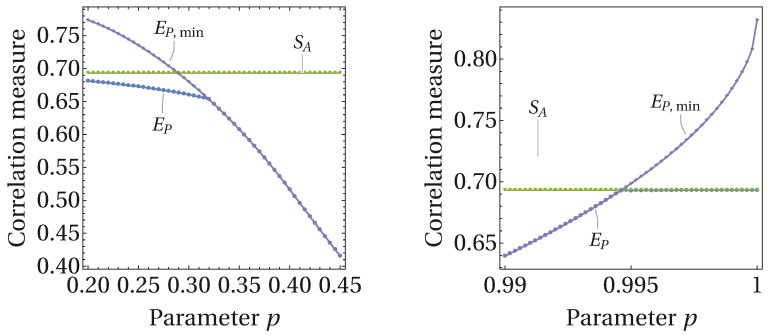

Figure 7.4: The detailed structure of the entanglement of purification for the Werner states of $0.2 \leq p \leq 0.45$ (left) and $0.99 \leq p \leq 1$ (right). There is a very tiny gap $S_A > E_P(A:B)$ in the phase (d) (except $p = 1$), though it is hard to observe them in the plot. (The figure is cited from [61])

is analogous to the free scalar field theory and the critical Ising spin chain. The symmetry is recovered and $S_{A'} = S_{B'}$ holds for phase (b) and (c). The Z_2 reflection symmetry is also broken in the phase (d).

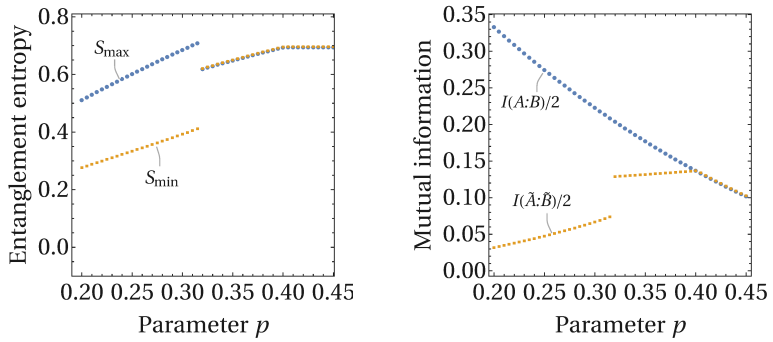

Figure 7.5: The Z_2 symmetry breaking, indicated by $S_{A'}$, $S_{B'}$ (left), and $I(A' : B')$ (right). There are two phase transition points at $p_1 \simeq 0.319$ and $p_2 \simeq 0.401$, which separate the phases (a) from (b), and (b) from (c), respectively. (The figure is cited from [61])

References

[1] Jacob D. Bekenstein. Black holes and entropy. *Phys. Rev. D*, 7:2333–2346, Apr 1973. 1

[2] S. W. Hawking. Particle Creation by Black Holes. *Commun. Math. Phys.*, 43:199–220, 1975. [,167(1975)]. 1

[3] Gerard 't Hooft. Dimensional reduction in quantum gravity. *Conf. Proc.*, C930308:284–296, 1993. 1

[4] Leonard Susskind. The World as a hologram. *J. Math. Phys.*, 36:6377–6396, 1995. 1

[5] Juan Martin Maldacena. The Large N limit of superconformal field theories and supergravity. *Int. J. Theor. Phys.*, 38:1113–1133, 1999. [Adv. Theor. Math. Phys.2,231(1998)]. 1

[6] Shinsei Ryu and Tadashi Takayanagi. Holographic derivation of entanglement entropy from AdS/CFT. *Phys. Rev. Lett.*, 96:181602, 2006. 1, 2.1

[7] Aitor Lewkowycz and Juan Maldacena. Generalized gravitational entropy. *JHEP*, 08:090, 2013. 1, 2.1

[8] Matthew J Donald, Michał Horodecki, and Oliver Rudolph. The uniqueness theorem for entanglement measures. *Journal of Mathematical Physics*, 43(9):4252–4272, 2002. 1, 3, 3.1.1

[9] Juan Martin Maldacena. Eternal black holes in anti-de Sitter. *JHEP*, 04:021, 2003. 1

[10] Veronika E. Hubeny, Mukund Rangamani, and Tadashi Takayanagi. A Covariant holographic entanglement entropy proposal. *JHEP*, 07:062, 2007. 1, 2.1

[11] Xi Dong, Aitor Lewkowycz, and Mukund Rangamani. Deriving covariant holographic entanglement. *JHEP*, 11:028, 2016. 1, 2.1

[12] Xi Dong. Holographic Entanglement Entropy for General Higher Derivative Gravity. *JHEP*, 01:044, 2014. 1

[13] Xi Dong and Aitor Lewkowycz. Entropy, Extremality, Euclidean Variations, and the Equations of Motion. 2017. 1

[14] Mark Van Raamsdonk. Comments on quantum gravity and entanglement. 2009. 1

[15] Mark Van Raamsdonk. Building up spacetime with quantum entanglement. *Gen. Rel. Grav.*, 42:2323–2329, 2010. [Int. J. Mod. Phys.D19,2429(2010)]. 1

[16] Juan Maldacena and Leonard Susskind. Cool horizons for entangled black holes. *Fortsch. Phys.*, 61:781–811, 2013. 1

[17] Mark Van Raamsdonk. Building up spacetime with quantum entanglement II: It from BC-bit. arXiv:1809.01197. 1

[18] David D. Blanco, Horacio Casini, Ling-Yan Hung, and Robert C. Myers. Relative Entropy and Holography. *JHEP*, 08:060, 2013. 1

[19] Daniel L. Jafferis, Aitor Lewkowycz, Juan Maldacena, and S. Josephine Suh. Relative entropy equals bulk relative entropy. *JHEP*, 06:004, 2016. 1

[20] Tadashi Takayanagi, Tomonori Ugajin, and Koji Umemoto. Towards an Entanglement Measure for Mixed States in CFTs Based on Relative Entropy. *JHEP*, 10:166, 2018. 1

[21] Masamichi Miyaji, Tokiro Numasawa, Noburo Shiba, Tadashi Takayanagi, and Kento Watanabe. Distance between Quantum States and Gauge-Gravity Duality. *Phys. Rev. Lett.*, 115(26):261602, 2015. 1

[22] Yuki Suzuki, Tadashi Takayanagi, and Koji Umemoto. Entanglement Wedges from the Information Metric in Conformal Field Theories. *Phys. Rev. Lett.*, 123(22):221601, 2019. 1

[23] Yuya Kusuki, Yuki Suzuki, Tadashi Takayanagi, and Koji Umemoto. Looking at Shadows of Entanglement Wedges. 12 2019. 1

[24] Pawel Caputa, Nilay Kundu, Masamichi Miyaji, Tadashi Takayanagi, and Kento Watanabe. Liouville Action as Path-Integral Complexity: From Continuous Tensor Networks to AdS/CFT. *JHEP*, 11:097, 2017. 1

[25] Ping Gao, Daniel Louis Jafferis, and Aron Wall. Traversable Wormholes via a Double Trace Deformation. *JHEP*, 12:151, 2017. 1

[26] Ahmed Almheiri, Xi Dong, and Daniel Harlow. Bulk Locality and Quantum Error Correction in AdS/CFT. *JHEP*, 04:163, 2015. 1

[27] Fernando Pastawski, Beni Yoshida, Daniel Harlow, and John Preskill. Holographic quantum error-correcting codes: Toy models for the bulk/boundary correspondence. *JHEP*, 06:149, 2015. 1

[28] Kotaro Tamaoka. Entanglement Wedge Cross Section from the Dual Density Matrix. *Phys. Rev. Lett.*, 122(14):141601, 2019. 1, 1, 2.4

[29] J. Levin and G. Smith. Optimized measures of bipartite quantum correlation. *IEEE Transactions on Information Theory*, 66(6):3520–3526, 2020. 1, 3.1.3, 3.1.4, 5, 9, 5.2.1

[30] Oliver DeWolfe, Joshua Levin, and Graeme Smith. Multipartite optimized correlation measures and holography. *Phys. Rev. D*, 102(6):066001, 2020. 1, 6

[31] Yoshifumi Nakata, Tadashi Takayanagi, Yusuke Taki, Kotaro Tamaoka, and Zixia Wei. Holographic Pseudo Entropy. 5 2020. 1

[32] Koji Umemoto and Tadashi Takayanagi. Entanglement of purification through holographic duality. *Nature Phys.*, 14(6):573–577, 2018. 1, 2.3, 2.3, 3.2.3, 5.2.3, 5.3.1

[33] Phuc Nguyen, Trithep Devakul, Matthew G. Halbasch, Michael P. Zaletel, and Brian Swingle. Entanglement of purification: from spin chains to holography. *JHEP*, 01:098, 2018. 1, 2.3

[34] Barbara M Terhal, Michał Horodecki, Debbie W Leung, and David P DiVincenzo. The entanglement of purification. *Journal of Mathematical Physics*, 43(9):4286–4298, 2002. 1, 2.4.1, 3.1.1, 3.1.1, 4, 4.3, 7.3.1, 7.3.1

[35] Hayato Hirai, Kotaro Tamaoka, and Tsuyoshi Yokoya. Towards Entanglement of Purification for Conformal Field Theories. *PTEP*, 2018(6):063B03, 2018. 1

[36] Ricardo Espíndola, Alberto Guijosa, and Juan F. Pedraza. Entanglement Wedge Reconstruction and Entanglement of Purification. *Eur. Phys. J.*, C78(8):646, 2018. 1

[37] Ning Bao, Aidan Chatwin-Davies, and Grant N. Remmen. Entanglement of Purification and Multiboundary Wormhole Geometries. *JHEP*, 02:110, 2019. 1

[38] Run-Qiu Yang, Cheng-Yong Zhang, and Wen-Ming Li. Holographic entanglement of purification for thermofield double states and thermal quench. *JHEP*, 01:114, 2019. 1

[39] Peng Liu, Yi Ling, Chao Niu, and Jian-Pin Wu. Entanglement of Purification in Holographic Systems. *JHEP*, 09:071, 2019. 1

[40] Wu-Zhong Guo. Entanglement of purification and projection operator in conformal field theories. *Phys. Lett.*, B797:134934, 2019. 1

[41] Mahdis Ghodrati, Xiao-Mei Kuang, Bin Wang, Cheng-Yong Zhang, and Yu-Ting Zhou. The connection between holographic entanglement and complexity of purification. *JHEP*, 09:009, 2019. 1

[42] Andrea Prudenziati. A geodesic Witten diagram description of holographic entanglement entropy and its quantum corrections. *JHEP*, 06:059, 2019. 1

[43] Ning Bao, Geoffrey Penington, Jonathan Sorce, and Aron C. Wall. Holographic Tensor Networks in Full AdS/CFT. arXiv:1902.10157. 1

[44] Komeil Babaei Velni, M. Reza Mohammadi Mozaffar, and M. H. Vahidinia. Some Aspects of Entanglement Wedge Cross-Section. *JHEP*, 05:200, 2019. 1

[45] Toshihiro Ota. Comments on holographic entanglements in cutoff AdS. 4 2019. 1

[46] Niko Jokela and Arttu Pönni. Notes on entanglement wedge cross sections. *JHEP*, 07:087, 2019. 1

[47] Wu-Zhong Guo. Entanglement of purification and disentanglement in CFTs. *JHEP*, 09:080, 2019. 1

[48] Yuya Kusuki and Kotaro Tamaoka. Dynamics of Entanglement Wedge Cross Section from Conformal Field Theories. arXiv:1907.06646. 1

[49] Jinwei Chu, Runze Qi, and Yang Zhou. Generalizations of Reflected Entropy and the Holographic Dual. *JHEP*, 03:151, 2020. 1

[50] Jan Boruch. Entanglement wedge cross-section in shock wave geometries. *JHEP*, 07:208, 2020. 1

[51] Aranya Bhattacharya. Multipartite purification, multiboundary wormholes, and islands in AdS_3/CFT_2. *Phys. Rev. D*, 102(4):046013, 2020. 1

[52] Chris Akers and Pratik Rath. Entanglement Wedge Cross Sections Require Tripartite Entanglement. *JHEP*, 04:208, 2020. 1

[53] Jonah Kudler-Flam and Shinsei Ryu. Entanglement negativity and minimal entanglement wedge cross sections in holographic theories. *Phys. Rev.*, D99(10):106014, 2019. 1, 2.4

[54] Yuya Kusuki, Jonah Kudler-Flam, and Shinsei Ryu. Derivation of Holographic Negativity in AdS_3/CFT_2. *Phys. Rev. Lett.*, 123(13):131603, 2019. 1, 2.4

[55] Souvik Dutta and Thomas Faulkner. A canonical purification for the entanglement wedge cross-section. arXiv:1905.00577. 1, 2.4

[56] Michael Freedman and Matthew Headrick. Bit threads and holographic entanglement. *Commun. Math. Phys.*, 352(1):407–438, 2017. 1

[57] Jonathan Harper and Matthew Headrick. Bit threads and holographic entanglement of purification. *JHEP*, 08:101, 2019. 1

[58] Ning Bao, Aidan Chatwin-Davies, Jason Pollack, and Grant N. Remmen. Towards a Bit Threads Derivation of Holographic Entanglement of Purification. *JHEP*, 07:152, 2019. 1

[59] Jonathan Harper. Multipartite entanglement and topology in holography. 6 2020. 1, 6

[60] Koji Umemoto and Yang Zhou. Entanglement of Purification for Multipartite States and its Holographic Dual. *JHEP*, 10:152, 2018. 1, 3.1, 3, 5, 3.1.3, 3.2, 3.3, 3.4, 3.5, 3.6, 3.7, 3.9

[61] Arpan Bhattacharyya, Alexander Jahn, Tadashi Takayanagi, and Koji Umemoto. Entanglement of purification in many body systems and symmetry breaking. *Phys. Rev. Lett.*, 122:201601, May 2019. 1, 4, 4.1, 4.2, 4.3, 4.4, 4.5, 4.6, 4.7, 4.8, 4.9, 4.10, 4.11, 7.1, 7.2, 7.3, 7.4, 7.5

[62] Pawel Caputa, Masamichi Miyaji, Tadashi Takayanagi, and Koji Umemoto. Holographic entanglement of purification from conformal field theories. *Phys. Rev. Lett.*, 122:111601, Mar 2019. 1, 3.2, 4

[63] Koji Umemoto. Quantum and Classical Correlations Inside the Entanglement Wedge. *Phys. Rev. D*, 100(12):126021, 2019. 1, 2.3, 3, 5, 5, 5.1, 5.2, 5.3, 5.4, 5.5, 5.6, 5.7, 5.8, 5.9, 5.10, 5.11

[64] Shinsei Ryu and Tadashi Takayanagi. Aspects of Holographic Entanglement Entropy. *JHEP*, 08:045, 2006. 2.1

[65] Massimiliano Rota and Sean J. Weinberg. New constraints for holographic entropy from maximin: A no-go theorem. *Phys. Rev.*, D97(8):086013, 2018. 2, 6

[66] Matthew Headrick and Tadashi Takayanagi. A Holographic proof of the strong subadditivity of entanglement entropy. *Phys. Rev.*, D76:106013, 2007. 2.1

[67] Patrick Hayden, Matthew Headrick, and Alexander Maloney. Holographic Mutual Information is Monogamous. *Phys. Rev.*, D87(4):046003, 2013. 2.1, 3, 7

[68] Ning Bao, Sepehr Nezami, Hirosi Ooguri, Bogdan Stoica, James Sully, and Michael Walter. The Holographic Entropy Cone. *JHEP*, 09:130, 2015. 2.1, 3, 3.1.4, 5.2.3

[69] Sergio Hernández Cuenca. Holographic entropy cone for five regions. *Phys. Rev.*, D100(2):026004, 2019. 2.1, 3

[70] Aron C. Wall. Maximin Surfaces, and the Strong Subadditivity of the Covariant Holographic Entanglement Entropy. *Class. Quant. Grav.*, 31(22):225007, 2014. 2.3, 3.2.2, 6

[71] Bartlomiej Czech, Joanna L. Karczmarek, Fernando Nogueira, and Mark Van Raamsdonk. The Gravity Dual of a Density Matrix. *Class. Quant. Grav.*, 29:155009, 2012. 2.3, 3.2.2

[72] Matthew Headrick, Veronika E. Hubeny, Albion Lawrence, and Mukund Rangamani. Causality & holographic entanglement entropy. *JHEP*, 12:162, 2014. 2.3, 3.2.2

[73] Brian Swingle. Entanglement Renormalization and Holography. *Phys. Rev.*, D86:065007, 2012. 2.4, 3.2

[74] Masamichi Miyaji and Tadashi Takayanagi. Surface/State Correspondence as a Generalized Holography. *PTEP*, 2015(7):073B03, 2015. 2.4, 3.2, 3.3.2

[75] Jonah Kudler-Flam, Masahiro Nozaki, Shinsei Ryu, and Mao Tian Tan. Quantum vs. classical information: operator negativity as a probe of scrambling. *JHEP*, 01:031, 2020. 2.4

[76] Jonah Kudler-Flam, Ian MacCormack, and Shinsei Ryu. Holographic entanglement contour, bit threads, and the entanglement tsunami. *J. Phys.*, A52(32):325401, 2019. 2.4

[77] Charles H. Bennett, David P. DiVincenzo, John A. Smolin, and William K. Wootters. Mixed-state entanglement and quantum error correction. *Phys. Rev. A*, 54:3824–3851, Nov 1996. 2.5

[78] V. Vedral, M. B. Plenio, M. A. Rippin, and P. L. Knight. Quantifying entanglement. *Phys. Rev. Lett.*, 78:2275–2279, Mar 1997. 2.5

[79] Patrick M Hayden, Michal Horodecki, and Barbara M Terhal. The asymptotic entanglement cost of preparing a quantum state. *Journal of Physics A: Mathematical and General*, 34(35):6891–6898, aug 2001. 2.5

[80] E. M. Rains. Rigorous treatment of distillable entanglement. *Phys. Rev. A*, 60:173–178, Jul 1999. 2.5

[81] Matthias Christandl and Andreas Winter. "squashed entanglement": An additive entanglement measure. *Journal of Mathematical Physics*, 45(3):829–840, 2004. 2.5, 3.3, 5.1.1

[82] Ryszard Horodecki, Paweł Horodecki, Michał Horodecki, and Karol Horodecki. Quantum entanglement. *Rev. Mod. Phys.*, 81:865–942, Jun 2009. 2.5, 3, 5.3

[83] Pavan Hosur, Xiao-Liang Qi, Daniel A. Roberts, and Beni Yoshida. Chaos in quantum channels. *JHEP*, 02:004, 2016. 3

[84] Massimiliano Rota. Tripartite information of highly entangled states. *JHEP*, 04:075, 2016. 3

[85] S. Mirabi, M. Reza Tanhayi, and R. Vazirian. On the monogamy of holographic n-partite information. *Phys. Rev. D*, 93:104049, May 2016. 3

[86] Laimei Nie, Masahiro Nozaki, Shinsei Ryu, and Mao Tian Tan. Signature of quantum chaos in operator entanglement in 2d CFTs. *J. Stat. Mech.*, 1909(9):093107, 2019. 3

[87] Mohsen Alishahiha, M. Reza Mohammadi Mozaffar, and Mohammad Reza Tanhayi. On the Time Evolution of Holographic n-partite Information. *JHEP*, 09:165, 2015. 3

[88] Dong Yang, Karol Horodecki, Michal Horodecki, Pawel Horodecki, Jonathan Oppenheim, and Wei Song. Squashed entanglement for multipartite states and entanglement measures based on the mixed convex roof. *IEEE Transactions on Information Theory*, 55(7):3375–3387, 2009. 3, 3.1.2, 3.3.1, 3.3.2

[89] David Avis, Patrick Hayden, and Ivan Savov. Distributed compression and multiparty squashed entanglement. *Journal of Physics A: Mathematical and Theoretical*, 41(11):115301, 2008. 3, 3.1.2, 3.3.1

[90] Shrobona Bagchi and Arun Kumar Pati. Monogamy, polygamy, and other properties of entanglement of purification. *Phys. Rev. A*, 91:042323, Apr 2015. 3.1.1

[91] Dong Yang, Michał Horodecki, and Z. D. Wang. An additive and operational entanglement measure: Conditional entanglement of mutual information. *Phys. Rev. Lett.*, 101:140501, Sep 2008. 5, 5, 5.1.2

[92] Robert R. Tucci. Entanglement of distillation and conditional mutual information. arXiv:quant-ph/0202144. 3.3

[93] Masamichi Miyaji, Tadashi Takayanagi, and Kento Watanabe. From path integrals to tensor networks for the AdS/CFT correspondence. *Phys. Rev.*, D95(6):066004, 2017. 3.3.2

[94] Pawel Caputa, Nilay Kundu, Masamichi Miyaji, Tadashi Takayanagi, and Kento Watanabe. Anti-de Sitter Space from Optimization of Path Integrals in Conformal Field Theories. *Phys. Rev. Lett.*, 119(7):071602, 2017. 3.3.2

[95] Sepehr Nezami and Michael Walter. Multipartite Entanglement in Stabilizer Tensor Networks. 2016. 3.3.2

[96] Masato Koashi and Andreas Winter. Monogamy of quantum entanglement and other correlations. *Phys. Rev. A*, 69:022309, Feb 2004. 3.3.2

[97] Arpan Bhattacharyya, Tadashi Takayanagi, and Koji Umemoto. Entanglement of Purification in Free Scalar Field Theories. *JHEP*, 04:132, 2018. 4, 4.1, 4.1, 4.1.2

[98] Luca Bombelli, Rabinder K. Koul, Joohan Lee, and Rafael D. Sorkin. A Quantum Source of Entropy for Black Holes. *Phys. Rev.*, D34:373–383, 1986. 4.1, 4.1.2, 7.1

[99] Noburo Shiba and Tadashi Takayanagi. Volume Law for the Entanglement Entropy in Non-local QFTs. *JHEP*, 02:033, 2014. 4.1, 7.1

[100] G. Vidal and R. F. Werner. Computable measure of entanglement. *Phys. Rev. A*, 65:032314, Feb 2002. 4.1.1, 7.1

[101] M. M. Wolf, G. Giedke, O. Krüger, R. F. Werner, and J. I. Cirac. Gaussian entanglement of formation. *Phys. Rev. A*, 69:052320, May 2004. 8

[102] Ben Ibinson, Noah Linden, and Andreas Winter. Robustness of quantum markov chains. *Communications in Mathematical Physics*, 277(2):289–304, Jan 2008. 4.2

[103] M. Christandl and A. Winter. Uncertainty, monogamy, and locking of quantum correlations. *IEEE Transactions on Information Theory*, 51(9):3159–3165, Sep. 2005. 4.2.1, 4.2.1, 5.1.1

[104] Pierre Pfeuty. The one-dimensional ising model with a transverse field. *Annals of Physics*, 57(1):79 – 90, 1970. 4.2.1

[105] Tobias J. Osborne and Michael A. Nielsen. Entanglement in a simple quantum phase transition. *Phys. Rev. A*, 66:032110, Sep 2002. 4.2.1

[106] P. R. Wells, C. M. Chaves, J. d'Albuquerque e Castro, and Belita Koiller. Correlations and werner states in finite spin linear arrays. *Applied Physics Letters*, 103(17):173105, 2013. 4.2.2

[107] M. C. Bañuls, J. I. Cirac, and M. B. Hastings. Strong and weak thermalization of infinite nonintegrable quantum systems. *Phys. Rev. Lett.*, 106:050405, Feb 2011. 4.2.2

[108] Jianxin Chen and Andreas Winter. Non-additivity of the entanglement of purification (beyond reasonable doubt). 2012/06/06 2012. 5.2.5, 7.3.1, 7.3.1

[109] Veronika E. Hubeny, Henry Maxfield, Mukund Rangamani, and Erik Tonni. Holographic entanglement plateaux. *JHEP*, 08:092, 2013. 5.3, 5.3.2, 5.3.3

[110] Matthew Headrick. General properties of holographic entanglement entropy. *JHEP*, 03:085, 2014. 5.3, 5.3.2

[111] L Henderson and V Vedral. Classical, quantum and total correlations. *Journal of Physics A: Mathematical and General*, 34(35):6899–6905, aug 2001. 5.3

[112] Harold Ollivier and Wojciech H. Zurek. Quantum discord: A measure of the quantumness of correlations. *Phys. Rev. Lett.*, 88:017901, Dec 2001. 5.3

[113] Nan Li and Shunlong Luo. Total versus quantum correlations in quantum states. *Phys. Rev. A*, 76:032327, Sep 2007. 5.3.1

[114] Zhengjun Xi, Xiao-Ming Lu, Xiaoguang Wang, and Yongming Li. Necessary and sufficient condition for saturating the upper bound of quantum discord. *Phys. Rev. A*, 85:032109, Mar 2012. 5.3.5

[115] Lin Zhang and Junde Wu. On conjectures of classical and quantum correlations in bipartite states. *Journal of Physics A: Mathematical and Theoretical*, 45(2):025301, 2012. 5.3.5

[116] A. Uhlmann. The "transition probability" in the state space of a *-algebra. *Reports on Mathematical Physics*, 9(2):273 – 279, 1976. 5.3.6

[117] Hugo A. Camargo, Lucas Hackl, Michal P. Heller, Alexander Jahn, Tadashi Takayanagi, and Bennet Windt. Entanglement and Complexity of Purification in (1+1)-dimensional free Conformal Field Theories. 9 2020. 6

[118] Thomas Faulkner, Aitor Lewkowycz, and Juan Maldacena. Quantum corrections to holographic entanglement entropy. *JHEP*, 11:074, 2013. 6

[119] Taylor Barrella, Xi Dong, Sean A. Hartnoll, and Victoria L. Martin. Holographic entanglement beyond classical gravity. *JHEP*, 09:109, 2013. 6

[120] Patrick Hayden, Richard Jozsa, Dénes Petz, and Andreas Winter. Structure of states which satisfy strong subadditivity of quantum entropy with equality. *Communications in Mathematical Physics*, 246(2):359–374, Apr 2004. 6

[121] William K. Wootters. Entanglement of formation of an arbitrary state of two qubits. *Phys. Rev. Lett.*, 80:2245–2248, Mar 1998. 7.3